

การสังเคราะห์พอลิโอสไตร์นปิดที่มีประจุบนพื้นผิวในขั้นตอนเดียวสำหรับดูดซับสี้อม



นางสาวบุญศรี คู่สุขธรรม

สถาบันวิทยบริการ

จุฬาลงกรณ์มหาวิทยาลัย

วิทยานิพนธ์นี้เป็นส่วนหนึ่งของการศึกษาตามหลักสูตรปริญญาวิทยาศาสตรดุษฎีบัณฑิต

สาขาวิชาวัสดุศาสตร์ ภาควิชาวัสดุศาสตร์


คณะวิทยาศาสตร์ จุฬาลงกรณ์มหาวิทยาลัย

ปีการศึกษา 2547

ISBN 974-17-5962-2

ลิขสิทธิ์ของจุฬาลงกรณ์มหาวิทยาลัย

ONE-POT SYNTHESIS OF POLYSTYRENE BEAD BEARING SURFACE CHARGE  
FOR DYE ADSORPTION



Miss Boonsri Kusuktham

สถาบันวิทยบริการ  
จุฬาลงกรณ์มหาวิทยาลัย

A Dissertation Submitted in Partial Fulfillment of the Requirements  
for the Degree of Doctor of Philosophy in Materials Science

Department of Materials Science

Faculty of Science

Chulalongkorn University

Academic year 2004

ISBN 974-17-5962-2

Thesis Title                                    ONE-POT SYNTHESIS OF POLYSTYRENE BEAD BEARING  
SURFACE CHARGE FOR DYE ADSORPTION

By    Miss Boonsri Kusuktham

Field of Study                                    Materials Science

Thesis Advisor                                   Associate Professor Kawee Srikulkit, Ph.D.

---

Accepted by the Faculty of Science, Chulalongkorn University in Partial  
Fulfillment of the Requirements for the Doctor's Degree

.....Dean of the Faculty of Science  
(Professor Piamsak Menasveta, Ph.D)

THESIS COMMITTEE

.....Chairman  
(Associate Professor Saowaroj Chuayujit)

.....Thesis Advisor  
(Associate Professor Kawee Srikulkit, Ph.D.)

..... Member  
(Associate Professor Werasak Udomkichdecha, Ph.D.)

..... Member  
(Assistant Professor Vimolvann Pimpan, Ph.D.)

.....Member  
(Assistant Professor Mongkol Sukwattanasinitt, Ph.D.)

.....Member  
(Associate Professor Pranee Phinyocheep, Doctorat de l'Universite' du Maine)

นางสาวบุญศรี คู่สุขธรรม : การสังเคราะห์พอลิस्टาไร์นปิดที่มีประจุบนพื้นผิวในขั้นตอนเดียวสำหรับดูดซับสีย้อม. (ONE-POT SYNTHESIS OF POLYSTYRENE BEAD BEARING SURFACE CHARGE FOR DYE ADSORPTION)  
 อ. ที่ปรึกษา : รศ. ดร. กาวี ศรีกุลกิจ, 237 หน้า. ISBN 974-17-5962-2.

พอลิस्टาไร์นปิดที่มีประจุที่ผิวเตรียมโดยปฏิกิริยาพอลิเมอไรเซชันแบบแขวนลอยในขั้นตอนเดียวของสตาไร์นและไดไวนิลเบนซีนที่มีแคทไอออนิกมอนอเมอร์ (3-เมทาคริลอิลอะมิโน) โพรพิลไตรเมทิลแอมโมเนียมคลอไรด์ (MAPTAC) โดยใช้โพแทสเซียมเพอร์ซัลเฟตและเอโซบิสไอโซบิวทิลไฮโดรเจนไตรลเป็นสารเริ่มปฏิกิริยา ขั้นแรก เริ่มจากการทำปฏิกิริยาพอลิเมอไรเซชันของ MAPTAC ตามระยะเวลาที่กำหนดเพื่อทำให้เกิดอนุกรมของพอลิ(3-เมทาคริลอิลอะมิโน) โพรพิลไตรเมทิลแอมโมเนียมคลอไรด์ (PMAPTAC) ขั้นที่สอง เติมสารผสมของสตาไร์น ไดไวนิลเบนซีน และสารเริ่มปฏิกิริยาเอโซบิสไอโซบิวทิลไฮโดรเจนไตรลลงในสารละลายของอนุกรมของ PMAPTAC จากนั้นปล่อยให้เกิดปฏิกิริยาพอลิเมอไรเซชันตามเวลาที่กำหนด ในระหว่างการเกิดปฏิกิริยาพอลิเมอไรเซชันของสตาไร์นและไดไวนิลเบนซีน อนุกรมของ PMAPTAC เข้าทำปฏิกิริยาที่ผิวปิดทำให้อนุภาคปิดที่ได้ประกอบด้วยชั้นจำนวนสองชั้น (จากการใช้กล้องจุลทรรศน์อิเล็กตรอนแบบส่องกราด) คือ แกนชั้นใน ซึ่งเป็นพอลิ(สตาไร์น-โค-ไดไวนิลเบนซีน) และชั้นนอก ซึ่งเกิดจากปฏิกิริยาโคพอลิเมอไรเซชันของสตาไร์น ไดไวนิลเบนซีน และอนุกรมของ PMAPTAC ซึ่งวิเคราะห์ด้วยอินฟราเรดสเปกโทรสโกปี โดยศึกษาปัจจัยที่มีผลต่อขนาดของอนุภาค การกระจายของขนาดอนุภาค และหมู่ฟังก์ชัน (functional group) ที่ผิวอนุภาค (ส่วนของ PMAPTAC) จากพารามิเตอร์ที่ทำการศึกษาทั้งหมด พบว่าปัจจัยสำคัญที่มีผลต่อการควบคุมขนาดของอนุภาค และหมู่ฟังก์ชันที่ผิวของอนุภาค คือ ชนิดของสารแรงดึงผิว และปริมาณของไดไวนิลเบนซีน การศึกษาการดูดซับสีแอนไอออนิกของปิดเพื่อประเมินลักษณะของปิดที่เป็นเรซินชนิดแลกเปลี่ยนไอออน กลไกการดูดซับเกิดจากการเกิดแรงดึงดูดของประจุต่างชนิดกันระหว่างหมู่ที่มีประจุบวกของปิดและหมู่ที่มีประจุลบของสี การดูดซับสอดคล้องกับแบบจำลองของแลงเมียร์

ภาควิชา วัสดุศาสตร์

ลายมือชื่อนิสิต .....

สาขาวิชา วัสดุศาสตร์

ลายมือชื่ออาจารย์ที่ปรึกษา.....

ปีการศึกษา 2547



##4473816323: MAJOR MATERIALS SCIENCE

KEY WORD: one-pot suspension polymerization / polymer bead / surface charge / anion exchange

BOONSRI KUSUKTHAM : ONE-POT SYNTHESIS OF POLYSTYRENE BEAD BEARING SURFACE CHARGE FOR DYE ADSORPTION. THESIS ADVISOR : ASSOC. PROF. KAWEE SRIKULKIT, Ph.D. 237 pp. ISBN 974-17-5962-2.

Preparation of polystyrene bead bearing surface charge was carried out using one pot suspension polymerization of styrene and divinylbenzene (DVB) in the presence of cationic functional monomer, (3-methacryloylamino) propyl trimethyl ammonium chloride (MAPTAC), using  $K_2S_2O_8$  and AIBN as initiators. Firstly, polymerization of MAPTAC in aqueous solution using  $K_2S_2O_8$  initiator was performed for the determined time to generate poly(3-methacryloylamino) propyl trimethyl ammonium chloride (PMAPTAC) radical. Secondly, the mixture of styrene, DVB, and AIBN initiator was fed into the solution of PMAPTAC radicals and then allowed the polymerization to proceed for another certain time. During the stage of polymerization of styrene and DVB, incorporation of PMAPTAC radicals onto the bead surface took place, resulting in the final bead particle comprised two layers (from SEM result); the inner core of the poly(styrene-co-DVB) support and the outer layer of copolymerization adduct of styrene, DVB, and PMAPTAC radical revealed by FTIR analysis. Factors affecting particle size, size distribution and surface functionality (PMAPTAC segment) were investigated. Of all synthetic parameters, types of surfactants and amounts of DVB were found to play an important role in controlling the particle size and the surface functionality, respectively. Anionic dye adsorption was carried out in order to evaluate the performance of the bead as ion exchange resin. Adsorption mechanism involved the opposite charge interaction between the bead cationic group and the dye anionic group. The adsorption capacities, following the Langmuir model, were also reported.

Department Materials Science

Student's signature .....

Field of study Materials Science

Advisor's signature .....

Academic year 2004

## ACKNOWLEDGEMENTS

I would like to express my sincere gratitude to my advisor Assoc. Prof. Dr. Kawee Srikulkit for his valuable guidance continuous interest and encouragement throughout this study.

I am grateful to Assoc. Prof. Saowaroj Chuayjuljit, Assoc. Prof. Dr. Weresak Udomkitchdecha, Asst. Prof. Dr. Vimolvan Pimpan, and Asst. Prof. Dr. Mongkol Sukwattanasinitt for their comments and the Department of Materials Science, Chulalongkorn University for the graduate courses.

I wish to express my appreciation to Assoc. Prof. Dr. Pranee Phinyocheep of the Faculty of Science, Mahidol University for her suggestion and many helpful discussion.

Finally, I would like to thank all of my friends for their helps throughout this work.



สถาบันวิทยบริการ  
จุฬาลงกรณ์มหาวิทยาลัย

## CONTENTS

|  | Page |
|--|------|
| Abstract (Thai).....                                 | iv   |
| Abstract (English).....                              | v    |
| Acknowledgements.....                                | vi   |
| List of Tables .....                                 | xii  |
| List of Figures .....                                | xv   |
| Chapter  |      |
| I Introduction .....                                 | 1    |
| II Literature Review .....                           | 5    |
| 2.1 Polymeric Bead : Synthesis and Application ..... | 5    |
| 2.1.1 Synthetic Organic Polymer.....                 | 5    |
| 2.1.2 Polysaccharides.....                           | 6    |
| 2.1.3 Inorganic Support.....                         | 6    |
| 2.1.4 Composite Support.....                         | 6    |
| 2.2 Preparation of Polymer Particle .....            | 10   |
| 2.2.1 Suspension Polymerization .....                | 11   |
| 2.2.2 Emulsion Polymerization .....                  | 23   |
| 2.2.3 The Role of Surfactants .....                  | 26   |
| 2.2.4 Application of Polymer Bead .....              | 31   |

| Contents (continued)                                   | Page |
|--|------|
| 2.3 Ion Exchange .....                                 | 34   |
| 2.3.1 Structure and Components of Ion Exchange .....   | 34   |
| 2.3.2 Organic Resin Exchangers .....                   | 37   |
| 2.4 Adsorption Isotherm .....                          | 38   |
| 2.4.1 Types of Adsorption Isotherm .....               | 38   |
| 2.4.2 Adsorption Isotherms in Solid-Liquid Systems ... | 42   |
| 2.5 Parameter of Color Removal .....                   | 44   |
| 2.5.1 Effect of Time .....                             | 44   |
| 2.5.2 Effect of Salt .....                             | 45   |
| 2.5.3 Effect of Temperature .....                      | 46   |
| 2.5.4 Effect of Particle Size .....                    | 48   |
| III Experimental.....                                  | 49   |
| 3.1 Chemicals and Equipment.....                       | 49   |
| 3.1.1 Chemicals.....                                   | 49   |
| 3.1.2 Equipment.....                                   | 50   |
| 3.2 Typical Synthesis of Poly (styrene-co-DVB) Beads   |      |
| Bearing Surface Charge.....                            | 51   |
| 3.2.1 General Procedure.....                           | 51   |
| 3.2.2 Effect of Polymerization Time of MAPTAC.....     | 54   |

| Content (continued)   | Page |
|---|------|
| 3.2.3 Effect of Copolymerization Time.....  | 54   |
| 3.2.4 Effect of Polymerization Temperature.....   | 55   |
| 3.2.5 Effect of Stirring Speed.....   | 56   |
| 3.2.6 Effect of Divinylbenzene.....   | 57   |
| 3.2.7 Effect of Surfactants.....  | 57   |
| 3.2.7.1 Effect of Nonionic Surfactant.....  | 57   |
| 3.2.7.2 Effect of Cationic Surfactant.....  | 58   |
| 3.3 Characterizations.....  | 59   |
| 3.3.1 Particle Size Measurement.....  | 59   |
| 3.3.2 Gel Permeation Chromatography (GPC).....  | 59   |
| 3.3.3 FTIR Analysis.....  | 60   |
| 3.3.4 Microscopic Studies.....  | 60   |
| 3.4 Dye Adsorption Studies.....   | 61   |
| 3.4.1 Determination of Dye Adsorption.....  | 61   |
| 3.4.2 Determination of Contact Time.....  | 61   |
| 3.4.3 Dye Adsorption Isotherms Study.....   | 61   |
| IV Results and Discussion.....  | 63   |
| 4.1 Fundamental Idea on One-Pot Synthesis of Polymeric<br>Beads Bearing Surface Charge..... | 63   |

| Content (continued)  | Page |
|--|------|
| 4.2 Parameters Influencing Particle Size and Particle Size |      |
| Distribution.....  | 68   |
| 4.2.1 Effect of Polymerization Time of MAPTAC.....         | 68   |
| 4.2.2 Effect of Copolymerization Time of                   |      |
| Styrene, DVB and PMAPTAC Oligomer                          |      |
| on Bead Formation.....                                     | 79   |
| 4.2.3 Effect of Copolymerization Temperature.....          | 83   |
| 4.2.4 Effect of Stirring Speed on Particle Size.....       | 88   |
| 4.2.5 Effect of Divinylbenzene Crosslinker on Bead         |      |
| Morphology and Surface Functionality.....                  | 90   |
| 4.2.6 Effect of Surfactants.....                           | 95   |
| 4.2.6.1 Effect of Nonionic Surfactant.....                 | 95   |
| 4.2.6.2 Effect of Cationic Surfactant.....                 | 100  |
| 4.3 Dye Adsorption Study of the Prepared Bead.....         | 108  |
| 4.3.1 Determination of Contact Time.....                   | 109  |
| 4.3.2 Adsorption Isotherm.....                             | 113  |
| 4.3.2.1 Effect of Particle Size on Adsorption              |      |
| Isotherm.....  | 118  |

| Content (continued)   | Page |
|---|------|
| 4.3.2.2 Effect of Temperature on Adsorption Isotherm.....                             | 122  |
| 4.3.3 Analysis of Adsorption Isotherm.....  | 124  |
| 4.3.3.1 Analysis Through Freundlich Isotherm.....                                     | 124  |
| 4.3.3.2 Analysis Through Langmuir Isotherm....  | 124  |
| V Conclusion.....   | 138  |
| References.....   | 141  |
| Appendices.....   | 150  |
| Appendix A Dye Adsorption of Polymer Bead at Various Condition of Polymerization..... | 151  |
| Appendix B Contact Time.....  | 157  |
| Appendix C Data of Adsorption Isotherm.....   | 164  |
| Appendix D Equilibrium Adsorption Isotherm Curve.....                                 | 206  |
| Appendix E Effect of Temperature on Adsorption Isotherm.....                          | 213  |
| Appendix F Freundlich Plots for Adsorption of Reactive dyes.....                      | 217  |
| Appendix G Langmuir Plots for Adsorption of Reactive dyes .....                       | 227  |
| Biography.....  | 237  |

## List of Tables

| Tables   | Page |
|--|------|
| 2.1 Types of heterogeneous polymerization systems .....                            | 10   |
| 2.2 Effect of Surfactants on Particle Size Distribution .....                      | 16   |
| 2.3 Porosity Data from Nitrogen Adsorption Analysis .....                          | 22   |
| 2.4 Component in Ion Exchange .....  | 35   |
| 3.1 Chemicals used in this thesis.....   | 50   |
| 3.2 Experimental conditions .....  | 53   |
| 3.3 Various polymerization time for suspension polymerization.....                 | 54   |
| 3.4 Various copolymerization time for suspension polymerization.....               | 55   |
| 3.5 Various polymerization temperature for suspension<br>polymerization.....       | 55   |
| 3.6 Various stirring speed for suspension polymerization.....                      | 56   |
| 3.7 Various amount of styrene, DVB, and AIBN for suspension<br>polymerization..... | 57   |
| 3.8 Various amount of cetyl alcohol for suspension<br>Polymerization.....          | 58   |
| 3.9 Various amount of CTAB for suspension polymerization.....                      | 59   |
| 4.1 Experimental conditions .....  | 65   |



| Tables (continued)  | Page |
|---|------|
| 4.2 Molecular weights of MAPTAC determined by<br>gel permeation chromatography .....  | 69   |
| 4.3 Molecular weights of PMAPTAC determined by<br>gel permeation chromatography .....   | 70   |
| 4.4 Effect of polymerization time of MAPTAC on particle size<br>and particle size distribution.....                                     | 74   |
| 4.5 Effect of polymerization time of MAPTAC on dye adsorption<br>of polymer beads .....   | 74   |
| 4.6 Effect of polymerization time between styrene, DVB, and<br>PMAPTAC radical on particle size and particle size<br>distribution ..... | 81   |
| 4.7 Effect of temperature on particle size and particle size<br>distribution .....  | 85   |
| 4.8 Effect of polymerization temperature on dye adsorption of<br>polymer bead .....   | 81   |
| 4.9 Effect of stirring speed on particle size and particle size<br>Distribution .....   | 88   |
| 4.10 Effect of DVB on particle size and particle size distribution.....   | 90   |

| Tables (continuted)   | Page |
|---|------|
| 4.11 The percent yield with the relation to the amount of cetyl alcohol..                             | 95   |
| 4.12 Effect of cetyl alcohol on particle size distribution and<br>size distribution.....              | 96   |
| 4.13 The relationship between the CTAB content and percent yield....                                  | 101  |
| 4.14 Effect of CTAB on particle size and particle size distribution.....                              | 101  |
| 4.15 Elements on polymer particle.....  | 105  |
| 4.16 Effect of CTAB content and particle size on dye adsorption.....                                  | 107  |
| 4.17 Effect of contact time on the adsorption of<br>C.I. Reactive Blue 171 by the polymer bead .....  | 109  |
| 4.18 Effect of contact time on the adsorption of<br>C.I. Reactive Red 195 by the polymer bead .....   | 110  |
| 4.19 Effect of contact time on the adsorption of<br>C.I. Reactive Yellow 84 by the polymer bead ..... | 110  |
| 4.20 Linear equation from Freundlich plots.....   | 129  |
| 4.21 Linear equation from Freundlich plots.....   | 130  |
| 4.22 Linear equation from Langmuir plots.....   | 136  |
| 4.23 Linear equation from Langmuir plots.....   | 137  |

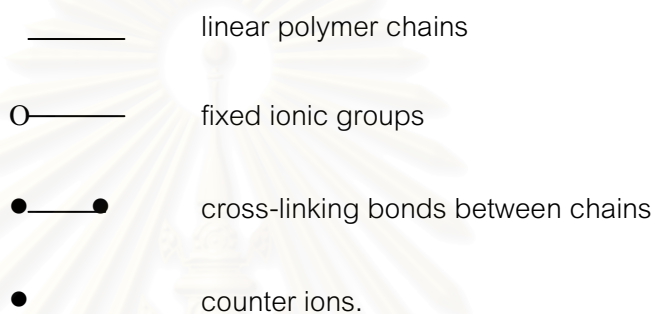
## List of Figures

| Figure  | Page |
|---|------|
| 2.1 Preparation of pore-matrix composite supports.....  | 7    |
| 2.2 Preparation of beaded interpenetrating networks.....  | 7    |
| 2.3 X-ray microprobe image of a cross-linked (network)<br>copolymer of dimethylacrylamide and vinylferrocene<br>formed within a preformed network of cross-linked<br>polydimethylacrylamide.....  | 8    |
| 2.4 Schematic presentation of core-shell grafts. (a) ideal structure<br>(b) typical structure, available via attachment of monomer on<br>the surface, followed by graft polymerization.....   | 9    |
| 2.5 Schematic representation of suspension polymerization (a) organic<br>comonomer mixture containing dissolved initiator; (b) aqueous<br>continuous phase containing dissolved polymeric suspension<br>stabilizer; (c) shearing to form comonomer liquid<br>droplets; (d) thermal polymerization to form solid polymer resin<br>beads..... | 12   |
| 2.6 Collision of polyisobutylene droplets.....  | 13   |

|  |    |
|--|----|
| 2.7 Action of porogen in forming porous morphology in a macroporous resin: (a) monomer, crosslinker and porogen isotropic solution; (b) polymerization; (c) polymer network forming; (d) porogen and network start to phase separate; (e) porogen phase acts as pore template; (f) porogen phase removal to yield pores (hatched area = crosslinked polymer; dots = porous phase)..... | 15 |
| 2.8 Effect of Aliquat 336 co-stabilizer concentration on PMMA particle size with different concentrations of poly(vinyl pyrrolidone) (PVP K-30).....   | 17 |
| 2.9 Evolution of number average diameter of droplets during the polymerization for different stirring rates.....   | 19 |
| 2.10 DSC thermograms of styrene/lauryl acrylate = 80/20 copolymer with different crosslinking densities: (----) first run; ( ) second run; (A) control; (B) 0.5 wt% DVB; (C) 5 wt% DVB; (D) 10 wt% DVB.....  | 20 |
| 2.11 Scanning electron micrographs of resin beads at dodecanol/toluene = 50/50 (magnification 500 X).....  | 22 |
| 2.12 Various possible mechanisms of droplet stabilization.....   | 28 |

2.13 Schematic representation of a modern ion exchange resin

The structure is based upon a random three-dimensional structure of linear polymer chain which are cross-linked at intervals along their length . . . . .35



2.14 Ion exchange with a solution . . . . .36




2.15 Langmuir plot for the removal of the three direct dyes.....40

2.16 A Freundlich plot for the adsorption of  $\text{Cu}^{2+}$  on modified cellulose at pH 5.0 and  $10^\circ\text{C}$  with  $63.5 \text{ mg/l Cu}^{2+}$  .....41

2.17 Classification of adsorption isotherm according to Giles et.al. Letters indicate class and numbers indicate subgroup..... 43

2.18 Effect of initial concentration of acid dye adsorption of TR 2B carbon mass = 1.7 g  $d_p = 355\text{-}500 \mu\text{m}$ , agitation time = 500 rpm.....44

| Figure (continued)  | Page |
|---|------|
| 2.19 Effect of NaCl concentration on the equilibrium adsorption isotherm at 30°C of Direct Blue 86 on PAE-Cell.....   | 45   |
| 2.20 (a) Effect of temperature on the equilibrium adsorption isotherm on PAE-Cell for C.I. Acid Blue 158. (b) Effect of temperature on the equilibrium adsorption isotherm on PAE-Cell for C.I. Direct Blue 86..... | 47   |
| 4.1 SEM micrographs of the bead structure and crossed-section of polymer bead.<br>(a), (b) bead structure<br>(c),(d) crossed-section of polymer bead .....  | 66   |
| 4.2 SEM micrograph of polystyrene.....  | 67   |
| 4.3 SEM micrographs of product in the case of no addition AIBN<br>(a) magnification 80X (b) magnification 100X .....  | 67   |
| 4.4 GPC chromatogram of MAPTAC monomer .....  | 71   |
| 4.5 GPC chromatogram of PMAPTAC at polymerization<br>time of 15 minutes.....  | 71   |
| 4.6 GPC chromatogram of PMAPTAC at polymerization<br>time of 30 minutes .....   | 72   |

| Figure (continued)   | Page |
|--|------|
| 4.7 GPC chromatogram of PMAPTAC at polymerization<br>time of 45 minutes.....   | 72   |
| 4.8 Particle size and distribution obtained from polymerization<br>times of MAPTAC 15-45 minutes.....  | 74   |
| 4.9 FT-IR spectrum of PMAPTAC .....  | 76   |
| 4.10 FTIR spectrum of polymer bead obtained from different<br>polymerization time of MAPTAC (a) polystyrene; (b) 15 min;<br>(c) 30 min; (d) 45 min.....  | 77   |
| 4.11 Schematic Diagram represents the formation of charge<br>bearing bead : <b>(a)</b> PMAPTAC radical in aqueous solution;<br><b>(b)</b> mixture of surfactant, styrene, DVB, and AIBN droplet<br>in the aqueous solution; <b>(c)</b> PMAPTAC radical diffused through<br>surfactant layer into gel bead surface; <b>(d)</b> the final bead bearing<br>surface charge onto the outer layer.....                           | 80   |
| <p>  = PMAPTAC radical      ..... = surfactant<br/>  = mixture of styrene, DVB, and AIBN droplet<br/>  = gel bead      ● = final bead bearing surface charge </p> |      |

| Figure (continued)   | Page |
|--|------|
| 4.12 Particle size and distribution obtained from styrene and PMAPTAC<br>polymerization times of 1-3 h.....                                  | 82   |
| 4.13 Particle size and distribution obtained from copolymerization<br>temperature of 60-80°C.....  | 84   |
| 4.14 SEM micrographs of polymer beads at different<br>polymerization temperatures.....   | 85   |
| (a) 70°C ; (b) 80°C  |      |
| 4.15 FTIR spectra of polymer bead obtain from different<br>polymerization temperatures (a) polystyrene; (b) 60°C;<br>(c) 70°C; (d) 80°C..... | 86   |
| 4.16 Effect of stirring speed on the particle size distribution .....  | 89   |
| 4.17 Particle size and distribution at DVB contents of 0.46-1.84 g.....  | 91   |
| 4.18 Comparison of SEM micrographs of polymer bead at<br>different amount of DVB.....  | 93   |
| (a) poly(styrene-co-DVB) bead (b) polymer bead at DVB<br>content of 0.46 g   |      |
| (c), (d) polymer bead at DVB content of 1.84 g   |      |
| 4.19 FTIR spectrum of polystyrene bead.....  | 94   |
| 4.20 FTIR spectrum of polymer bead at DVB content of 0.46 g.....   | 94   |



| Figure (continued)  | Page |
|---|------|
| 4.21 Particle size and distribution at cetyl alcohol content of<br>0-0.005 g.....   | 97   |
| 4.22 Particle size and distribution at cetyl alcohol content of<br>0.01-0.03 g..... | 97   |
| 4.23 SEM micrographs of polymer bead in the absence of<br>cetyl alcohol.....        | 99   |
| (a) magnification 59X (b) magnification 450X  |      |
| (c) magnification 450X  |      |
| 4.24 SEM micrographs of polymer bead at cetyl alcohol<br>content 0.01 g.....        | 100  |
| (a) magnification 100X (b) magnification 350X                                       |      |
| 4.25 Particle size and distribution at different CTAB content.....                  | 102  |
| 4.26 FTIR spectrum of polystyrene bead.....   | 104  |
| 4.27 FTIR spectrum of polymer bead at CTAB content of 0.002 g...                    | 104  |
| 4.28 SEM micrographs of polymer bead with different amount of<br>CTAB.....          | 106  |
| (a), (b) CTAB content of 0.002 g  |      |
| (c),(d) CTAB content of 0.004 g   |      |
| (e), (f) CTAB content of 0.005 g  |      |

| Figure (continued)  | Page |
|---|------|
| 4.29 Effect of contact time on the adsorption of reactive blue<br>by the polymer bead at temperature of 80°C.....   | 111  |
| 4.30 Effect of contact time on the adsorption of reactive red<br>by the polymer bead at temperature of 80°C.....    | 112  |
| 4.31 Effect of contact time on the adsorption of reactive yellow<br>by the polymer bead at temperature of 80°C..... | 112  |
| 4.32 Equilibrium adsorption isotherms of reactive blue.....   | 115  |
| on polymer bead at particle of 150 $\mu\text{m}$ .  |      |
| (a) at room temperature      (b) at temperature of 80°C   |      |
| 4.33 Equilibrium adsorption isotherms of reactive red .....   | 116  |
| on polymer bead at particle of 150 $\mu\text{m}$ .  |      |
| (a) at room temperature      (b) at temperature of 80°C   |      |
| 4.34 Equilibrium adsorption isotherms of reactive red<br>on polymer bead at particle of 150 $\mu\text{m}$ .....     | 117  |
| (a) at room temperature      (b) at temperature of 80°C   |      |
| 4.35 Effect of particle size on the equilibrium adsorption<br>isotherm of reactive blue at room temperature.....    | 119  |
| 4.36 Effect of particle size on the equilibrium adsorption<br>isotherm of reactive blue at temperature of 80°C..... | 119  |

| Figure (continued)   | Page        |
|--|-------------|
| 4.37 Effect of particle size on the equilibrium adsorption<br>isotherm of reactive red at room temperature.....  | 120         |
| 4.38 Effect of particle size on the equilibrium adsorption<br>isotherm of reactive red at temperature of 80°C.....                                     | 120         |
| 4.39 Effect of particle size on the equilibrium adsorption<br>isotherm of reactive yellow at room temperature.....                                     | 121         |
| 4.40 Effect of particle size on the equilibrium adsorption<br>isotherm of reactive.....  | 121         |
| 4.41 Effect of temperature on the equilibrium adsorption isotherm<br>of reactive blue on polymer bead at particle size of 150 $\mu\text{m}$ ...        | 123         |
| 4.42 Effect of temperature on the equilibrium adsorption isotherm<br>of reactive red on polymer bead at particle size<br>of 150 $\mu\text{m}$ .....    | 123         |
| 4.43 Effect of temperature on the equilibrium adsorption<br>isotherm of reactive yellow on polymer bead at<br>particle size of 150 $\mu\text{m}$ ..... | 124         |
| 4.44 Freundlich plots for the adsorption of reactive blue on<br>bead 150 $\mu\text{m}$ .....   | 126         |
| (a) at room temperature  | (b) at 80°C |

| Figure (continued)   | Page |
|--|------|
| 4.45 Freundlich plots for the adsorption of reactive red on<br>bead 150 $\mu\text{m}$ .....                      | 126  |
| (a) at room temperature      (b) at 80°C   |      |
| 4.46 Freundlich plots for the adsorption of reactive yellow<br>on bead 150 $\mu\text{m}$ .....                   | 128  |
| (a) at room temperature      (b) at 80°C   |      |
| 4.47 Langmuir plots for the adsorption of reactive blue on<br>bead at particle size of 150 $\mu\text{m}$ .....   | 133  |
| (a) at room temperature      (b) at 80°C   |      |
| 4.48 Langmuir plots for the adsorption of reactive red on<br>bead at particle size of 150 $\mu\text{m}$ .....    | 134  |
| (a) at room temperature      (b) at 80°C   |      |
| 4.49 Langmuir plots for the adsorption of reactive yellow on<br>bead at particle size of 150 $\mu\text{m}$ ..... | 135  |
| (a) at room temperature      (b) at 80°C   |      |

## CHAPTER I

### INTRODUCTION

Adsorption is one of treatment technique for removal of textile dye waste commonly containing anionic dyes such as unfixed reactive dyes, the widely used dyes for the coloration of cellulose. Discharged unfixed reactive dyes have been problematic compounds in textile effluents as they are highly water-soluble and cannot be removed by traditional aerobic biological wastewater treatment system (i.e. activated sludge and trickling filters), resulting in highly colored effluent entering the receiving water body. [1] Typical dye adsorbents include agricultural by-products, [2-3] activated carbon [4-5] and metal sludge. [6-8] Agriculture based adsorbents usually contain negative charge which repels anionic dyes. They can be modified in low pH conditions to reduced coulombic repulsion but this means a higher cost of pH adjustment and COD increase. Activated carbon is an expensive material while metal sludge is cheap but leachable to release toxic heavy metal ions. Adsorbents based on synthetic polymers are commercially available and they have mostly found application in areas of chromatography, [9] water softening and small ionic species [10] such as counter anions [11-12] and cations. [13] Their adsorption capacity of very large molecules such as most of synthetic dyes is extremely low and costly to be applied.

Most ion exchange bead resins are manufactured by a suspension polymerization of styrene using divinylbenzene (DVB) as a crosslinking agent. [14-16] The polymeric bead is needed to be chemically activated in order to make it capable of exchanging ions. Functional groups are chemically attached to the bead as a source of charge. Each active group has a fixed electrical charge, which is balanced by the equivalent number of oppositely charged ions. Strong base exchangers are based upon quaternary ammonium groups ( $-NR_3^+$ ), where R may be a methyl, ethyl or other organic substituents. Activation of polystyrene/DVB bead involves two-step processes; chloroethylation and subsequently treated with ammonia or primary, secondary or tertiary alkyl amine. [17] It can be seen that several involved reaction steps with requirement of toxic chemicals contribute to the high cost of the final resins which make them too expensive for treatment of textile dye wastewater.

It is of interest to prepare anion exchange resin by a single batch process at the ultimate aim of resins suitable for textile dye adsorption. In this work, a suspension polymerization of styrene and divinylbenzene was carried out in an aqueous solution of functional monomer (3-(methacryloylamino) propyl trimethyl ammonium chloride : MAPTAC, a cationic monomer). The functional monomer was firstly initiated by potassium persulfate to generate short chain length of PMAPTAC radical (the functional group). Styrene and divinylbenzene mixture containing AIBN initiator was fed after the certain time. It is expected that the surface of poly(styrene-co-DVB) bead would be

functionalized by the graft reaction of PMAPTAC radical with available surface monomer.

#### Objectives of this research

- To prepare an ion exchange adsorbent for removal of unfixed reactive dyes.
- To investigate the adsorption isotherm of prepared ion exchange adsorbent.

#### Scope of the present thesis

1. Synthesis of adsorbent bead by a polymerization of styrene with poly((3-methacryloylamino propyl) trimethyl ammonium chloride) (PMAPTAC) using co-initiators, potassium persulfate and 2,2'-azobis(isobutyronitrite)

2. Investigation of several parameters influencing particle size and particle size distribution as follows:

2.1 Polymerization time of MAPTAC

2.2 Copolymerization time of styrene, DVB, and PMAPTAC radical

2.3 Polymerization temperature

2.4 Agitation speed

2.5 Amount of divinylbenzene (crosslinking agent)

2.6 Type and amount of surfactants

### 3. Characterization of adsorbent bead

3.1 Gel permeation chromatography (GPC) was employed to determine molecular weight of PMAPTAC.

3.2 FT-IR spectroscopy was used to determine the functional groups.

3.3 Scanning electron microscope (SEM) equipped with X-Ray microanalysis was used to analyze the surface and the elements of the bead.

### 4. Adsorption properties of adsorbent

The following parameters were studied

4.1 Type of reactive dyes (blue, red, and yellow) on adsorption isotherm

4.2 Temperature on adsorption isotherm

4.3 Concentration of dyes

4.4 Particle size of beads on adsorption isotherm

สถาบันวิทยบริการ  
จุฬาลงกรณ์มหาวิทยาลัย



## CHAPTER II

### LITERATURE REVIEW

#### 2.1 Polymer Bead : Synthesis and Applications [18]

Polymeric beads are widely used as packing materials in the field of separation technology including chromatography, bio-product separation, solid phase synthesis and water treatment and precious metals extraction. Polymer supports and gels are produced from a wide range of natural and synthetic sources and by numerous manufacturing processes and technologies. For example, beads of polystyrene resins are produced by oil-in-water (o/w) suspension polymerization, whereas polyacrylamide gels are obtained by water-in-oil (w/o) suspension polymerization. Microspherical products based on polysaccharides and silica are manufactured by a number of related processes. Types of polymer beads are divided in details as follows.

##### 2.1.1 Synthetic Organic Polymers

Synthetic organic polymers used as polymer supports or polymeric reagents are mainly based on polystyrene and polyacrylamides. Polymethacrylates and poly(vinyl alcohol) are also used to a lesser extent. Beads of polycondensates such as phenolic and polycarbonate resins can be produced readily by suspension polycondensation but polycondensates are generally less suitable for the development of polymer supports.

### 2.1.2 Polysaccharides

Beads of polysaccharide resins (gels) are produced by a variety of closely related suspension processes. Most of the techniques developed for the preparation of polysaccharide beads resins are based on droplet formation processes more or less similar to water-in-oil suspension polymerization. The samples of polysaccharide beads are agarose, cellulose, and dextran.

### 2.1.3 Inorganic Supports

Porous silica (silica gel) is widely used as a sorbent, catalyst and polymer support. Related sorbent such as alumina is also used to a lesser extent. Controlled pore glass has attracted considerable interest in recent years for enzyme immobilization and chromatography.

### 2.1.4 Composite Supports

Most of polymers have defined characteristics within relatively sharp boundaries. For example, polyacrylamide is strongly hydrophilic and not suitable for use in organic media. In order to benefit from the desirable features of different polymer types, and at the same time minimize their shortcomings, attempts have been directed towards the design of composite and multicomponent polymer supports. The variety of composite polymer supports are shown as follows:

## 1. Pore-matrix composites

This category of composite supports has attracted considerable interest owing to its simple design and ease of production, as illustrated in Figure 2.1.

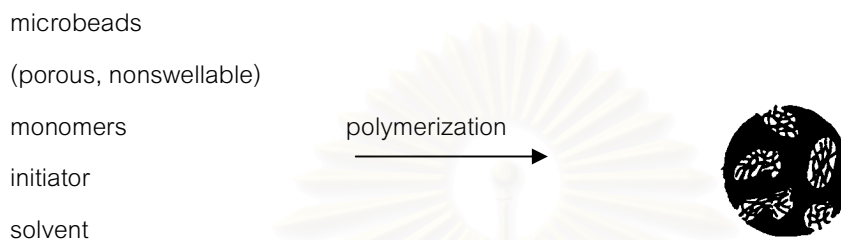


Figure 2.1 Preparation of pore-matrix composite supports.

A porous inorganic support (e.g. porous silica) is soaked in a solution of the organic monomer mixture, usually containing a cross-linker and initiator. Subsequent polymerization under carefully controlled condition leads to the formation of the desired organic polymer within the pores of the beaded inorganic support.

## 2. Interpenetrating networks

Beaded polymer supports composing of two interpenetrating networks are produced according to the scheme shown in Figure 2.2.

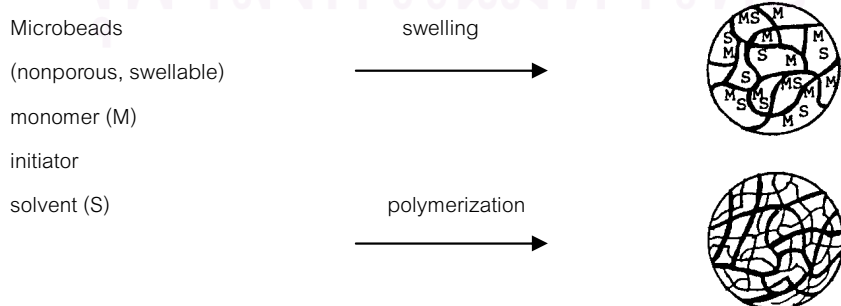


Figure 2.2 Preparation of beaded interpenetrating networks.

The method involves the formation of one cross-linked polymer network within the matrix of a preformed beaded polymer. Figure 2.3 shows an X-ray microprobe image of a copolymer of vinylferrocene within a beaded polydimethylacrylamide matrix.

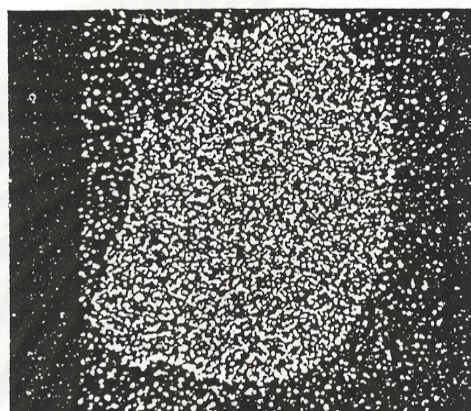


Figure 2.3 X-ray microprobe image of a cross-linked (network) copolymer of dimethylacrylamide and vinylferrocene formed within a preformed network of cross-linked polydimethylacrylamide.

### 3. Core-shell grafts

An ideal model of a core-shell graft composite having a rigid core and relatively long flexible graft chain, is shown in Figure 2.4.

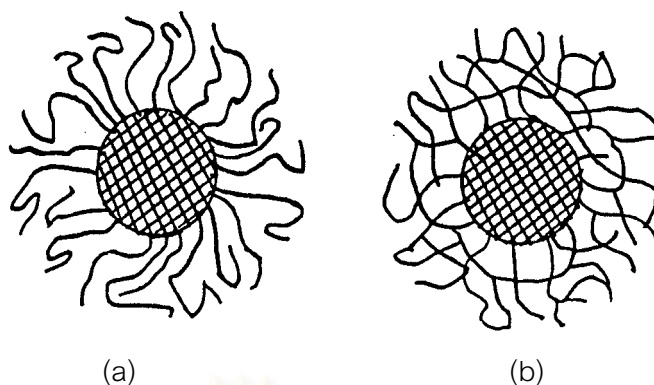


Figure 2.4 Schematic presentation of core-shell grafts: (a) ideal structure (b) typical structure, available via attachment of monomer on the surface, followed by graft polymerization.

The rigid core may be an inorganic material (e.g. glass) or an organic polymer (e.g. polystyrene). Such an ideally grafted surface can be produced by attaching specifically monofunctionalized linear chain to suitably activated surfaces. A more practical approach is, however, the attachment of initiator groups or vinyl residues to the surface, followed by direct graft polymerization. Graft polymerization onto the surface of the core produces a different shell structure.

#### 4. Pellicular supports

Pellicular supports are essentially similar to core-shell grafts shown in Figure 2.4. However, the term "pellicular" is used to describe materials in which the outer shell is relatively thicker than that in core-shell supports. In addition, in pellicular supports the shell is deliberately cross-linked by the inclusion of a cross-linking monomer, and the shell may or may not be covalently attached to the core. Here again,

the pellicular terminology is equally used whether the core is rigid or porous.

## 2.2 Preparation of Polymer Particle

Several process methods for preparing polymer particle, such as emulsion polymerization [19-21], suspension polymerization [15-16 ; 22] , and dispersion polymerization [ 23-26] have been reported. These polymerization methods are rather complicated and require numerous time-consuming reaction steps and procedure. Different types of heterogeneous polymerization systems are shown in Table 2.1

Table 2.1 Types of heterogeneous polymerization systems [20]

| Type       | Particle radius      | Initiator     | Continuous phase                             | Particles  |
|------------|----------------------|---------------|--|--|
| emulsion   | 50-300 $\mu\text{m}$ | water soluble | water  | initially absent, monomer-swollen polymer particles form |
| suspension | $\geq 1 \mu\text{m}$ | oil soluble   | water  | monomer and formed polymer in pre-existing droplets      |
| dispersion | $\geq 1 \mu\text{m}$ | oil soluble   | organic<br>(poor solvent for formed polymer) | initially absent, monomer-swollen polymer particles form |

The term dispersion polymerization was defined as a modified suspension polymerization that produced particles in the 10  $\mu\text{m}$  range. This is the range between suspension (100-1000  $\mu\text{m}$ ) and emulsion (0.01-0.1  $\mu\text{m}$ ). Normal suspension polymerization is a reaction in bulk; the initiator is soluble in the monomer droplets, which are stabilized in the aqueous phase by a surface active agent. In emulsion

polymerization, on the other hand, the initiator is usually water soluble and the radicals are formed in the aqueous phase. These radicals enter a monomer-swollen emulsifier micelle and polymerize the solubilized monomer. [27]

## 2.2.1 Suspension Polymerization [18 ; 28]

### 2.2.1.1 Components in Suspension Polymerization

In a typical suspension polymerization system, one or more water-insoluble monomers containing oil-soluble initiator (s) are dispersed in the continuous aqueous phase by a combination of strong stirring and the use of small amounts of suspending agents (stabilizers). Suitable conditions of mechanical agitation are maintained while the monomer droplets are slowly converted from a highly mobile liquid state, through a sticky syrup-like dispersion (conversion 20-60%), to hard solid polymer particles (beads or resins) (conversion 70%). Schematic representation of suspension polymerization is shown in Figure 2.5.

สถาบันวิทยบริการ  
จุฬาลงกรณ์มหาวิทยาลัย



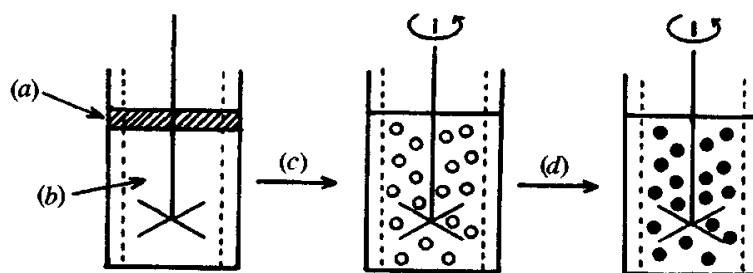


Figure 2.5 Schematic representation of suspension polymerization (a) organic comonomer mixture containing dissolved initiator; (b) aqueous continuous phase containing dissolved polymeric suspension stabilizer; (c) shearing to form comonomer liquid droplets; (d) thermal polymerization to form solid polymer resin beads.

The stabilizers hinder the coalescence of the monomer droplets first, and later stabilize the polymer beads whose tendency to agglomerate may become critical when the polymerization has advanced to the point where the polymer beads become sticky.

#### 2.2.1.2 Particle Formation [28-29]

Particle size, particle size distribution, and particle morphology affect the polymer's handling, storage, processing, and application characteristics. The particle formation mechanisms can be divided into three stages.

1. In first stage, a liquid-liquid dispersion exists; the liquid monomer is dispersed in the form of small droplets, stabilized by combined actions of the rotating stirrer and the suspending agents.



2. In second stage, a break-up-coalescence dynamic equilibrium of monomer-polymer droplets seems to determine the final particle size. The viscosity of the droplets increases with increasing the conversion. The droplets break up by the impeller shear stress and coalesce back after collision with each other. The collision of the droplets is shown in Figure 2.6.

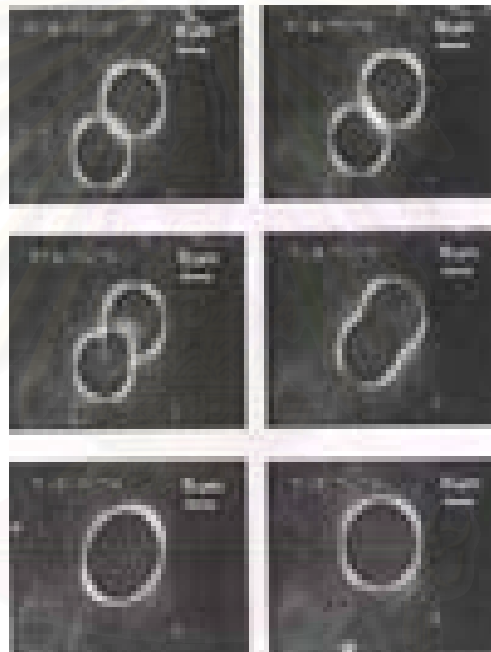


Figure 2.6 Collision of polyisobutylene droplets.

3. In third stage, the polymer particles are solid and they do not stick any more. After this point, the viscosity of polymer particles is too high, so they cannot be broken up, and their diameter remains constant.

### 2.2.1.3 Morphology [29]

Morphology of styrene-divinylbenzene particle is divided in two types as following.

#### 1. Gel-type resins

When the comonomer mixture in a suspension polymerization consists only of styrene and divinylbenzene (plus the polymerization initiator), the product generally consists of hard glassy transparent resin beads. The percentage of divinylbenzene can be varied in principle from 0-100% but typically for most resin applications the range 0.5-20% is more usual. The resin have very low surface area in the dry state. The diffusion of even small molecules through this polymeric glass is very slow.

#### 2. Macroporous resins

Macroporous resin is used to indicate a class of resins which have a permanent well developed porous structure even in the dry state. If a suspension polymerization of a styrene-divinylbenzene mixture is carried out with the comonomer mixture also containing an appropriate organic solvent (dilute or porogen) at some appropriate level then the internal structure (morphology) of the product resin beads can be very different to that of a gel-type resin. In particular, removal of the solvent or porogen at the end of the polymerization can leave resin beads which are hard but opaque and with a rough surface. The polymer matrix is rather heterogeneous or non-uniform. These materials can have much higher surface areas in the dry state than gel-type resins. Porous morphology in a macroporous resin is shown in Figure 2.7.

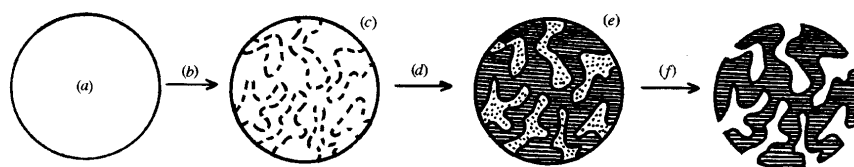


Figure 2.7 Action of porogen in forming porous morphology in a macroporous resin: (a) monomer, crosslinker and porogen isotropic solution; (b) polymerization; (c) polymer network forming; (d) porogen and network start to phase separate; (e) porogen phase acts as pore template; (f) porogen phase removal to yield pores (hatched area = crosslinked polymer; dots = porous phase).

#### 2.2.1.4 Synthesis of Polymer Bead by Suspension Polymerization

##### 2.2.1.4.1 Gel Type

Balakrishnan et.al. [30] studied the effects of surfactant on particle size distribution in suspension copolymerization of styrene. The polymerization contained 2% divinylbenzene and 25% vinylbenzyl chloride by weight using 165 g styrene and 0.5 wt% AIBN at a stirring speed of 300 rpm with gelatin and poly(diallyldimethyl ammonium chloride) as suspension stabilizers. The mixture is stirred and heated at 70°C for 60 min. The effects of nonionic surfactant (Triton X-100) and anionic surfactant (sodium dodecylbenzene sulfonate; SDBS) was shown in Table 2.2.

The nonionic Triton X-100 has no major effect, but the anionic sodium dodecylbenzene sulfonate at or below its critical micelle concentration in water ( $1.1 \times 10^{-3}$  M) causes the formation of a large fraction of particles smaller than  $74 \mu\text{m}$  (200 mesh) and prevents the formation of particle larger than  $250 \mu\text{m}$  (60 mesh)

Table 2.2 Effect of Surfactants on Particle Size Distribution

| Surfactant concentration<br>(M)     | Wt. of product<br>(g) | % polymer on mesh sieve size |     |     |     |     |
|-------------------------------------|-----------------------|------------------------------|-----|-----|-----|-----|
|                                     |                       | 60                           | 100 | 200 | 325 | 400 |
| none                                | 139                   | 29                           | 60  | 11  | 0   | 0   |
| Triton X-100, $1.20 \times 10^{-4}$ | not determine         | 10                           | 60  | 25  | 5   | 5   |
| SDBS, $1.10 \times 10^{-3}$         | 90                    | 0                            | 17  | 44  | 17  | 11  |
| SDBS, $5.50 \times 10^{-4}$         | 111                   | 0                            | 28  | 36  | 13  | 5   |
| SDBS, $2.75 \times 10^{-4}$         | 107                   | 0                            | 12  | 56  | 17  | 6   |

Poly (methyl methacrylate) particles ranging in diameter from 2 to  $10 \mu\text{m}$  were prepared by dispersion polymerization. The effect of cationic co-stabilizer (methyl tricaprylyl ammonium chloride; Aliquat 336) was studied. Aliquat 336 were added as solution in methanol, with concentration of 0.0-4.8 wt% base on recipe (25g). The result was shown in Figure 2.8.

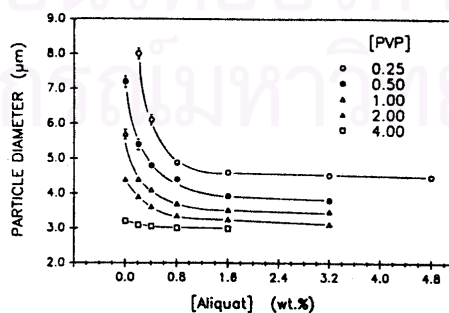


Figure 2.8 Effect of Aliquat 336 co-stabilizer concentration on PMMA particle size with different concentrations of poly(vinyl pyrrolidone) (PVP K-30).

The particle size decreased with increasing concentration of Aliquat 336 and then leveled off. The influence of the co-stabilizer was strong for the lower concentration of poly(vinyl pyrrolidone) (as the stabilizer). At a PVP K-30 concentration lower than 2 wt%, monodisperse particles could not be obtained without co-stabilizer. The addition of Aliquat 336 not only decreased the particle size, but also improved the monodispersity. On the other hand, with a PVP K-30 concentration of 4 wt%, monodisperse particles could be obtained without co-stabilizer, and the addition of Aliquat 336 only reduced the particle size slightly. [31]

Particles of methyl methacrylate (MMA) and glycidyl methacrylate (GMA) copolymer were prepared by the method of dispersion polymerization. Prior to polymerization, MMA, GMA and *N,N*-methylenebismethacrylamide were mixed with methanol in a 250 ml flask to form a solution of monomer. A mixture of initiator (AIBN), steric stabilizer (PVP), cetyl alcohol and methanol was added to the solution of monomers. The mixture was polymerized at 55°C for 48 h.

The addition of 0.5 wt% cetyl alcohol led to an increase in particle size and a more spherical shape. When the mass ratio of GMA to MMA was 0.1, for example, the particle size increases from 2.7 to 3.9  $\mu\text{m}$  in the presence of cetyl alcohol. The reason could be that cetyl alcohol could associate with PVP, and hence retard the adsorption rate of PVP onto the nuclei, consequently resulting in an increased final particle size.

[32]

Cetyl alcohol has been used as the co-stabilizer to improve the monodispersity of particles in the dispersion polymerization of styrene by Tserg et.al . [24] Their result also indicate that the nonionic cetyl alcohol as the co-stabilizer leads to a larger particle size in comparison with anionic surfactant Aerosol OT.

Carlos et.al. [33] studied the influence of the stirring rate on the final mean particle size in suspension copolymerization of methyl methacrylate-styrene. The result is shown in Figure 2.9.

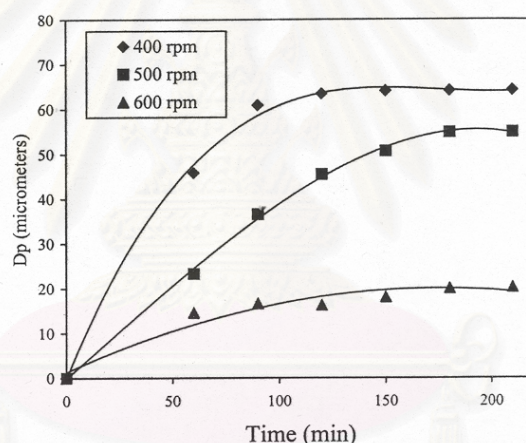


Figure 2.9 Evolution of number average diameter of droplets during the polymerization for different stirring rates.

The particle size increases as the reaction progresses, until reaching a certain maximum value. The final value is between 180 and 210 min from the beginning of the experiment. The higher the agitation rate, the lower the particle size is attained with time.

Jyongrik and Beom-Seok [34] prepared crosslinked styrene-alkyl acrylate copolymers for oil absorbency application. Suspension polymerization was carried out using benzoyl peroxide as an initiator. Crosslinked copolymers were synthesized by adding divinyl benzene (DVB) as a crosslinking agent. The effect of DVB on glass transition temperature was shown in Figure 2.10.

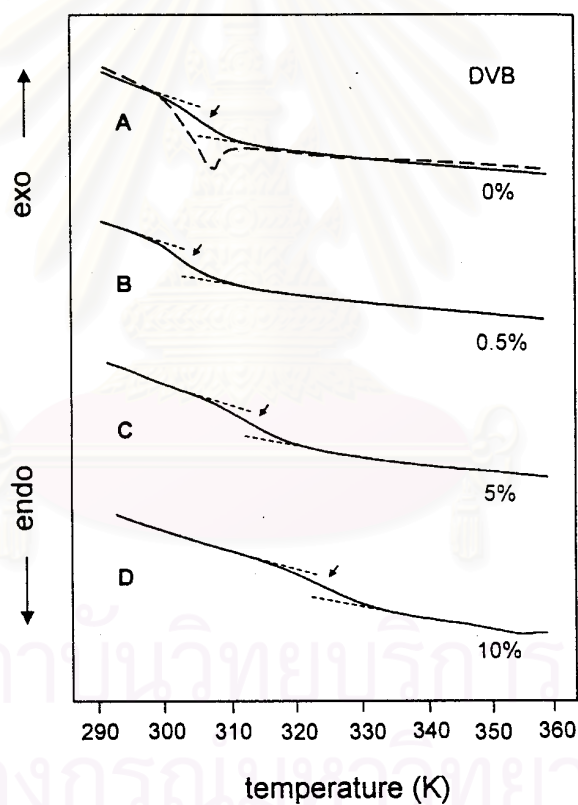


Figure 2.10 DSC thermograms of styrene/lauryl acrylate = 80/20 copolymer with different crosslinking densities: (----) first run; (—) second run; (A) control; (B) 0.5 wt% DVB; (C) 5 wt% DVB; (D) 10 wt% DVB.

The change in glass transition temperature depends upon the degree of crosslinking. At a low degree of crosslinking (0.5 wt% DVB), the  $T_g$  of the crosslinked copolymers was lower than or similar to that of the uncrosslinked ones. At a high degree of crosslinking, the  $T_g$  increased with increasing crosslinking density.

#### 2.2.1.4.2 Macroporous Resin

The main interest in macroporous exchanger is due to the performance of these resins being better than that of conventional gel-type materials mainly with respect to thermal stability and exchange kinetics. The proper pore size can be achieved by using mixtures of good and bad solvents. The increasing of the good solvent proportion in the diluent mixture reduces the pore size and the total porosity. [9]

Carelinho and Lima [35] studied the influence of diluents on the formation of porous structure in ion exchanger resins based on 2-vinylpyridine and divinylbenzene, by suspension polymerization. Ion-exchange resins were synthesized in the presence of *n*-heptane and diethyl phthalate as diluents. It was found that only in the presence of *n*-heptane, porous resins were produced.

Li et.al. [36] prepared polystyrene for size exclusion chromatography. The macroporous resins were prepared by suspension polymerization. For a typical preparation, 50 g of 4-methylstyrene and 50 g of 1,2-bis (*p*-vinyl phenyl) ethane with AIBN (3.4 wt% relative to monomer) as an initiator and porogen (dodecanol/toluene;



porogen: monomer = 1.4 : 1 v/v) were dispersed in water phase. The reactor was stirred at 500 rpm for 2 h at 40°C under nitrogen atmosphere, followed by polymerization at 250 rpm and 70°C for 24 h. The results was shown in Table 2.3 and Figure 2.11.

The surface porosity is seen to increase with the percentage of nonsolvent (dodecanol) in the porogen mixture. At a dodecanol percentage of 50% and above, the resin shows a cauliflower-like surface morphology.

Table 2.3 Porosity Data from Nitrogen Adsorption Analysis

| Dodecanol/toluene(nonsolvent/solvent) | Total pore volume (ml/g) | Surface area (m <sup>2</sup> /g) |
|---------------------------------------|--------------------------|----------------------------------|
| 0/100                                 | 0.005                    | 1.9                              |
| 30/70                                 | 0.025                    | 9.0                              |
| 40/60                                 | 0.370                    | 92.2                             |
| 50/50                                 | 0.726                    | 88.8                             |
| 60/40                                 | 0.342                    | 46.7                             |

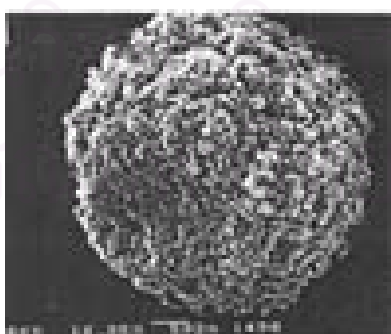


Figure 2.11 Scanning electron micrographs of resin beads at dodecanol/toluene = 50/50 (magnification 500X).

### 2.2.2 Emulsion Polymerization

There have been several reports describing the preparation of monodisperse polymer microspheres. These studies were concerned with synthetic methods involving emulsion and soap-free polymerizations.

Emulsifier-free emulsion copolymerization of styrene with two different amino-containing cationic monomers by using 2,2'-azobis(2-amidinopropane) dihydrochloride as an initiator was studied. It was found that the particle size decreased upon increasing the ionic monomer concentration. The presence of very small amounts of functional monomer strongly affected the particle size because of the electrostatic stabilization conferred by the cationic groups to the growing particles. The incorporation of a part of functional monomer in the particles by copolymerization can occur during the nucleation step, where copolymerization of styrene with the comonomer takes place in water phase. Furthermore, the synthesis of cationic hydrophobic particle (polystyrene), upon using an ionic monomer in the polymerization, led to the formation of a population of small polymer chains that mainly located at the outer shell of the particle during and after particle growth [37].

Zuifang et.al. [21] studied the synthesis of cationic polymer particle by emulsifier-free emulsion copolymerization of styrene with quaternary ammonium cationic monomers. The presence of the ionic monomeric repeating units along the copolymer chains could make the mechanism for particle formation more complicated. Firstly, the

incorporation of ionic monomer into the growing oligomeric radicals must have an influence on nucleation process. The nucleation only occurs when a certain molar fraction of the styrene has been incorporated into the copolymer chains. Secondly, the presence of the ionic monomeric repeating units at particle surfaces must contribute to particle-electrostatic stabilization. Final particle size normally decreases with increasing ionic monomer concentration in a certain range.

The presence of more ionic groups at particle surfaces certainly enhances the electrostatic repulsion forces between the particles and hence, the coagulation of primary particles would be restricted. Furthermore, if the particle surface-charge density is high enough, the electrostatic layer at the particle surface could prevent likely charged primary free radicals (generated in aqueous phase) from entering. As a result, the polymerization of styrene inside the particles could be also restricted .

The polymer microspheres were synthesized by emulsion copolymerization of styrene with vinyl benzyl terminated poly(methacrylic acid) (PMA) macromonomer in an aqueous ethanol solution. In these copolymerization system, the macromonomer acted not only as a comonomer but also as a stabilizer. The particle diameters obtained from water-soluble initiator system showed smaller values than those obtained from water-insoluble initiator system.

The copolymerization mechanism for both systems could be explained as follows. The copolymerization in AIBN system was a heterogeneous process in which a

water-insoluble styrene was dispersed in ethanol/water in the form of droplets. The droplets were stabilized with PMA macromonomers. Polymerization was initiated by means of a monomer-soluble initiator (AIBN) so that the locus of polymerization was in the individual droplets. The whole process may therefore be viewed as being made up of many separate bulk polymerizations. As polymerization proceeded, the polystyrene particles continued to grow. At final stage of the polymerization, polystyryl radicals were terminated with a combination process.

The copolymerization in  $K_2S_2O_8$  system was also a heterogeneous process. Water-soluble initiator ( $K_2S_2O_8$ ) was used so that the initial locus of polymerization was in aqueous phase. The polymer was formed as a latex of polystyrene particles stabilized by PMA macromonomers. Reaction of primary radicals with monomer molecules present in aqueous phase produced short-chain radicals that were captured by the emulsified monomer droplets. The propagation of polystyryl radicals proceeded with a living radical-like mechanism. As polymerization proceeded, the latex particles continued to grow. The surface areas were stabilized with not only PMA macromonomers but also with sulfate ions. Therefore, the particle sizes were smaller than those obtained in AIBN system. [38]

## 2.2.3 The Role of Surfactants

### 2.2.3.1 The Stability of Dispersion

The use of both polymers and lower molecular weight surface-active species to stabilize dispersion is widely practiced. Friberg et.al. [39] interpreted the experimental evidence that interfacial layer containing the surfactant and water have a marked effect on dispersion stability by suggesting that the droplets would exhibit a reduced attraction potential energy owing to the fact that each droplet is surrounded by a layer of surfactant phase. Likewise, these authors have considered the changes in hydrodynamic interactions in droplet region, which affects the aggregation kinetics, and would thus affect observed coalescence rates.

The classes of materials constitute which are used as stabilizers [40].

#### 1. Electrolytes

The action of electrolytes is to impart a weak electrical double layer that retards the close approach, and thus coalescence, of individual drop in the dispersion phase.

#### 2. Polymeric materials

By proper choice of chemical composition, such materials can be made to adsorb at the interface between the continuous and dispersed phases. By their presence, such materials can reduce the energetic driving force to coalescence by lowering the interfacial tension and/or forming a mechanical barrier between drops.

Polymers can form at the interface that retards the approach and coalescence of individual droplets. The polymeric nature of the materials means that each molecule can be strongly adsorbed at many sites on the interface. As a result, the chance of desorption is greatly reduced or effectively eliminated.

### 3. Solid particles

It has been known for sometimes that the particles of colloidal dimensions (less than 1  $\mu\text{m}$  in diameter, for example) that are wetted by both aqueous and organic liquids can form stabilizing films and produce both oil-in-water and water-in-oil emulsions with significant stability. Stabilization by solid particle relies upon the specific location of the particles at the interface to produce a strong, rigid barrier that prevents or inhibits the coalescence of droplets. It may also impart a degree of electrostatic repulsion that enhance the overall stabilizing power of the system.

### 4. Surfactant

The last major class is the surfactants that adsorb at the interfaces and produce electrical, mechanical, and steric barrier to drop coalescence, in addition to their role in lowering the interfacial free energy between the dispersed and continuous phases. Various possible mechanisms of droplet stabilization is shown in Figure 2.12.

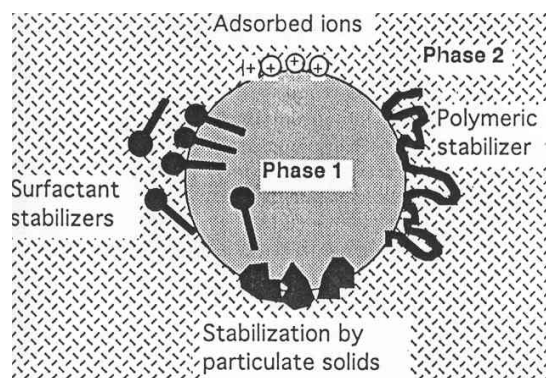


Figure 2.12 Various possible mechanisms of droplet stabilization.

Several investigations have demonstrated that surfactant concentration can influence stability. At low surfactant concentration, the major instability is due to flocculation of the oil droplets. The upper concentration is also well define, with one of two types of instability being observed. The first type of instability occurring with more water-soluble surfactants, is a rapid flocculation and creaming without any accompanying separation of free oil. The second type of instability occurs with more oil-soluble surfactants and is an extremely rapid coalescence with separation of free oil.

#### 2.2.3.2 The Polymer-Surfactant Interactions [40]

The force controlling surfactant interaction with polymers are identical to those involved in other solution or interfacial properties, namely Van der Waals or dispersion forces, the hydrophobic effect, dipolar and acid-base interactions, and electrostatic interactions. The relative importance of each type of interaction will vary with the natures of the polymer and the surfactant.



In the case of surfactants, four general types of polymers can be defined related to the electronic nature of the species: anionic, cationic, nonionic, and amphoteric. Each polymer type will exhibit characteristic interactions with each surfactant class, with variation occurring within each group.

#### 1. Nonionic polymers

The primary driving force for surfactant-polymer interaction will be Van der Waals forces and the hydrophobic effect. Dipolar and acid-base interactions may be present, depending upon the exact nature of the system. Ionic interactions will be minimal or nonexistent. For the polymer, it is reasonable to infer that the importance of the hydrophobic effect will be related to the ability of the polymer to undergo hydrogen bonding with the solvent (water), as well as the relative availability of nonpolar binding sites along the polymer chain.

The interaction between ionic surfactant/nonionic polymer is hydrophobic. The work on cationic surfactant/nonionic polymer interaction has utilized long-chain alkylammonium surfactants. It has been found that the interaction between such species becomes stronger as the chain length of the surfactant increases, reflecting the greater drive to substitute surfactant/polymer for surfactant/water and polymer/water interactions.

The relative binding strengths between nonionic polymers and cationic or anionic surfactants are difficult to compare. The general trends are that with a given



polymer, anionic will exhibit stronger interactions than analogous cationic surfactants, all other things being equal.

The interactions between nonionic surfactants and nonionic polymers has been much less intensively studied than those for ionic surfactants. A nonionic surfactant bound to a strongly hydrophobic polymer.

## 2. Ionic polymers

For interactions between ionic polymers (polyelectrolytes) and surfactants with those for nonionic polymers, it is obvious that the presence of discrete electrical charges along the polymer backbone introduces the possibility (and probability) of Coulombic interaction, in addition to the nonionic factors.

Interactions between surfactants and polymers of similar charge are usually minimal, with electrostatic repulsion serving to inhibit the effectiveness of any non-Coulombic attractions. This is especially true for polymers having relatively high charge densities along the chain. When opposite charges are present, however, the expected high degree of interaction is usually found to occur.

### 2.2.3.3 Surfactant Adsorption and The Nature of Solid Surface

The nature of the solid surface involving in the adsorption process is a major factor affecting the manner and the extent of surfactant adsorption.

Adsorption of surfactant onto nonpolar surface is primarily by dispersion force interactions. From aqueous solution, it is obvious that an orientation of the adsorbed molecules will be such that the hydrophobic groups are associated with the solid surface with the hydrophilic group directed toward the aqueous phase. Holloway reported that nonionic surfactant was adsorbed on the beads of polystyrene divinylbenzene matrix. [41]

The potential forces operating at a polar surface include the ever-present dispersion forces, dipolar interactions and hydrogen bonding and the acid-base interactions. The relative balance between the dispersion forces and the uniquely polar interactions is important in determining the mode of surfactant adsorption. If the dispersion forces predominate, for example, adsorption will occur in a manner essentially equivalent to that for the nonpolar surfaces. If, on the other hand, polar interactions dominate, adsorption may occur in a reverse mode; that is, the surfactant molecule will be oriented with the hydrophilic head group at the solid surface and the hydrophobic group set toward the aqueous phase.

#### 2.2.4 Application of Polymer Bead

Applications of poly(styrene-divinylbenzene) particle are as the stationary phase for size exclusion and ion-exchange chromatography and the catalytic support.

## 1. Separation media for chromatography

Marina et.al. [42] studied effect of divinylbenzene content on the porous and chromatographic properties of poly(styrene-co-divinylbenzene) beads. The beads prepared from a mixture containing more crosslinking monomer have better mechanical stability, and columns packed with these beads exhibit better flow properties and higher separation efficiencies.

Ching Wang et.al. [43] prepared macroporous poly(styrene-co-divinylbenzene) beads for separation media. Protein separation were performed in the reversed-phase mode on a 30X4.6 mm i.d. column with a solvent gradient from 20 to 60 vol% acetonitrile in water containing 0.1vol% trifluoroacetic acid.

The use of high flow rates is advantageous as it accelerates the separation of protein decreasing the analysis times while preserving the resolution power.

## 2. Oil absorbency

Jyongrik and Beom-Seok [34] prepared crosslinked styrene-alkyl acrylate copolymers for oil absorbency. Suspension polymerization was carried out using benzoyl peroxide as an initiator with varying monomer feed ratio. At low concentration of acrylate, most of the sample beads remained, not dissolving in oil (kerosene oil) due to the lack of acrylate units with oil affinity. With increasing the concentration of acrylate, the copolymer included more portions of the acrylate units. The mixture resulted in a clear solution with small amounts of beads swollen. At high concentration of acrylate,

however, the copolymer was fully swollen in oil without dissolving.

### 3. Polymer Sorbents [44]

It is well known that the sorbents containing hydrazide, amidooxyme, and carboxylic groups have high complex-forming capability.

Porous sorbents of acrylonitrile copolymer were prepared from the solution of 15% copolymer of acrylonitrile-methylmethacrylate-2-acrylamido methylpropensulfonic acid in dimethylformamide at 60°C under continuous stirring in water bath. Then, 1% LiNO<sub>3</sub> and 3% glycerine were added to the polymer solution. The homogenized mixture was pipetted at constant volume rate into distilled water. The granules obtained were porous. The sorbent obtained was modified with hydroxylamine, sodium hydroxide, and hydrazine hydrochloride under optimal condition to obtain amidooxyme, carboxylic acid, and hydrazide groups. The results showed high ability to form complexes with Pb(II) and Cu(II) ions. The polymer sorbents reached maximum adsorption capacity of 0.29 and 0.90 mg eq/g for Pb(II) and Cu(II) ions respectively.

### 4. Cation exchange resin

Ogawa et.al. [45] prepared copolymer beads of maleic anhydride (MA)-styrene (ST)-divinylbenzene (DVB). A mixture of 84 g of MA, 36 ml of ST, 36 ml of DVB, 62 ml of benzene, 62 ml of dioxane, and 3.2 g of benzoyl peroxide were added to a suspending medium of 540 ml of glycerol containing hydroxyethyl cellulose (1.1 g) and sodium

chloride (27 g). The polymerization was carried out at 70°C for 2 h. About 60 g of white spherical bead (35-60 mesh) were obtained. After that the resin was refluxed with 100 ml of 2 N sodium hydroxide and then washed with 2 N hydrochloric acid and water and dried. The beads obtained seemed to be useful as a starting material for ion exchange or chelating resin.

## 2.3 Ion Exchange

### 2.3.1 Structure and Components of Ion Exchange

Ion exchange, by common definition, are insoluble solid materials which carry exchangeable cations or anions. Ion exchangers consist of a framework carrying a positive or negative electric surplus charge which is compensated by mobile counter ions of opposite sign [46]. The structure of ion exchange is shown in Figure 2.13

สถาบันวิทยบริการ  
จุฬาลงกรณ์มหาวิทยาลัย

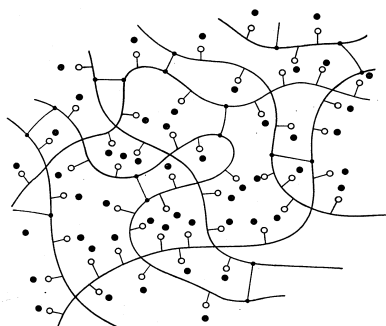
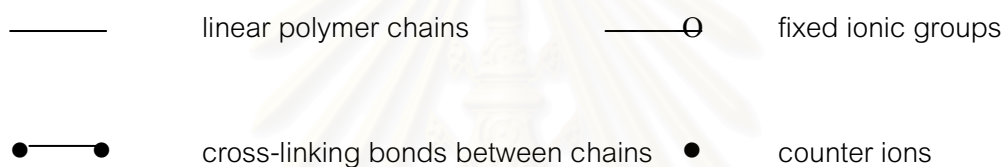


Figure 2.13 Schematic representation of a modern ion exchange resin. The structure is based upon a random three-dimensional structure of linear polymer chain which are cross-linked at intervals along their length .



The counter ions, are free to move through the matrix (fixed ion) by diffusion or under electrical field and may be replaced by other counter ions (same sign) from solution, in the process of ion exchange. The material is a cation or an anion exchanger according to the counter ions are cations or anion, respectively. The situation is summarized in Table 2.4.

Table 2.4 Component in Ion Exchange [46]

| Exchanger type   | Fixed charge | Counter ion | Co-ion     |
|------------------|--------------|-------------|------------|
| cation exchanger | anion (-)    | cation (+)  | anion (-)  |
| anion exchanger  | cation (+)   | anion (-)   | cation (+) |

Ions of the same sign as the fixed charge are known as co-ions, both in solution and when present within the exchanger pores. The co-ions will, however, affect the equilibrium if they form complexes or ion pairs with one or other of the counter ions in the solution, effectively reducing the concentration of that free ion and so its uptake into the exchanger.

Ion exchange resembles sorption in that, in both cases, a dissolved species is taken up by a solid. The characteristic difference between the two phenomena is that ion exchange, in contrast to sorption, is a stoichiometric process. Every ion which is removed from the solution is replaced by an equivalent amount of another ionic species of the same sign. In sorption, on the other hand, a solute (an electrolyte or nonelectrolyte) is taken up without being replaced by another species. Schematic of ion exchange with a solution is shown in Figure 2.14.

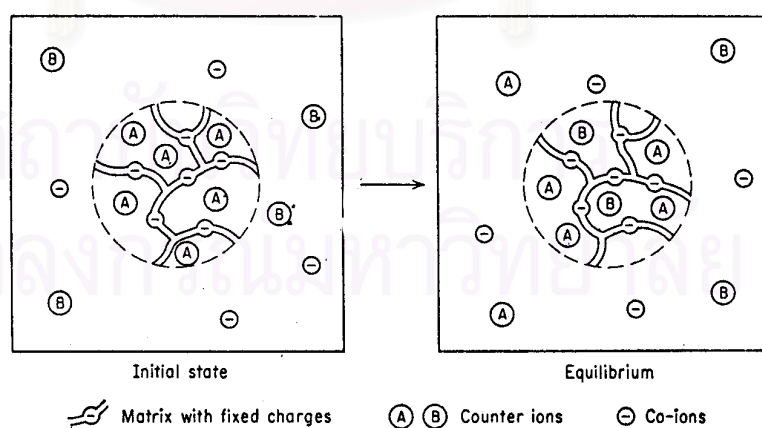


Figure 2.14 Ion exchange with a solution [47].

A cation exchanger containing counter ions A is placed in a solution containing counter ions B (left). The counter ions are redistributed by diffusion until equilibrium is attained (right)

### 2.3.2 Organic Resin Exchangers

The majority of these exchangers are based upon a matrix of cross-linked polystyrene. Upon this chemically and physically robust structure a very wide range of functional groups may be bound, each corresponding to a new type of exchanger. By a pearl copolymerization process it is possible to obtain almost completely spherical beads in a wide range of particle sizes according to requirements.

#### 2.3.2.1 Styrenic Anion Exchange Resins [46]

Anionic exchange resins are usually based on an amine or ammonium grouping as a source of positive fixed charge. Strong base exchangers are based upon quaternary ammonium groups ( $-NR_3^+$ ), where R may be a methyl, ethyl or other organic substituents. The polystyrene-divinylbenzene copolymer has proved to be the most usual matrix. The beads are chloromethylated and subsequently treated with ammonia or primary, secondary or tertiary alkyl amine.



### 2.3.2.2 Styrenic Cation Exchange Resins [48]

The copolymer of styrene and divinylbenzene is carried out by sulfonation of the matrix with hot sulfuric acid thereby introducing the sulfonic acid functional group giving a strongly acidic cation exchange resin.

## 2.4 Adsorption Isotherm

The relation, at constant temperature, between the amount adsorbed on the bead and the equilibrium pressure, or concentration of the fluid, is known as the adsorption isotherm.

### 2.4.1 Types of Adsorption Isotherm

The distribution of dye between the adsorbent and the solution, at equilibrium, has been expressed using various equations. Two widely used forms are the Langmuir and Freundlich isotherm.

#### 1. Langmuir Isotherm [49]

The Langmuir isotherm is valid for monolayer adsorption on a surface containing a finite number of identical site. Langmuir isotherm can be expressed as

$$C_e/q_e = 1/Q_0b + C_e/Q_0$$

$Q_0$  = maximum amount of adsorbate per gram of adsorbent (mg/g)

$b$  = Langmuir constant (l/mg)

= adsorption coefficient

$C_e$  = equilibrium concentration of dye in solution (mg/l)

$q_e$  = milligrams of dye adsorbed per gram of adsorbent at equilibrium (mg/g)

A plot of  $C_e/q_e$  versus  $C_e$  should yield a straight line having a slope  $1/Q_0$  and an intercept of  $1/Q_0b$  from which the value of  $Q_0$  and  $b$  may be readily obtained.

Figure 2.15 showed the plot of  $C_e/q_e$  versus  $C_e$  for the adsorption of three direct dyes on polyamide-epichlorohydrin-cellulose at 30°C. The results showed that the adsorption followed Langmuir isotherm. [51]

สถาบันวิทยบริการ  
จุฬาลงกรณ์มหาวิทยาลัย

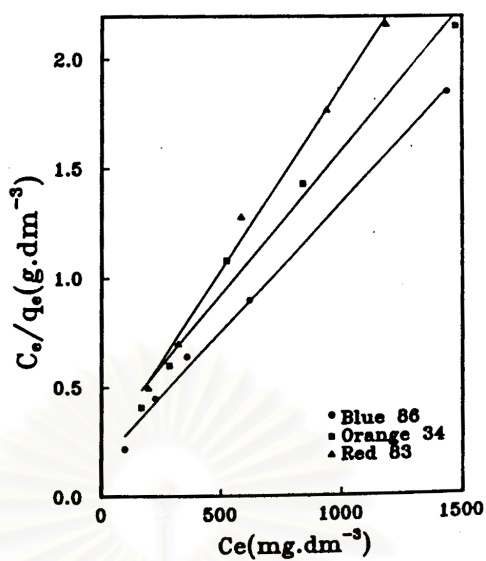


Figure 2.15 Langmuir plot for the removal of the three direct dyes.

## 2. Freundlich Isotherm [49]

The Freundlich equation is used for heterogeneous surface (rough surface).

The Freundlich equation has the general form

$$\log q_e = \log k + \frac{1}{n} \log C_e$$

$$q_e = (C_o - C_e) V / W$$

$C_o$  = initial dye concentration (mg/g)

$C_e$  = equilibrium concentration of dye in solution (mg/l)

$V$  = volume of dye solution

$W$  = the amount of adsorbent required to adsorb dye (g)

$q_e$  = milligrams of dye adsorbed per gram of adsorbent at equilibrium

(mg/g)

- k = indicator of adsorption capacity  
 = constant in Freundlich isotherm (l/g)
- n = Freundlich exponent

The values of  $k$  and  $1/n$  are equal to the intercept and slope of the straight line, respectively. For favorably adsorbed chemical,  $1/n$  is between 0 and 1. For unfavorably adsorbed chemicals,  $1/n$  is greater than 1. For chemicals that are not adsorbed,  $1/n$  approaches infinity (or very large). The magnitude of the exponent  $n$  give an indication of the favorability and capacity of the adsorbent/adsorbate system. Value of  $n > 1$  represents favorable adsorption conditions according to the theories.

Linear plot of  $\log q_e$  versus  $\log C_e$  shows that adsorption follows Freundlich isotherm. Figure 2.16 shows typical Freundlich plots for the adsorption of  $\text{Cu}^{2+}$  on modified cellulose adsorbent. [50]

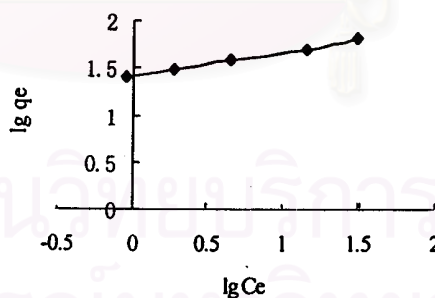


Figure 2.16 A Freundlich plot for the adsorption of  $\text{Cu}^{2+}$  on modified cellulose at pH 5.0 and  $10^\circ\text{C}$  with  $63.5 \text{ mg/l Cu}^{2+}$ .

The Freundlich adsorption equation was as follow:

$$\log q_e = 1.4094 + 0.2672 \log C_e$$

Where  $k = 25.67$  and  $1/n = 0.2672$ . The results show that the adsorption has a high adsorption capacity, and the adsorption of  $\text{Cu}^{2+}$  ion on adsorbent is feasible ( $1/n = 0.2672$ ).

#### 2.4.2 Adsorption Isotherms in Solid-Liquid Systems [40]

Giles et.al. examined several liquid adsorption isotherms and classified them into four categories with subdivision for each type as shown in Figure 2.17. The main classification is based on the initial slope of the isotherm, and the sub-classification on the shape at higher concentration.

The L class is of the so-called Langmuir type. This class is the most common and is identified by having its initial region (L1) convex to the concentration axis. As the concentration of adsorbate increases, the isotherm may reach a plateau (L2), followed by a reaction convex to the concentration axis (L3). If the L3 region attains a second plateau, the region is designated L4. Under some circumstance, a maximum may be obtained (L5).

The S class of isotherms, the initial slope is concave to the concentration axis (S1) and is often broken by a point of inflection (S2) leading to the characteristic S

shape (S3). Further concentration increases may then parallel those of the L class, including the presence of a maximum. The S class is obtained if (i) the solvent is strongly adsorbed, (ii) there is strong inter-molecular attraction within the adsorbed layer, (iii) the adsorbent is macro-functional.

The H class occurs where there is high affinity between the adsorbate and adsorbent which is shown even in very dilute solutions. Thus it can result from chemisorption or from the adsorption of polymers or ionic micelles. Higher concentrations lead to similar changes to those found in the L and S classes.

The final type of isotherm is the C class. This class indicates constant partition of the adsorbate between the solution and the adsorbent. It appears mainly with textile fibers, into which the solute penetrates to further extents as its concentration in the solution is increased.

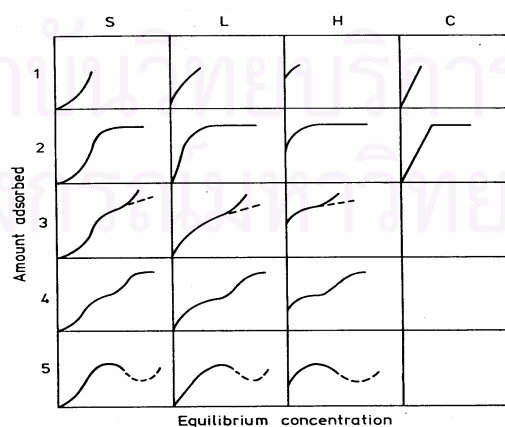


Figure 2.17 Classification of adsorption isotherm according to Giles et al. Letters indicate class and numbers indicate subgroup.

## 2.5 Parameters for Color Removal

### 2.5.1 Effect of Time

Ahmed and Ram [52] presented the removal of basic dye from wastewater using silica as adsorbent. The results indicated that the removal of dye initially increases with time, but attains an equilibrium within 30-40 min. Adsorption of the actual amount of dye increase with an increase in the concentration of the dye solution.

Walker and Weatherley [53] studied the kinetic of adsorption by using granular activated carbon as the adsorbent and acid dyestuff Tectilon Red 2B as the adsorbate. A fixed volume stirred tank reactor was used to study the kinetics of adsorption. Contact time experiments provide the kinetic data in the form of concentration decay ( $C_t / C_0$ ) VS. time curves. The results obtained are shown in Figure 2.18.

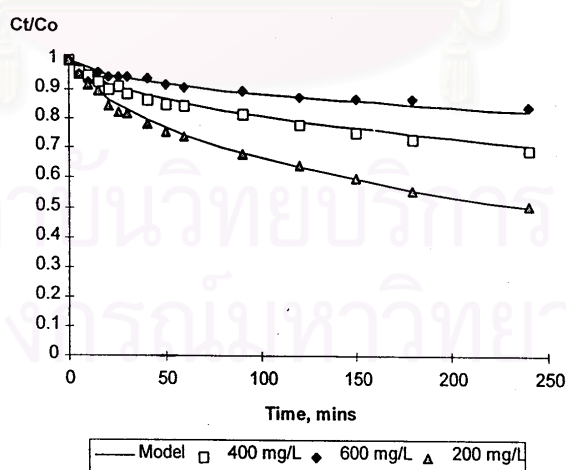


Figure 2.18 Effect of initial concentration of acid dye adsorption of TR 2B carbon mass = 1.7 g  $d_p = 355-500 \mu\text{m}$ , agitation time = 500 rpm.

It was apparent that the adsorption curves decayed with contact time.

The chemisorption is the likely process of acid dye adsorption on to activated carbon.

### 2.5.2 Effect of Salt

The removal of color from effluents using polyamide-epichlorohydrin-cellulose polyamide (PAE-Cell) was studied. The adsorbent used in this study was prepared by the reaction of adipic acid, diethylenetriamine, epichlorohydrin, and  $\alpha$ -cellulose. The effect of salt on dye adsorption was shown in Figure 2.19.

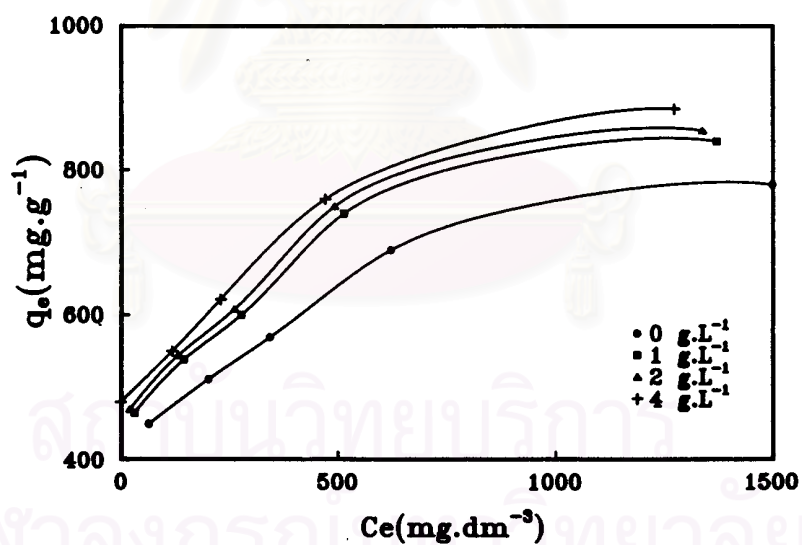


Figure 2.19 Effect of NaCl concentration on the equilibrium adsorption isotherm at 30°C of Direct Blue 86 on PAE-Cell.



The results showed that the affinity formed between Direct Blue 86 and PAE-Cell increased with the NaCl content. Hence, the adsorption capacity of PAE-Cell improve with the NaCl content in the dye bath. [54]

Morais et.al. [55] presented the reactive dye removal from wastewater by adsorption on eucalyptus bark. The effect of NaCl concentration and temperature were studied. It was observed that an increase in NaCl concentration caused an adsorption capacity to increase at  $\text{pH} \geq 2.00$  and to decrease at  $\text{pH} 1.00$ . For temperatures higher than room temperature, an adsorption capacity decreased with increasing the temperatures. The best value recorded for the adsorption capacity was about 90 mg of dye/g of dry bark. It was obtained at  $\text{pH} 2.50$  for a sodium chloride concentration of 50 g/l, an initial dye concentration equal to 500 ppm, a bark concentration equal to 2 g/l and at  $18^\circ\text{C}$ .

### 2.5.3 Effect of Temperature [54]

The temperature of a solution affects two major aspects of adsorption: the rate of diffusion of the adsorbate molecules through the solution to the adsorbent, and the solubility of the adsorbate and the swelling property of the adsorbent. The effect of temperature on the adsorption of dyes such as Direct Blue 86 and Acid Blue 158 on PAE-Cell is shown in Figure 2.20.

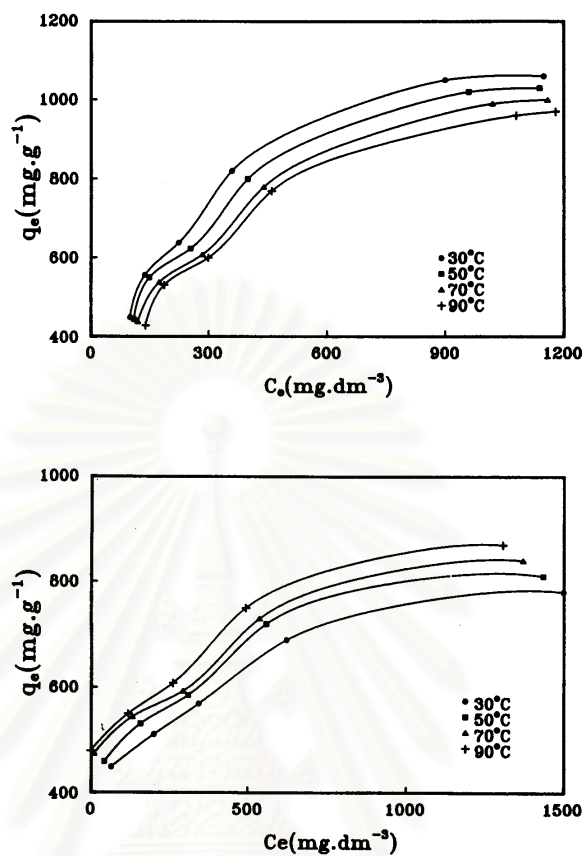


Figure 2.20 (a) Effect of temperature on the equilibrium adsorption isotherm on PAE-Cell for C.I. Acid Blue 158. (b) Effect of temperature on the equilibrium adsorption isotherm on PAE-Cell for C.I. Direct Blue 86.

The results show two completely different effects. For dyes such as Acid Blue 158, the adsorption capacity of PAE-Cell decreases with increasing temperature. This is possibly due to the exothermic effect from the surroundings during the adsorption process. On the other hand, the capacity of PAE-Cell for dyes such as Direct Blue 86 increases with the temperature. This phenomenon is possibly due to the endothermic

effect from the surroundings during the adsorption process. It may increase the mobility of the large dye ion, hence, increasing the rate of diffusion of the dye molecules through the solution to PAE-Cell.

#### 2.5.4 Effect of Particle Size

Joseph [56] prepared an ion exchange resin from sugarcane bagasse to remove reactive dye from wastewater. Bagasse was reacted with *N*-(3-chloro-2-hydroxypropyl) trimethyl ammoniumchloride and crosslinked with epichlorohydrin. A crosslinked, quaternized bagasse sample were milled.

The dye-adsorption kinetics of the bagasse-derived resin at 25°C were examined and found to vary greatly with resin particle size. Particles smaller than 75  $\mu\text{m}$  reached 95% of their maximal binding capacity within five minutes. Particles that were 75-100  $\mu\text{m}$  required 15 minutes to achieve 95% of their final dye capacity. Larger particles took progressively longer to equilibrate with dye.

The decrease in particle size of adsorbent increased the dye uptake and decreased the equilibrium time. [57]

## CHAPTER III

### EXPERIMENTAL

#### 3.1 Chemicals and Equipment

##### 3.1.1 Chemicals

All the following chemicals were used as purchased. The details of chemicals used in this thesis were shown in Table 3.1

Table 3.1 Chemicals used in this thesis

| Chemicals name   | Formula  | Source                           |
|--|--|----------------------------------|
| 2,2'-azobis (isobutyronitrile)<br>(AIBN)   | $(\text{CH}_3)_2\text{C}(\text{CN})-\text{N}=\text{N}-(\text{CN})\text{C}(\text{CH}_3)_2$                        | Siam Chemical<br>Industry Co,Ltd |
| benzoyl peroxide (BPO)   | $\text{C}_6\text{H}_5-\text{CO}-\text{O}-\text{O}-\text{CO}-\text{C}_6\text{H}_5$                                | Fluka                            |
| potassium persulfate (KPS)   | $\text{K}_2\text{S}_2\text{O}_8$   | M&B Laboratory<br>Chemical       |
| 3-(methacryloylamino) propyl<br>trimethyl ammonium chloride<br>(MAPTAC), 50 wt% solution | $\text{CH}_2=\text{CCH}_3-\text{CO}-\text{NH}(\text{CH}_2)_3-\text{N}^+(\text{CH}_3)_3\text{Cl}^-$<br>MW = 220.5 | Aldrich<br>Company               |
| styrene  | $\text{CH}_2=\text{CHC}_6\text{H}_5$   | Fluka                            |
| acetone  | $\text{CH}_3-\text{CO}-\text{CH}_3$  | P.P.M. Chemical                  |

Table 3.1 Chemicals used in this thesis (continued)

| Chemicals name                               | Formula   | Source                               |
|--|---|--------------------------------------|
| cetyl alcohol                                | $\text{CH}_3-(\text{CH}_2)_{14}-\text{CH}_2-\text{OH}$<br>MW = 242.4  | Union Chemical                       |
| divinylbenzene (DVB)                         | $\text{CH}_2=\text{CHC}_6\text{H}_4-\text{CH}=\text{CH}_2$            | Fluka                                |
| hexadecyltrimethylammonium<br>bromide (CTAB) | $\text{CH}_3-(\text{CH}_2)_{15}-\text{N}^+(\text{CH}_3)_3\text{Br}^-$ | Fluka                                |
| poly(vinyl alcohol) (PVA)<br>MW 115,000      | $[\text{CH}_2-\text{CH}-\text{OH}]_n$                                 | BDH Laboratory<br>Reagent            |
| sodium carbonate                             | $\text{Na}_2\text{CO}_3$  | APS Ajax Finechem                    |
| sodium chloride                              | $\text{NaCl}$   | BDH Laboratory<br>Reagent            |
| reactive dyes                                |   | Modern Dyestuff<br>& Pigment.,Co.Ltd |
| - C.I. Reactive Blue 171                     | Azo, monochlorotriazinyl  |                                      |
| - C.I. Reactive Red 195                      | Monoazo   |                                      |
| - C.I. Reactive Yellow 84                    | Azo, monochlorotriazinyl  |                                      |
| wetting agent (Tergitol NP-15)               | Nonylphenol Ethoxylate  | Union Carbide                        |

### 3.1.2 Equipment

1. Fourier-Transform Infrared Spectrometer, Omic Nicolet Impact 400 D
2. Gel Permeation Chromatography, PL-GPC 110
3. Laboratory Test Sieve (mesh number G-140), Endecotts Ltd London England
4. Rotary Dyeing Machine & Steel Pots, Ahiba AG CH-4127 (Ahiba Polymat)

5. Scanning Electron Microscope (SEM) equipped with X-ray microanalysis,  
Philip XL 30 CP
6. Ultraviolet Spectrophotometer, Specord S 100
7. Glasswares
  - beakers
  - condensers
  - cylinders
  - erlenmeyer flasks
  - three necked round bottom flasks
  - pipettes
  - stirring rod
  - volumetric flasks

### 3.2 Typical Synthesis of Poly (styrene-co-DVB) Beads Bearing Surface Charge

#### 3.2.1 General Procedure

Synthesis of poly (styrene-co-DVB) beads was conducted in two steps; the polymerization of MAPTAC in aqueous continuous phase and then surface functionalization of styrene and DVB droplets with the PMAPTAC radicals. Typical experimental was described as follows:

In first step, 90 ml of 0.1 wt% PVA aqueous solution was added into a 500 ml three-neck round bottomed flask which was immersed in a thermostat oil bath as a source of constant heat supplier. The reaction flask was equipped with a mechanical stirrer, a thermometer, a reflux condenser, and a nitrogen gas inlet tube. The suspending agent solution was preheated to desired temperature and kept constant for 30 minutes. MAPTAC and  $K_2S_2O_8$  initiator were well-mixed before adding into the reaction flask in which the suspending agent was stirred at a constant speed. The reaction was allowed to proceed for a determined time.

In second step, a mixture of styrene, DVB, surfactant, and AIBN initiator were added into the reaction flask and copolymerization reaction was continued for a period of set time. At the end of reaction the polymeric particles were formed. After that, the polymeric beads were filtered and washed with distilled water, and followed by acetone and then dried at room temperature. The product yield was calculated. The experimental conditions were varied as shown in Table 3.2.

In this experiment, various influencing parameters of polymerization, including polymerization time of MAPTAC, copolymerization time between styrene, DVB, and PMAPTAC radicals, polymerization temperature, agitation speed, amount of divinylbenzene, type and amount of surfactant, were studied.

Table 3.2 Experimental conditions

| Reagents and condition                                       | conditions  | wt% (based on styrene) |
|--|-------------|------------------------|
| MAPTAC   | 2.25 g      | 55.15                  |
| K <sub>2</sub> S <sub>2</sub> O <sub>8</sub>                 | 0.09 g      | 4.00*                  |
| 0.1 wt% PVA solution   | 90 ml       | -                      |
| polymerization time of MAPTAC                                | 15-45 min   | -                      |
| styrene  | 4.08 g      | -                      |
| DVB  | 0.46-1.84 g | 11.27-45.10            |
| surfactant   |             |                        |
| - cetyl alcohol  | 0-0.03 g    | 0-0.74                 |
| - CTAB   | 0-0.005 g   | 0-0.12                 |
| AIBN   | 0.10-0.13 g | 2.20**                 |
| polymerization time of styrene,<br>DVB, and PMAPTAC radicals | 1 –3 h      | -                      |
| polymerization temperature                                   | 60-80 °C    | -                      |
| stirring speed   | 200-400 rpm | -                      |

\* based on the amount of MAPTAC

\*\* based on the amount of styrene and DVB



### 3.2.2 Effect of Polymerization Time of MAPTAC

Effect of polymerization time of MAPTAC was undertaken. The polymerization of MAPTAC was carried out with various reaction times as shown in Table 3.3. Then, a mixture of styrene, DVB, surfactant, and AIBN were added into the reaction flask and the copolymerization reaction was continued at temperature of 70°C for 1 h. The obtained polymer beads were then subjected to determine particle size and particle size distribution and dye adsorption.

Table 3.3 Various polymerization times for suspension polymerization

| Batch | Polymerization time (min) |
|-------|---------------------------|
| 1     | 15                        |
| 2     | 30                        |
| 3     | 45                        |

### 3.2.3 Effect of Copolymerization Time

The polymerization was carried out at reaction time of MAPTAC for 30 min. Then, a mixture of styrene, DVB, surfactant, and AIBN were added into the reaction flask. Effect of copolymerization time of styrene, DVB, and MAPTAC radical was undertaken as shown in Table 3.4. The obtained polymeric beads were collected, weighed, and followed by characterization.

Table 3.4 Various copolymerization times for suspension polymerization

| Batch | Copolymerization time (h) |
|-------|---------------------------|
| 1     | 1                         |
| 2     | 2                         |
| 3     | 3                         |

### 3.2.4 Effect of Polymerization Temperature

The polymerization of MAPTAC radicals, styrene and DVB was repeated. It was carried out at polymerization time of MAPTAC for 30 min and copolymerization time of MAPTAC radical, styrene, and DVB was carried out for 1 h. Effect of polymerization temperature was undertaken as shown in Table 3.5. The obtained polymeric beads were collected, weighed, and followed by characterization.

Table 3.5 Various polymerization temperature for suspension polymerization

| Batch | Polymerization temperature (°C) |
|-------|---------------------------------|
| 1     | 60                              |
| 2     | 70                              |
| 3     | 80                              |

### 3.2.5 Effect of Stirring Speed

The polymerization of MAPTAC radicals, styrene and DVB was repeated. It was carried out at a temperature of 70°C. Effect of stirring speed was undertaken as shown in Table 3.6. The obtained polymeric beads were collected and weighted, and followed by characterization.

Table 3.6 Various stirring speeds for suspension polymerization

| Batch | Stirring speed (rpm) |
|-------|----------------------|
| 1     | 200                  |
| 2     | 300                  |
| 3     | 400                  |

### 3.2.6 Effect of Divinylbenzene

The polymerization of MAPTAC radicals, styrene and DVB was repeated. It was carried out at a stirring speed of 300 rpm. The amount of DVB was varied as shown in Table 3.7. The obtained polymeric beads were collected, weighted, and followed by characterization.

Table 3.7 Various amounts of styrene, DVB, and AIBN for suspension polymerization

| Batch | Amount of      |            |                               |             |
|-------|----------------|------------|-------------------------------|-------------|
|       | Styrene<br>(g) | DVB<br>(g) | DVB<br>(wt% based on styrene) | AIBN<br>(g) |
| 1     | 4.08           | 0.46       | 11.25                         | 0.10        |
| 2     | 4.08           | 0.92       | 22.55                         | 0.11        |
| 3     | 4.08           | 1.84       | 45.10                         | 0.13        |

### 3.2.7 Effect of Surfactants

#### 3.2.7.1 Effect of Nonionic Surfactant

The polymerization was carried out at DVB content 0.46 g. The amount of cetyl alcohol content was varied as shown in Table 3.8. The obtained polymeric beads were collected, weighed, and followed by characterization.

สถาบันวิทยบริการ  
จุฬาลงกรณ์มหาวิทยาลัย

Table 3.8 Various amounts of cetyl alcohol for suspension polymerization

| Batch | Amount of cetyl alcohol (g) |
|-------|-----------------------------|
| 1     | 0                           |
| 2     | 0.002                       |
| 3     | 0.003                       |
| 4     | 0.004                       |
| 5     | 0.005                       |
| 6     | 0.01                        |
| 7     | 0.02                        |
| 8     | 0.03                        |

### 3.2.7.2 Effect of Cationic Surfactant

Cetyl alcohol was replaced by cationic surfactant (CTAB). The amount of CTAB was varied as shown in Table 3.9. The obtained polymeric beads were collected, weighed, and followed by characterization.

Table 3.9 Various amounts of CTAB for suspension polymerization

| Batch | Amount of CTAB (g) |
|-------|--------------------|
| 1     | 0                  |
| 2     | 0.002              |
| 3     | 0.003              |
| 4     | 0.004              |

### 3.3 Characterizations

#### 3.3.1 Particle Size Measurement

The final polymer beads were sieved into discrete particle size ranges by using Laboratory Test Sieve (mesh number 6-140) (Endecotts Ltd. London England).

#### 3.3.2 Gel Permeation Chromatography (GPC)

GPC experiment was carried out to obtain the information of the molecular weight (MW) distribution of PMAPTAC radicals. Separate polymerization of MAPTAC was conducted at temperature of 70°C under a nitrogen atmosphere in a three-neck round-bottomed flask. After the reaction proceeded for a determined time, the polymerization was stopped by adding hydroquinone. The products obtained were dried and their molecular weight (MW) were determined using gel permeation chromatography. The analysis conditions were as follow : 0.1 M sodium nitrate :

acetonitrile (80 :20) as a eluent, temperature of 30°C; flow rate 1.0 ml/min. Column was packed with Shodex Asahipak GS-220 HQ with MW resolving range 200-3000. Detection was obtain by Refractive Index Detector. Polysaccharide standard kits were used as relative standards.

### 3.3.3 FTIR Analysis

FTIR spectra of polystyrene, PMAPTAC, and polymer beads were recorded in KBr pellets using Omnic Nicolet Impact 400 D FTIR Spectrophotometer. The sample was prepared in KBr pellets press. The recording parameters were as follows : scan rate 32 sec, wave number : 4000-400  $\text{cm}^{-1}$ .

### 3.3.4 Microscopic Studies

The particle structure and the surface morphology of polymer beads were observed with Scanning Electron Microscope (SEM,XL 30 CP. Philips). The sample for cross sectional view was prepared by sectioning bead which was embedded in epoxy resin and observed using SEM. Some samples were determined the element on the surface of polymer bead by SEM equipped with X-ray microanalysis.

### 3.4 Dye Adsorption Studies

#### 3.4.1 Determination of Dye Adsorption

Firstly, the solution containing 0.1 wt% reactive dye, 10 g/l NaCl, and 1 g/l wetting agent was prepared. To the 20 ml test tube, 1 g adsorbent beads and 10 ml reactive dye solution was added. The mixture was stirred at 100 rpm for 1 min and standed for 24 h to allow equilibrium adsorption. The initial dye concentration and residual dye concentration were measured using a Specord S 100 UV spectrophotometer at the maximum wavelength ( $\lambda_{\max}$ ) of the absorbance.

#### 3.4.2 Determination of Contact Time

The contact time measurement of dye adsorption properties of polymer beads with particle sizes ranging from 150 and 500  $\mu\text{m}$  was carried out at the temperature of 80°C. The beads (0.5 g) and the volume of the dye solution at the concentrations of 3500 mg/l (5 ml) and wetting agent of 1 g/l in a test tube were stirred with a magnetic stirrer at 100 rpm. The concentration of remaining dye was monitored at certain intervals by Specord S 100 UV spectrophotometer at the  $\lambda_{\max}$  of the absorbance.

#### 3.4.3 Dye Adsorption Isotherms Study

The equilibrium adsorption isotherm was determined by mixing 0.5 g of polymer beads (particle size ranging from 150 to 500 microns) with 5 ml of reactive dyes solution (blue, red, and yellow) and wetting agent 1 g/l in a test tube at room temperature for



24 h and at a temperature of 80°C for determine time (20 minute). Each isotherm consisted of seven different concentrations varied from 500 to 3500 mg/l of dye. The tubes containing dye solution and polymer beads were stirred with a magnetic stirrer at 100 rpm for 1 min. The equilibrium concentrations of different combinations were measured by UV spectrophotometer and referenced with the calibration curve.



สถาบันวิทยบริการ  
จุฬาลงกรณ์มหาวิทยาลัย

## CHAPTER IV

### RESULTS AND DISCUSSION

#### 4.1 Fundamental Idea on One-Pot Synthesis of Polymeric Beads Bearing Surface Charge

Polymeric beads bearing surface charge were prepared by suspension polymerization of 3-(methacryloylamino) propyl trimethyl ammonium chloride (MAPTAC), styrene, divinylbenzene (DVB) using two initiators system: water soluble  $K_2S_2O_8$  and oil soluble AIBN. Firstly, MAPTAC was polymerized in aqueous solution of PVA as a stabilizing agent for desired periods of times using  $K_2S_2O_8$  initiator. Then the mixture of surfactant, styrene, DVB, and AIBN was fed quickly into the reactor meanwhile agitating continuously. At this stage, the droplets were formed and uniformly dispersed in the aqueous solution of growing polymeric chain of PMAPTAC radicals. The droplet sizes were dependent on the stirring speed, the polymerization temperature and the types of surfactants. Furthermore, at this stage AIBN would begin to initiate the copolymerization of styrene and DVB to transform into gel bead. Meanwhile, it was expected that PMAPTAC radicals would diffuse through surfactant layer into gel bead surface to undergo the reaction with available styrene or DVB monomers present at bead surface. As polymerization proceeded, the gel bead was gradually transformed into solid particle

having cationic charge surface layer. Compared to typical ion exchange poly(styrene-co-DVB) beads which are also produced by suspension polymerization but it is further required for surface functionalization step in order to introduce desirable functional groups such as cations or anions.[17] In this study, the incorporation of charge onto poly (styrene-co-DVB) bead surface was undertaken in a single batch reaction. Typical morphology and the cross section view of the bead was obtained using SEM analysis and shown in Figure 4.1. The particle viewed by SEM image exhibits a round-shaped bead which is uniquely different from the smooth spherical particle typically obtained from conventional synthesis. [58] The cross section view further proves that the bead comprises two layers : the inner core represents the poly(styrene-co-DVB) support and the outer layer is the copolymerization product of surface styrene, DVB and PMAPTAC radical capable of diffusing through surfactant layer during the polymerization process. The percentage yield for each synthesis batch was about 45% on average.

Primary investigation revealed that there were three major parameters influencing the formation of spherical bead bearing surface functional group including DVB, the type of surfactants and initiators. Therefore, the experimental conditions were designed as shown in Table 4.1. In the case of no addition of AIBN, the major population of large agglomerate of  $\sim 3,000 \mu\text{m}$  was formed, reflecting the collapse of polymer particles existing largely in the aqueous phase (Figure 4.2). When excess amount of cationic surfactant (CTAB) was employed, the powder was obtained instead due to

significant reductive of surface tension at the droplet interface. The spherical shape with surface functional group was formed when the appropriate amount of DVB crosslinker and surfactant was used in the presence of AIBN in the oil phase. Detailed discussion on each effect is presented as follows.

Table 4.1 Experimental conditions

| Reagents and condition                                       | conditions            | wt% (based on styrene) |
|--|-----------------------|------------------------|
| MAPTAC   | 2.25 g                | 55.15                  |
| K <sub>2</sub> S <sub>2</sub> O <sub>8</sub>                 | 0.09 g                | 4.00*                  |
| 0.1 wt% PVA solution   | 90 ml                 | -                      |
| polymerization time of MAPTAC                                | 15-45 min             | -                      |
| styrene  | 4.08 g                | -                      |
| DVB  | 0.46-1.84 g           | 11.27-45.10            |
| surfactant ; cetyl alcohol or CTAB                           | 0-0.03 g or 0-0.005 g | 0-0.74 or 0-0.12       |
| AIBN   | 0.10-0.13 g           | 2.20**                 |
| polymerization time of styrene, DVB,<br>and PMAPTAC radicals | 1-3 h                 | -                      |
| polymerization temperature                                   | 60-80 °C              | -                      |
| stirring speed   | 200-400 rpm           | -                      |

\* based on the amount of MAPTAC

\*\* based on the amount of styrene and DVB

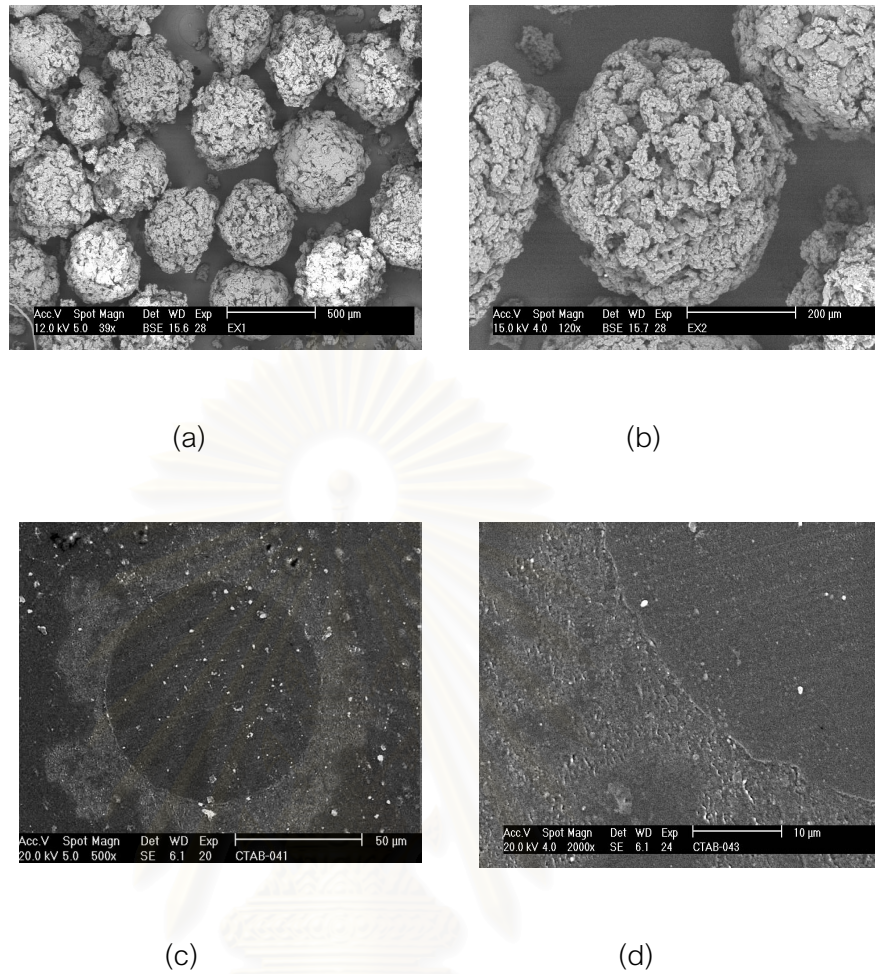


Figure 4.1 SEM micrographs of the bead structure and cross-section of polymer bead.

(a), (b) whole bead structure

(c),(d) cross-section of polymer bead

สถาบันวิทยบริการ  
จุฬาลงกรณ์มหาวิทยาลัย

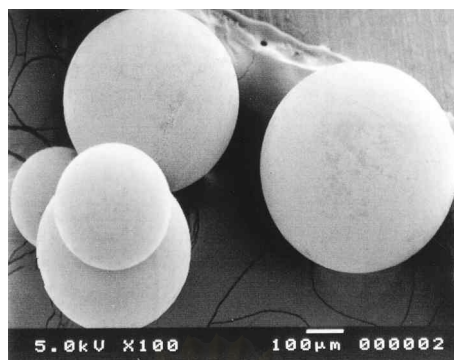
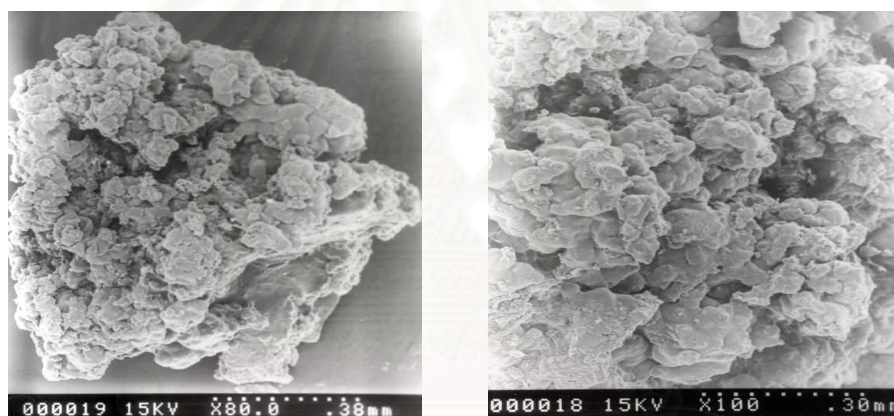


Figure 4.2 SEM micrograph of virgin polystyrene.



(a)

(b)

Figure 4.3 SEM micrographs of product in the case of no addition of AIBN.

(a) magnification 80X

(b) magnification 100X

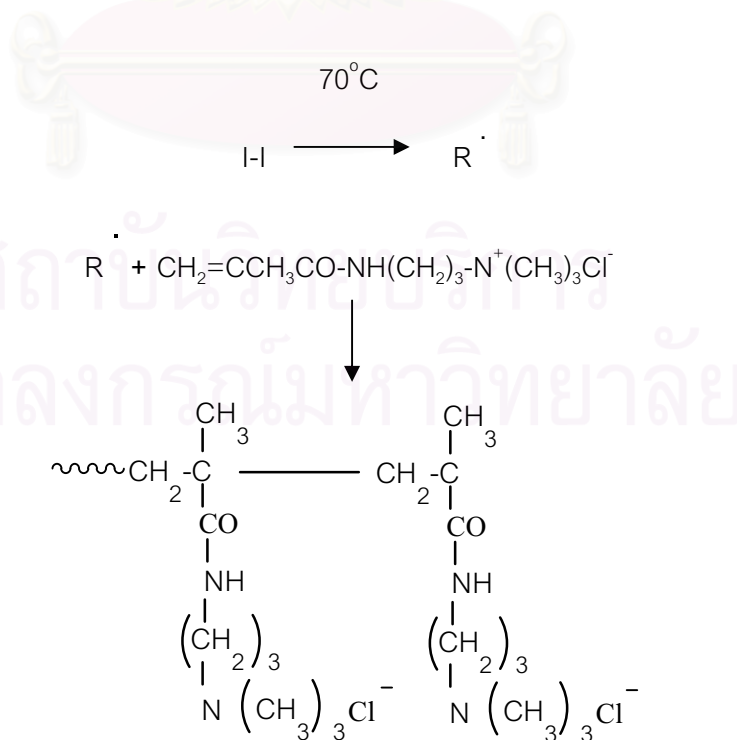


## 4.2 Parameters Influencing Particle Size and Particle Size Distribution

The effect of several parameters were investigated in controlling the particle size, size distribution and properties of the adsorbent, including polymerization time of MAPTAC, copolymerization time between styrene, DVB, and PMAPTAC radical, polymerization temperature, agitation speed, amount of divinylbenzene and surfactant. The effects of this parameters were studied. The results obtained are reported below.

### 4.2.1 Effect of Polymerization Time of MAPTAC

At the beginning, the radical polymerization of MAPTAC was carried out in aqueous solution at a temperature of 70°C using  $K_2S_2O_8$  as an initiator in order to generate the PMAPTAC radicals. The polymerization reaction is represented as shown below.



Since it was anticipated that the chain length of PMAPTAC radical governed its subsequent reactivity with styrene monomer to obtain surface functionalized bead. Separate experiment for determination of the molecular weight of PMAPTAC radical was performed. Three reaction batches which differed in the polymerization time of MAPTAC(15, 30 and 45 minutes, respectively) were carried out. The characterization of quenched PMAPTAC oligomer by gel permeation chromatography (GPC) analysis was separately performed to obtain the information of its molecular weight and weight distribution. The results of molecular weights of PMAPTAC oligomers are shown in Table 4.2-4.3 and Figures 4.4-4.7, respectively.

Table 4.2 Molecular weights of MAPTAC determined by gel permeation chromatography

| $\overline{M}_n$ | $\overline{M}_w$ | $\overline{M}_v$ |
|------------------|------------------|------------------|
| 259              | 263              | 262              |

สถาบันวิทยบริการ  
จุฬาลงกรณ์มหาวิทยาลัย



Table 4.3 Molecular weights of PMAPTAC determined by gel permeation chromatography

| Polymerization time of<br>MAPTAC (min) | Peak<br>number | $\overline{M}_n$ | $\overline{M}_w$ | $\overline{M}_v$ | Polydispersity<br>index |
|--|----------------|------------------|------------------|------------------|-------------------------|
| 15                                     | 1              | 2191             | 2239             | 2233             | 1.02                    |
|  | 2              | 659              | 667              | 666              | 1.01                    |
|  | 3              | 218              | 220              | 220              | 1.01                    |
| 30                                     | 1              | 2126             | 2194             | 2184             | 1.03                    |
|  | 2              | 661              | 667              | 666              | 1.01                    |
|  | 3              | 234              | 235              | 234              | 1.00                    |
| 45                                     | 1              | 2256             | 2292             | 2287             | 1.02                    |
|  | 2              | 648              | 653              | 652              | 1.01                    |
|  | 3              | 221              | 222              | 222              | 1.00                    |

สถาบันวิทยบริการ  
จุฬาลงกรณ์มหาวิทยาลัย

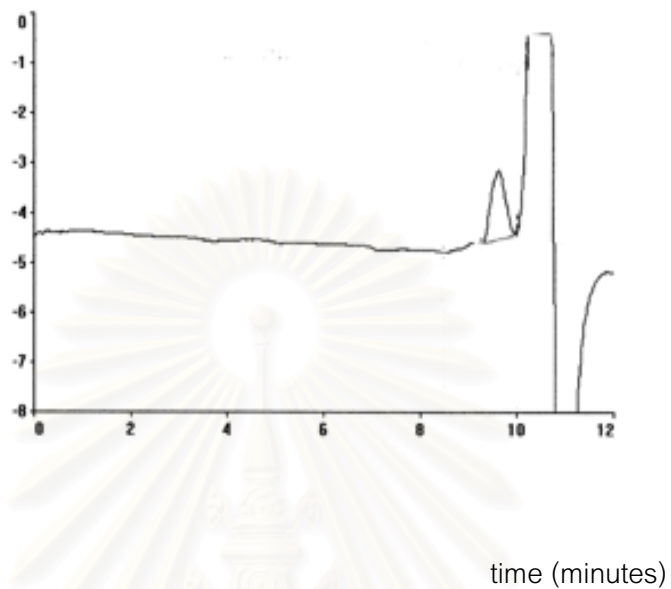


Figure 4.4 GPC chromatogram of MAPTAC monomer.

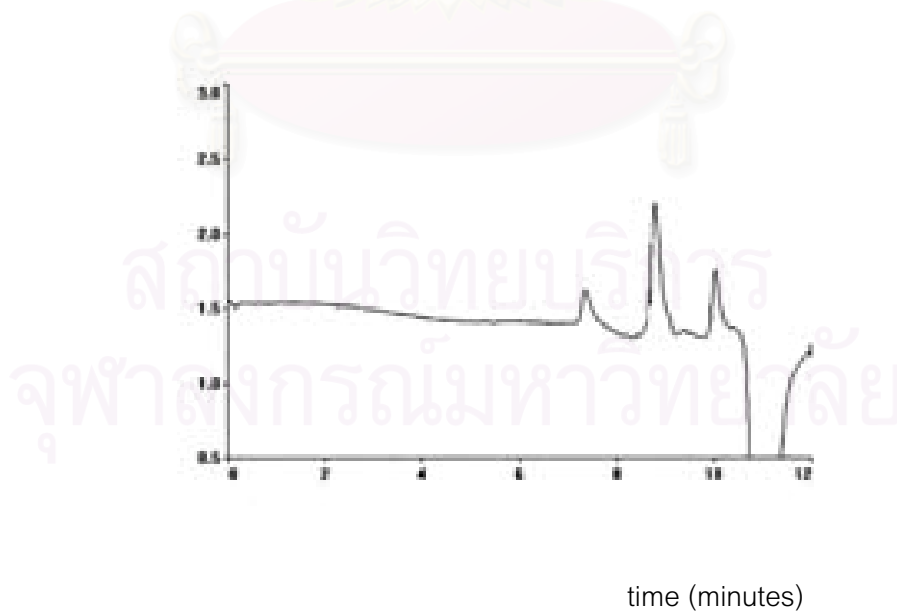


Figure 4.5 GPC chromatogram of PMAPTAC at polymerization time of 15 minutes.

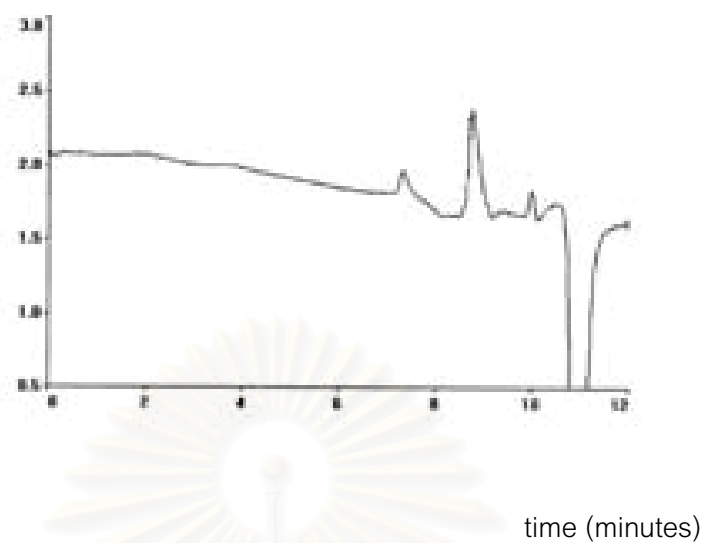


Figure 4.6 GPC chromatogram of PMAPTAC at polymerization time of 30 minutes.

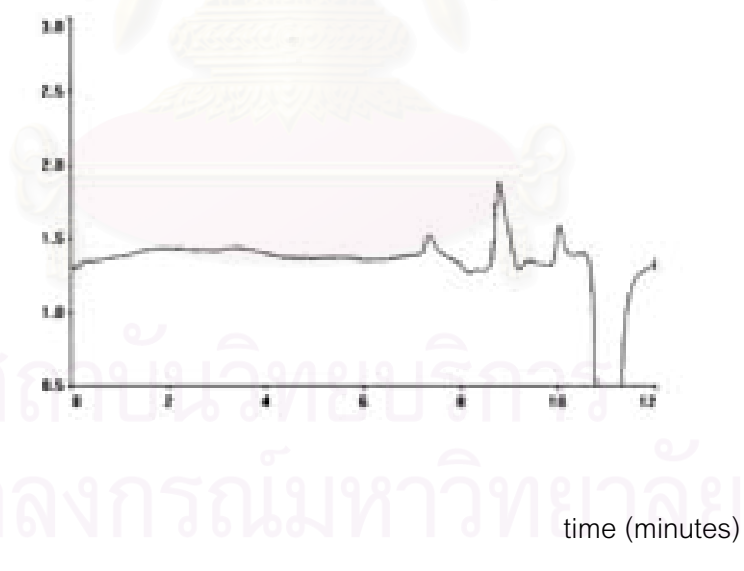


Figure 4.7 GPC chromatogram of PMAPTAC at polymerization time of 45 minutes.

The typical GPC chromatograms (Figures 4.5-4.7) show peaks corresponding to the molecular weights of 2,000 and 600. Another peak with the molecular weight of 200 probably represents the unreacted monomer. They show that the molecular weight of PMAPTAC oligomers obtained from various polymerization times are not different, reflecting the characteristic of free radical chain polymerization in terms of high percent conversion achievable at the beginning of polymerization. From this experiment, it was found that the short chain PMAPTAC radical of MW of  $\sim 600$  was the major reaction product. Therefore, it was expected that there was no difference in the reactivity of PMAPTAC radicals obtained from the different reaction time of MAPTAC. Since generated PMAPTAC radical was considered to behave like polyelectrolyte it, therefore, was capable of enhancing the stabilization of styrene droplets by electrostatic effect during bead formation stage. [59-60]

After obtaining the information of the generated PMAPTAC radical, the effects of polymerization time of MAPTAC on the particle size, size distribution and property, the polymerization time of MAPTAC were studied. Polymerization of styrene and DVB droplets containing AIBN initiator was carried out in the aqueous solution of PMAPTAC oligomer. The experimental results obtained are shown in Table 4.4 and Figure 4.8.

Table 4.4 Effect of polymerization time of MAPTAC on particle size distribution

| Particle size ( $\mu\text{m}$ ) | Product weight distribution (%)        |       |       |
|---------------------------------|--|-------|-------|
|                                 | Polymerization time of MAPTAC (minute) |       |       |
|                                 | 15                                     | 30    | 45    |
| 106                             | 0.73                                   | 0.15  | 1.03  |
| 125                             | 0.95                                   | 0.23  | 1.56  |
| 150                             | 10.58                                  | 2.28  | 11.96 |
| 300                             | 15.56                                  | 16.79 | 8.02  |
| 500                             | 47.23                                  | 54.17 | 53.97 |
| 1000-1800                       | 24.94                                  | 26.38 | 23.46 |
| 3000-3500                       | 0                                      | 0     | 0     |

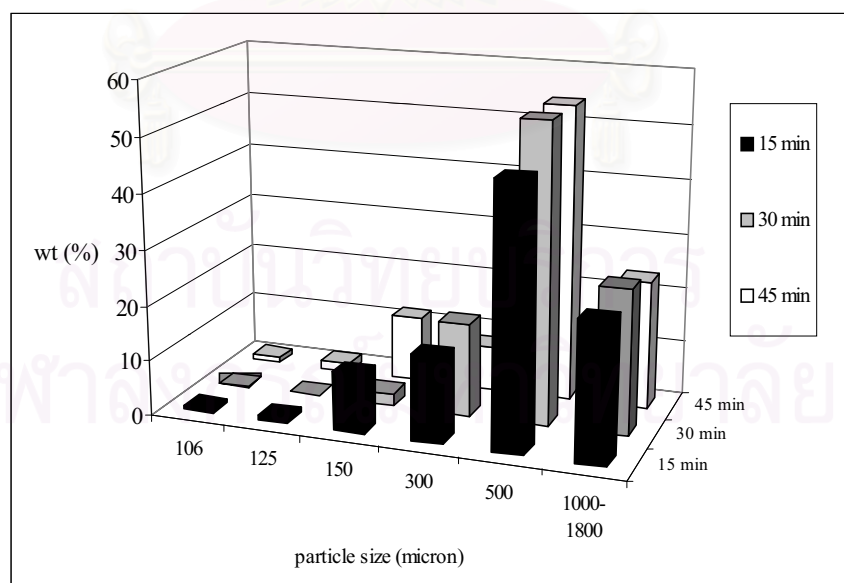


Figure 4.8 Particle size and distribution obtained from polymerization times of MAPTAC

15-45 minutes.

The synthesized products of each batch were measured and the percent yields are 46.42, 40.13, and 43.45 respectively. Figure 4.8 shows the particle sizes and size distribution of the resulting polymer beads achieved as a function of polymerization time of MAPTAC. The particle size found ranges widely from 100  $\mu\text{m}$  to  $\sim 2000 \mu\text{m}$  with a mean size of 500  $\mu\text{m}$ . These results suggest that the polymerization time of MAPTAC in the studying range did not cause the difference in the final particle size.

It should be noted that when the applications of the bead are concerned the small particle size with large surface as well as high surface charge density is preferable. In this work, attempt to incorporate the surface charge density onto bead surface was carried out during the polymerization process. Hence, the surface charge density was greatly dependent on the PMAPTAC radical capability of attaching to bead surface. The reason for varying polymerization times of MAPTAC was to generate the different chain length radicals in order to optimize the bead surface charge density. Unfortunately, based on the results of molecular weight determination, nearly identical molecular weight was found in all cases of polymerization times.

FTIR spectroscopy was chosen to identify the functional group (cationic charge) on the bead surface and the results are shown in Figures 4.9-4.10. The absorption bands at  $3400 \text{ cm}^{-1}$  and  $1700 \text{ cm}^{-1}$  corresponding to the absorbances of NH and C=O functional groups are indicative of the attachment of PMAPTAC segment on the bead particle. The results show that the peak intensities of bead functional groups obtained

from various polymerization times of MAPTAC are not significantly different. This implies that the effect of varying polymerization times of MAPTAC from 15 to 45 minutes brought about indifference in the surface charge density as a result of indifference in chain length of PMAPTAC radicals.

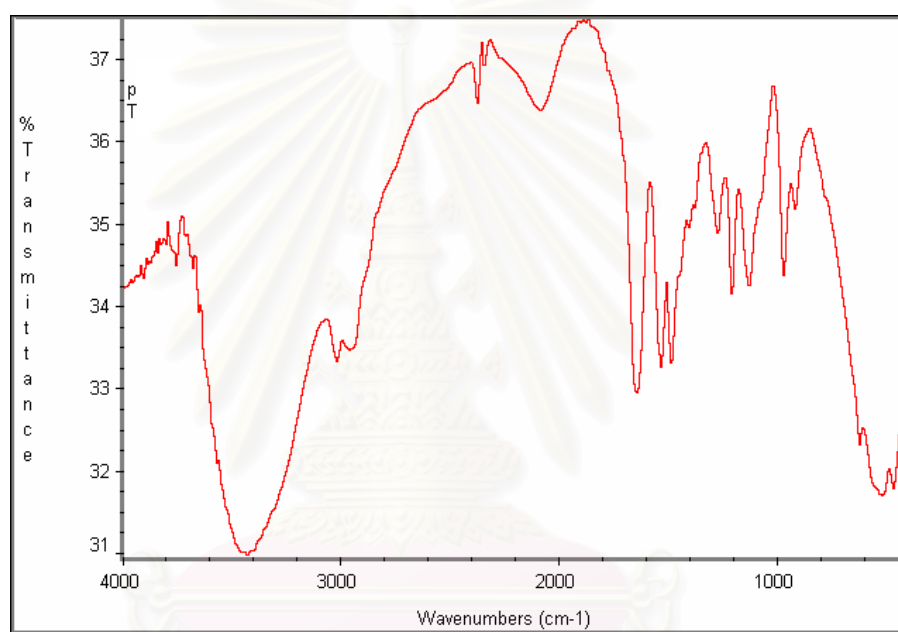


Figure 4.9 FT-IR spectrum of PMAPTAC.

สถาบันวิทยบริการ  
จุฬาลงกรณ์มหาวิทยาลัย

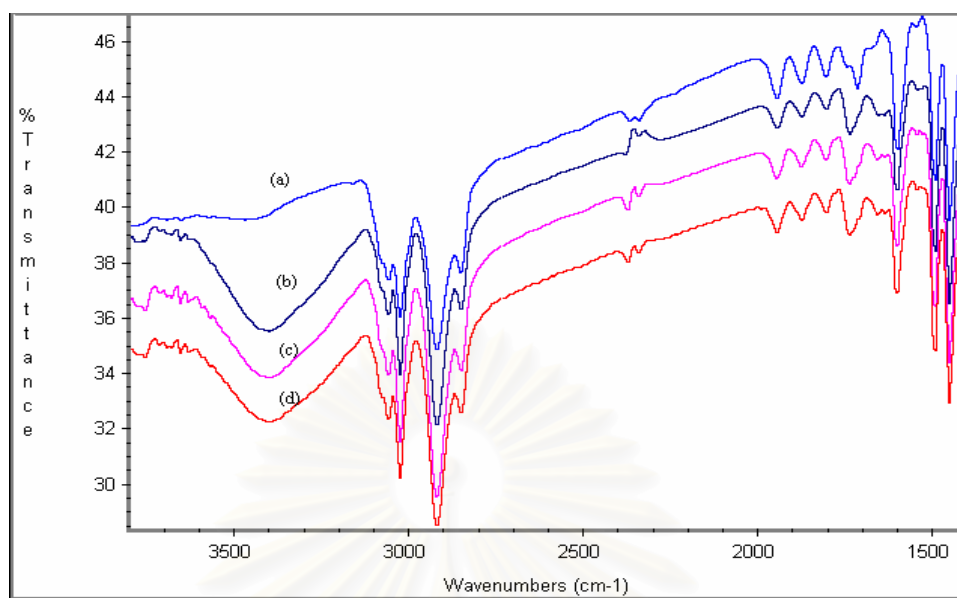


Figure 4.10 FTIR spectra of polymer bead obtained from different polymerization time of MAPTAC (a) polystyrene; (b) 15 min; (c) 30 min; (d) 45 min.

Further dye adsorption study of the beads from each batch was performed in order to choose the optimum polymerization of PMAPTAC for latter experiments. The prepared beads were immersed in the reactive dye solution and allowed to obtain adsorption equilibrium for 24 h. The dye adsorption performance was spectrophotometrically measured. The experimental results obtained are shown in Table 4.5.



Table 4.5 Effect of polymerization time of MAPTAC on dye adsorption of polymer beads

| Polymerization time of MAPTAC<br>(minutes) | Dye adsorption by bead (mg dye/g adsorbent) |
|--|---|
| Polystyrene bead                           | 0.03  |
| 15   | 3.90  |
| 30   | 4.53  |
| 45   | 4.04  |

From this result, it will be seen that the dye adsorption were 3.90-4.53 mg/g. Dye adsorption of polymer bead depended on functional group in PMAPTAC and particle size of polymer. The effect of varying polymerization time of MAPTAC on dye adsorption of polymer bead was not different. For the further experiments throughout, the constant polymerization time of MAPTAC of 30 min was chosen.

สถาบันวิทยบริการ  
จุฬาลงกรณ์มหาวิทยาลัย

#### 4.2.2 Effect of Copolymerization Time of Styrene, DVB and PMAPTAC Oligomer on Bead Formation

The copolymerization reaction of styrene, DVB, and PMAPTAC radical was carried out at the constant temperature in the solution of the PMAPTAC oligomer after 30 minutes of the polymerization time of MAPTAC . The well-mixed liquid of styrene, DVB and AIBN initiator was quickly fed onto the PMAPTAC oligomer solution. The liquid droplet was formed by means of agitation and the droplet size was controlled by means of the stirring speed. At this stage, the polymerization time was varied from 1-3 h. It was expected that the copolymerization reaction between styrene and DVB initiated by AIBN occurred at once inside the liquid droplet. Simultaneously, the PMAPTAC radical would diffuse through the surfactant layer and undergo the reaction with styrene monomer available on the liquid droplet surface. The copolymerization reaction between styrene and DVB resulted in the transformation of droplet liquid into the spherical solid particle. While the attachment of PMAPTAC segment onto the bead surface led to the formation of polystyrene bearing cationic surface charge as shown previously. The model of charge bearing bead formation may be proposed as in Figure 4.11.

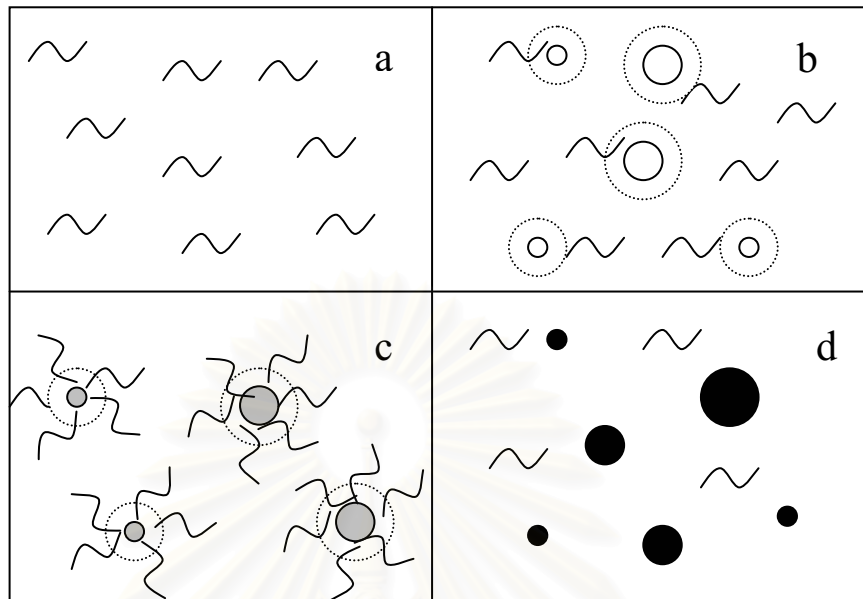


Figure 4.11 Schematic Diagram represents the formation of charge bearing bead :  
**(a)** PMAPTAC radical in aqueous solution; **(b)** mixture of surfactant, styrene, DVB, and AIBN droplet in the aqueous solution; **(c)** PMAPTAC radical diffused through surfactant layer into gel bead surface; **(d)** the final bead bearing surface charge onto the outer layer.

~ = PMAPTAC radical ..... = surfactant

○ = mixture of styrene, DVB, and AIBN droplet

● = gel bead

● = final bead bearing surface charge

The particle size of beads was also determined and the results obtained are shown in Table 4.6 and Figure 4.12.

Table 4.6 Effect of polymerization time between styrene, DVB, and PMAPTAC radical on particle size and particle size distribution

| Particle size ( $\mu\text{m}$ ) | Product weight distribution (wt %)                  |       |       |
|---------------------------------|---|-------|-------|
|                                 | Polymerization time between styrene and PMAPTAC (h) |       |       |
|                                 | 1   | 2     | 3     |
| 106                             | 0   | 0.15  | 0     |
| 125                             | 0.18  | 0.23  | 0.66  |
| 150                             | 4.05  | 2.28  | 11.93 |
| 300                             | 9.09  | 16.79 | 15.27 |
| 500                             | 53.65   | 54.17 | 51.38 |
| 1000-1800                       | 33.03   | 26.38 | 20.76 |
| 3000-3500                       | 0   | 0     | 0     |

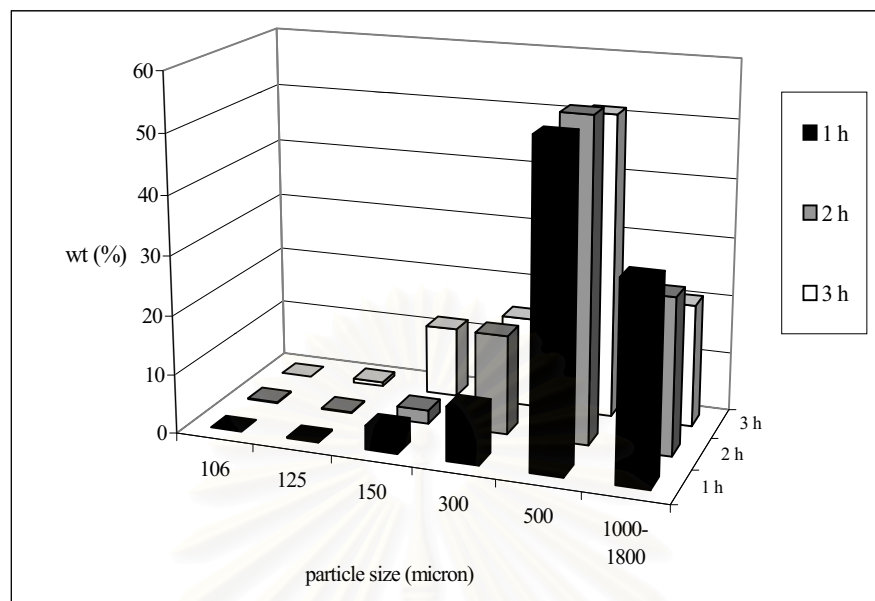


Figure 4.12 Particle size and distribution obtained from styrene and PMAPTAC polymerization times of 1-3 h.

The synthesized products of each batch were measured and the percent yield found were 45.60, 40.13, and 41.65, for 1, 2 and 3 h respectively. From the Figure 4.12, it can be seen that varying of copolymerization times from 1 to 3 hours had little effect on the mean particle size which was found about  $\sim 500 \mu\text{m}$ . From there results, the polymerization time for 1 h was chosen as the suitable condition.

#### 4.2.3 Effect of Copolymerization Temperature

In this experiment, beads bearing cationic charge surface were synthesized at the reaction temperatures ranging from 60-80°C which are the dissociation temperature of both initiators, potassium persulfate and AIBN. The other synthetic parameters were kept constant as follows; the polymerization time of MAPTAC was 30 min at fixed stirring speed of 300 rpm. DVB and cetyl alcohol content were 11.27 wt% and 0.25 wt% (based on styrene), respectively. Table 4.7 and Figure 4.13 show the relationship between the particle size and size distribution with the reaction temperature.

Table 4.7 Effect of temperature on particle size and particle size distribution

| Particle size ( $\mu\text{m}$ ) | Product weight distribution (wt%)  |       |       |
|---------------------------------|------------------------------------|-------|-------|
|                                 | Temperature ( $^{\circ}\text{C}$ ) |       |       |
|                                 | 60                                 | 70    | 80    |
| 106                             | 0                                  | 0     | 0     |
| 125                             | 0.31                               | 0.18  | 0.46  |
| 150                             | 16.26                              | 4.05  | 4.50  |
| 300                             | 39.10                              | 9.09  | 6.37  |
| 500                             | 35.79                              | 53.65 | 28.90 |
| 1000-1800                       | 8.53                               | 33.03 | 59.76 |
| 3000-3500                       | 0                                  | 0     | 0     |

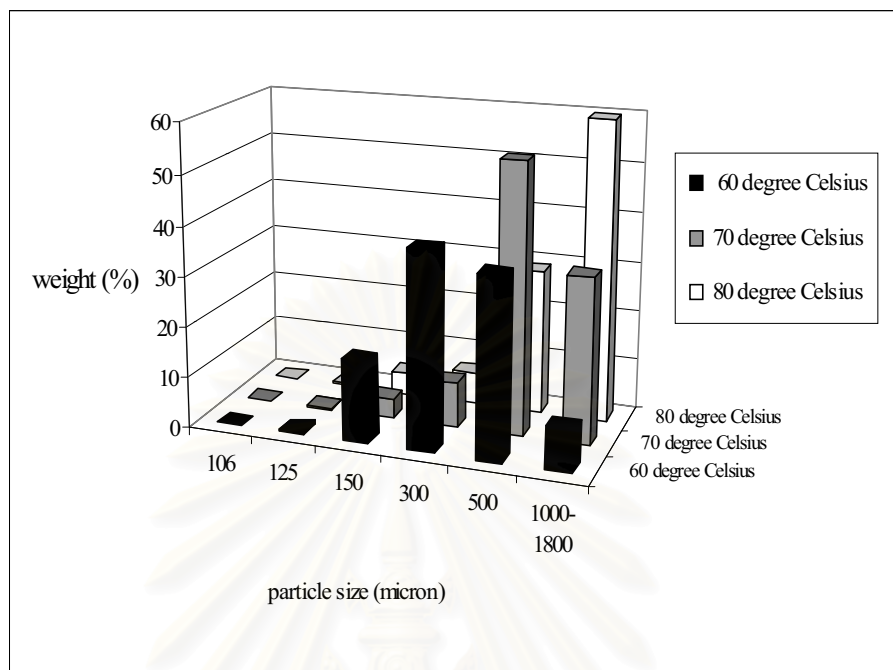


Figure 4.13 Particle size and distribution obtained from copolymerization temperature of 60-80°C.

The synthesized products of each batch were measured and the percent yields found were 36.03, 45.60, and 41.56, at 60, 70 and 80°C respectively. The results show that the reaction temperatures of 60°C tended to produce the small particle size with broad size distribution in the range of 106 to 1000  $\mu\text{m}$ . At temperature of 70°C, the particle size tended to increase from 150-300  $\mu\text{m}$  to 500  $\mu\text{m}$  whilst the reaction temperature of 80°C yielded most of large particle size of 1000  $\mu\text{m}$  with narrow size distribution. Similar observation was reported by Shen et. al.. [26] It was speculated that an increase in the reaction temperature normally causes the decrease in the adsorption rate of PVA due to its increasing solubility in water [61] leading to coalescence of

styrene-DVB droplets. Moreover, higher temperatures resulted in faster polymerization rate, further accelerating the conversion of coalesced droplet into stable particle. The SEM micrographs of polymer beads at different polymerization temperatures are shown in Figure 4.14.

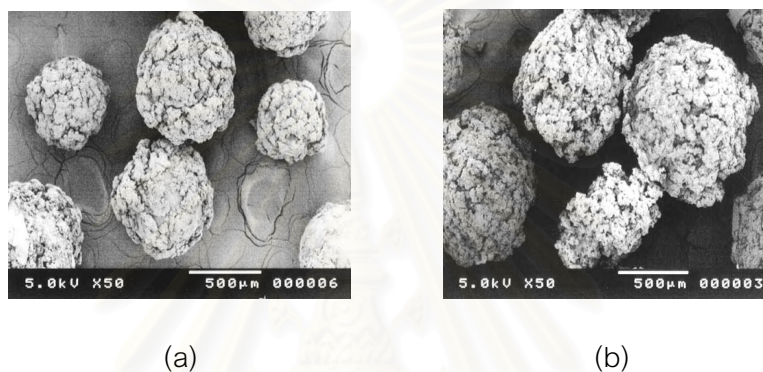


Figure 4.14 SEM micrographs of polymer beads at different polymerization temperatures.

(a) 70°C ; (b) 80°C

Figure 4.15 shows FTIR spectra of bead functional groups obtained from different polymerization temperatures. The results show that the peak intensities of the carbonyl group increase with increasing polymerization temperatures, implying an increase in the agglomerate outer layer. As a result this effect further contributed to the increase in the final particle size with relation to polymerization temperature.



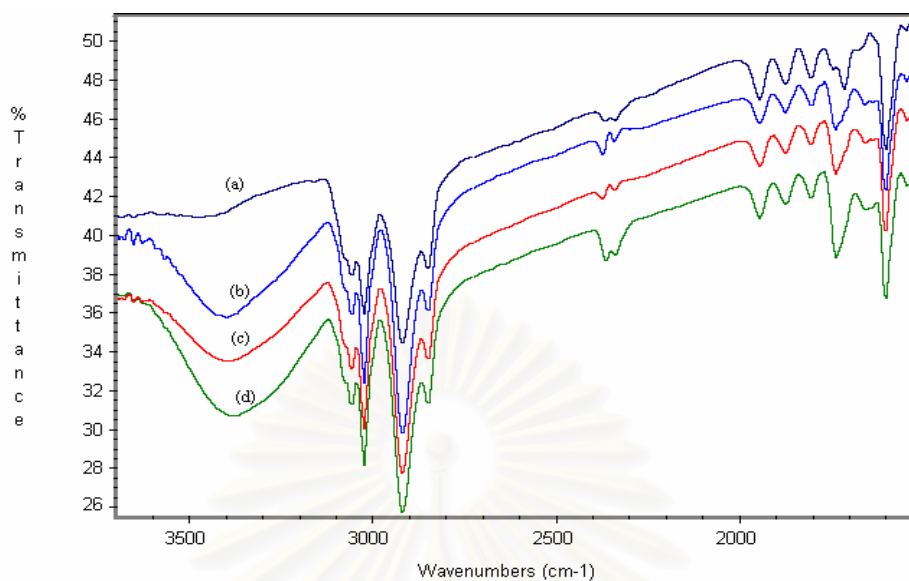


Figure 4.15 FTIR spectra of polymer bead obtain from different polymerization temperatures (a) polystyrene; (b) 60°C; (c) 70°C; (d) 80°C.

The experiment was undertaken to determine suitable condition for preparation of polymer bead. So, the polymer beads were used to adsorb reactive dye. The result obtains are shown in Table 4.8.

สถาบันวิทยบริการ  
จุฬาลงกรณ์มหาวิทยาลัย

Table 4.8 Effect of polymerization temperature on dye adsorption of polymer bead

| Polymerization temperature (°C) | Dye adsorption by bead (mg dye/g adsorbent) |
|---------------------------------|---|
| Polystyrene bead                | 0.03  |
| 60                              | 1.34  |
| 70                              | 4.53  |
| 80                              | 4.32  |

From this result, it will be seen that at temperature of 60°C the dye adsorption of polymer bead was lower than other temperatures. This can be explained that at temperature of 60°C the reaction between PMAPTAC and styrene was very low, therefore, the dye adsorption of polymer particle was not much. When the reaction temperature increased from 60°C to 80°C the dye adsorption increased. This was due to the reaction between PMAPTAC and styrene increased.

At temperature of 80°C, most of particle size was about 1000  $\mu\text{m}$  which larger than at temperature of 70°C. Therefore, the reaction temperature of 70°C was chosen as the suitable polymerization temperature.

#### 4.2.4 Effect of Stirring Speed on Particle Size

In suspension polymerization, agitation during polymerization is necessary to keep the oil phase properly dispersed. The stirring speed, therefore, greatly affects the final particle size. Hence, in this experiment, three stirring speeds of 200, 300, and 400 rpm were employed at the polymerization temperature of 70°C. The synthesis products of each batch were measured and the percent yields found were 23.11, 45.60, and 42.66, respectively. The effect of stirring speed in the particle size and size distribution are presented and shown in Table 4.9 and Figure 4.16.

Table 4.9 Effect of stirring speed on particle size and particle size distribution

| Particle size ( $\mu\text{m}$ ) | Product weight distribution (%) |       |       |
|---------------------------------|---------------------------------|-------|-------|
|                                 | Stirring speed (rpm)            |       |       |
|                                 | 200                             | 300   | 400   |
| 106                             | 0                               | 0     | 0.37  |
| 125                             | 0                               | 0.18  | 1.62  |
| 150                             | 6.30                            | 4.05  | 85.06 |
| 300                             | 11.47                           | 9.09  | 8.02  |
| 500                             | 59.44                           | 53.65 | 4.93  |
| 1000-1800                       | 22.78                           | 33.03 | 0     |
| 3000-3500                       | 0                               | 0     | 0     |

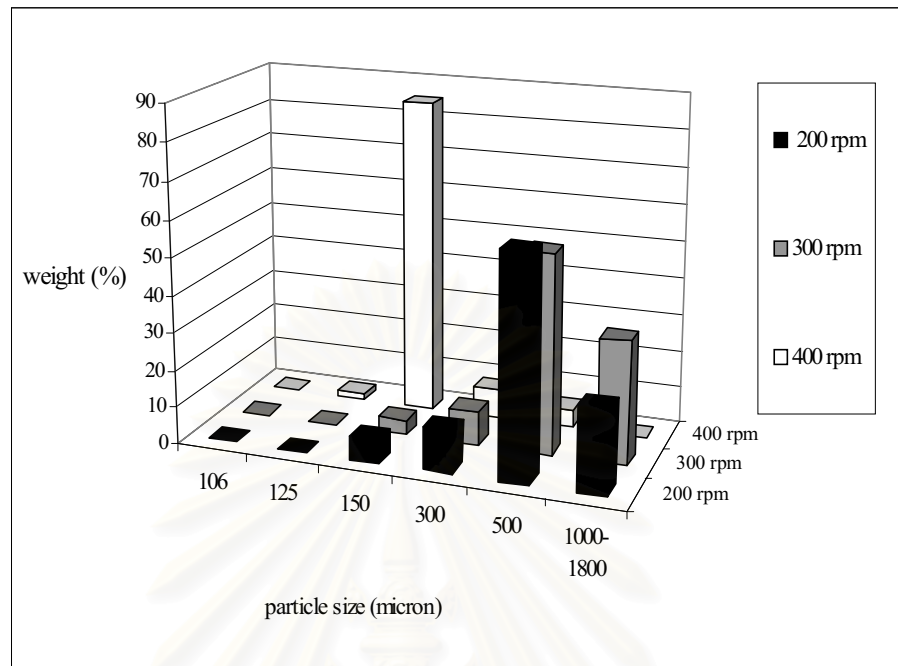


Figure 4.16 Effect of stirring speed on the particle size distribution

From Figure 4.16, the stirring speeds of 200 and 300 rpm produce the bead particle with the majority size falling around 500  $\mu\text{m}$ . In the case of 400 rpm stirring speed, the smaller particle size of 150  $\mu\text{m}$  is mainly obtained.

The results shown in Figure 4.16 indicate that the particle size is strongly dependent on the stirring speed; the higher the stirring speed (400 rpm), the smaller the particle size. Basically, the two phases system in suspension polymerization cannot be maintained without agitation which controls the balance between droplet breakage and coalescence. At higher stirring speed, the balance is shifted towards the rate of drop breakage, resulting in smaller drop size. As can be seen from the figure, an increase in

the rate of stirring speed tended to produce an increase in the population of final particles with smaller size.

#### 4.2.5 Effect of Divinylbenzene Crosslinker on Bead Morphology and Surface Functionality

It is well understood that the presence of crosslinking agent is responsible for the spherical shape of bead particle with the good mechanical property. In this study, divinylbenzene (DVB) was used as a crosslinker. To study the effect of DVB, other synthesis parameters such as polymerization time and temperature as well as stirring speed were controlled. Amounts of divinylbenzene was varied from 11.27-45.10 wt% (based on styrene). The synthesis products of each batch were measured and the percent yields found were 45.60, 44.82 and 53.98, at DVB content 0.46, 0.92 and 1.84 g respectively. The effect of DVB on polymer particle was shown in Table 4.10 and Figure 4.17.

Table 4.10 Effect of DVB on particle size and particle size distribution

| Particle size ( $\mu\text{m}$ ) | Product weight distribution (%) |       |       |
|---------------------------------|---------------------------------|-------|-------|
|                                 | DVB content (g)                 |       |       |
|                                 | 0.46                            | 0.92  | 1.84  |
| 106                             | 0                               | 0     | 0     |
| 125                             | 0.18                            | 0     | 0     |
| 150                             | 4.05                            | 2.74  | 2.58  |
| 300                             | 9.09                            | 33.07 | 25.99 |
| 500                             | 53.65                           | 63.79 | 70.42 |
| 1000-1800                       | 33.03                           | 0.39  | 1.01  |
| 3000-3500                       | 0                               | 0     | 0     |

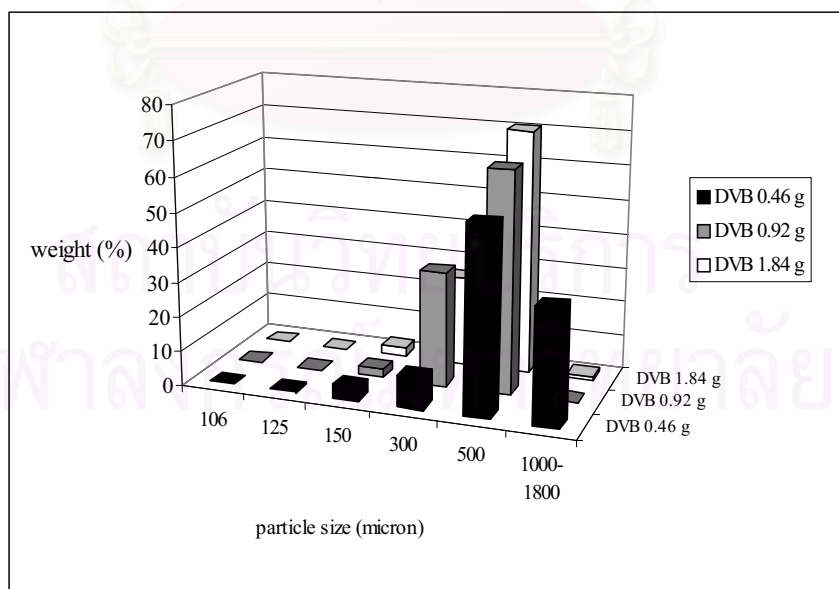


Figure 4.17 Particle size and distribution at DVB contents of 0.46-1.84 g.

It can be seen that an increase in the content of DVB does not bring about the change in the final particle size which is found, in average, in the range of 500  $\mu\text{m}$  for all synthesis batches. On the other hand, the surface morphology revealed by SEM exhibits coarse surface with various degree of surface irregularity which decreased with increasing the amount of DVB. Figure 4.18 show a comparison of SEM micrographs of polymer bead with different amounts of DVB. As DVB content increased, the polymer bead gave rise to smoother surface particle. From the study of Kangwansupamonkon et.al., [62] the presence of divinylbenzene enhanced the copolymerization rate of styrene and divinylbenzene in droplet phase, leading to rapid conversion of droplet with subsequent reduced reactivity of growing polymeric radicals on the droplet surface. Due to less availability of reactive species at the interface, incorporation capability of PMAPTAC radicals would be successively reduced when the amount of divinylbenzene rose, evidenced by smoother bead surface with increased amount of DVB observed from SEM micrographs.

Figures 4.19-4.20 show FTIR spectra of polystyrene bead and polymer beads at DVB content of 0.46 g. The results show the adsorption bands at  $3400\text{ cm}^{-1}$  and  $1700\text{ cm}^{-1}$  corresponding to the absorbances of NH and C=O functional groups. In conclusion, DVB content of 0.46 g was chosen for preparation of polymer bead.

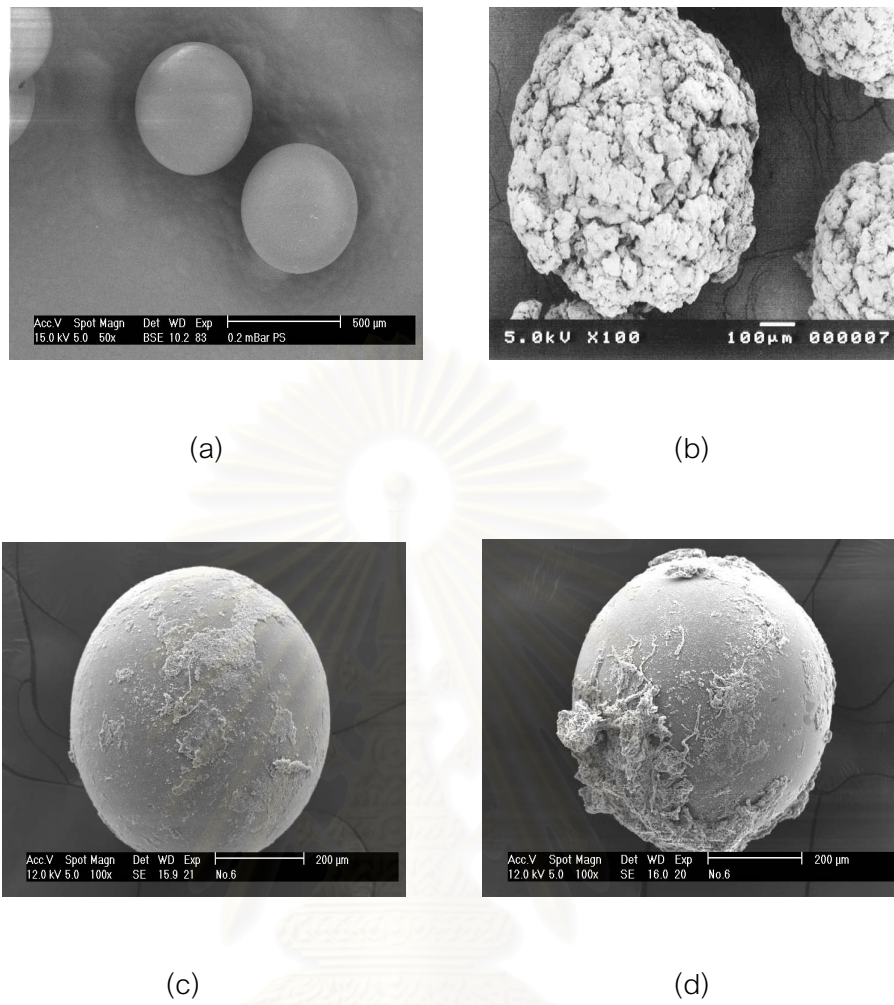


Figure 4.18 Comparison of SEM micrographs of polymer bead at different amount of DVB.

(a) poly(styrene-co-DVB) bead      (b) polymer bead at DVB content 0.46 g

(c), (d) polymer bead at DVB content 1.84 g



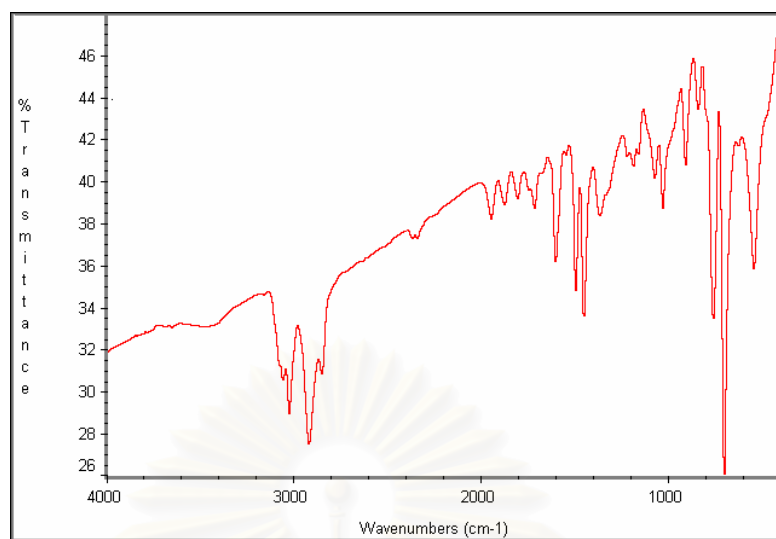


Figure 4.19 FTIR spectrum of polystyrene bead.

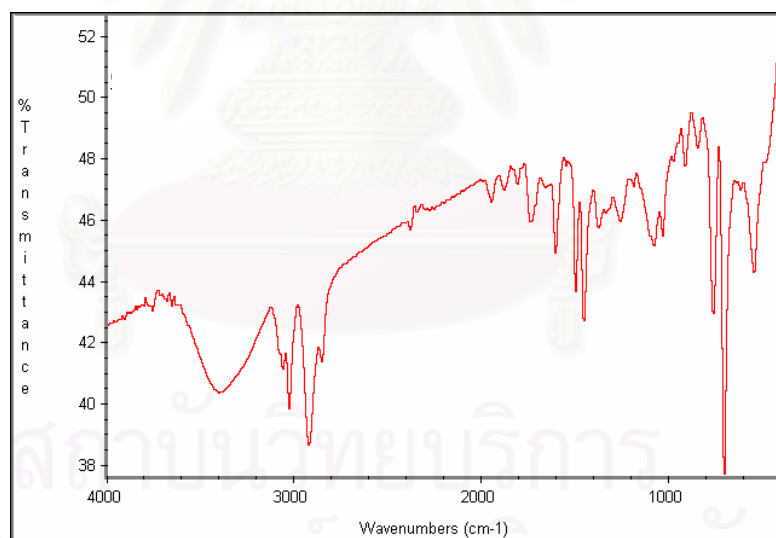


Figure 4.20 FTIR spectrum of polymer bead at DVB content of 0.46 g.

#### 4.2.6 Effect of Surfactants

The role of surfactants in suspension polymerization is to stabilize the droplet phase during polymerization. In this work, it was found that the presence of surfactant enhanced the incorporation capability of PMAPTAC radicals into the bead surface by decreasing the surface tension at the interface. Two types of surfactants were investigated; nonionic surfactant (cetyl alcohol) and cationic surfactant (CTAB).

##### 4.2.6.1 Effect of Nonionic Surfactant

Cetyl alcohol was added into the system prior to the addition of styrene and DVB. The amounts of cetyl alcohol were varied from 0-0.74 wt% (based on styrene). The percent yields obtained are given in Table 4.11. Effect of cetyl alcohol on the particle size and particle size distributions are shown in Table 4.12 and Figures 4.21-4.22.

Table 4.11 The percent yield with the relation to the amount of cetyl alcohol

| Cetyl alcohol content (g) | % Yield |
|---------------------------|---------|
| 0                         | 45.46   |
| 0.002                     | 43.41   |
| 0.003                     | 41.46   |
| 0.004                     | 46.20   |
| 0.005                     | 45.96   |

Table 4.11 The percent yield with the relation to the amount of cetyl alcohol (continued)

| Cetyl alcohol content (g) | % Yield |
|---------------------------|---------|
| 0.004                     | 46.20   |
| 0.005                     | 45.96   |
| 0.01                      | 45.60   |
| 0.02                      | 45.22   |
| 0.03                      | 48.13   |

Table 4.12 Effect of cetyl alcohol on particle size distribution and size distribution

| Particle size ( $\mu\text{m}$ ) | Product weight distribution (%) |       |       |       |       |       |       |       |
|---------------------------------|---------------------------------|-------|-------|-------|-------|-------|-------|-------|
|                                 | Cetyl alcohol content (g)       |       |       |       |       |       |       |       |
|                                 | 0                               | 0.002 | 0.003 | 0.004 | 0.005 | 0.01  | 0.02  | 0.03  |
| 125                             | 0                               | 0     | 0.23  | 0.38  | 0.54  | 0.18  | 0.30  | 0     |
| 150                             | 1.78                            | 0.99  | 2.85  | 1.99  | 6.12  | 4.05  | 2.47  | 0.95  |
| 300                             | 2.59                            | 2.42  | 4.70  | 2.79  | 8.69  | 9.09  | 4.37  | 1.97  |
| 500                             | 81.04                           | 69.96 | 69.08 | 66.51 | 57.63 | 53.65 | 29.78 | 21.81 |
| 1000-1800                       | 14.59                           | 21.76 | 17.67 | 23.62 | 21.15 | 33.03 | 63.08 | 75.27 |
| 3000-3500                       | 0                               | 4.87  | 5.47  | 4.71  | 5.86  | 0     | 0     | 0     |

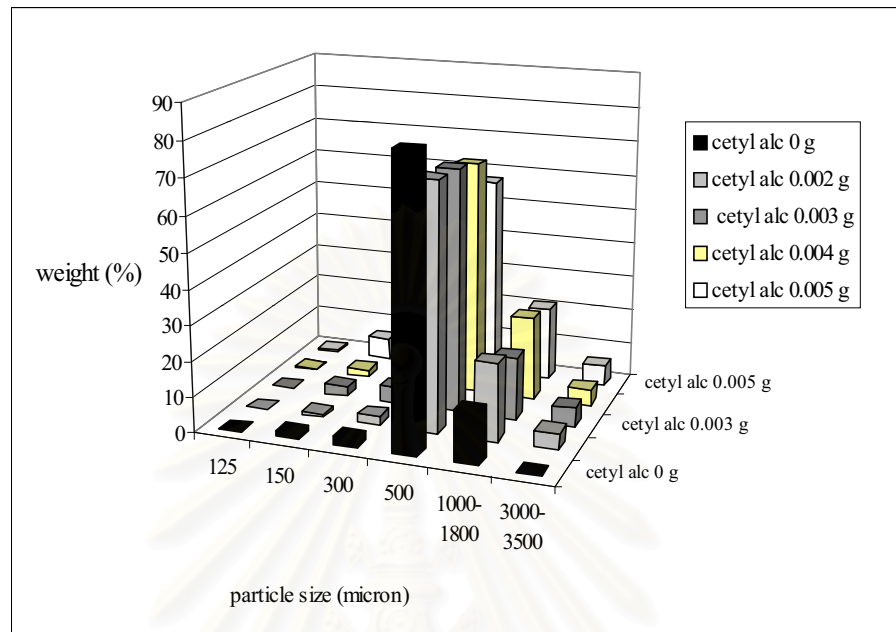


Figure 4.21 Particle size and distribution at cetyl alcohol content of 0-0.005 g.

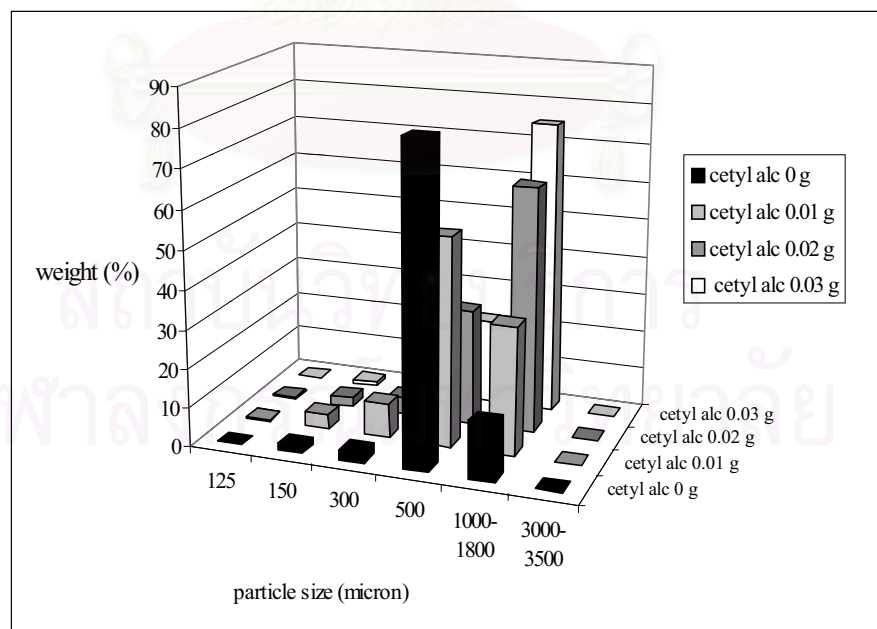


Figure 4.22 Particle size and distribution at cetyl alcohol content of 0.01-0.03 g.

The use of cetyl alcohol tended to produce large particle size with the majority of population falling in the range of 500 - 1800  $\mu\text{m}$ . Broader size distribution was also observed when compared with the case of without cetyl alcohol addition. It is well documented that, in suspension polymerization, suspending agent such as PVA is a dominant factor by providing the protective layer resulting from the surface adsorption. [63] The suspending agent molecules adsorbed by monomer droplets locate at the monomer/water interface which would give coalescence resistance to droplets.

Bao and Brooks [64] reported that nonionic surfactants which have more affinity with monomer droplet than PVA, would be absorbed on the monomer/water interface better than PVA, and a part of interface originally occupied by PVA molecules would become occupied by nonionic surfactant molecules. Thus, the protection ability of suspending agent would decrease because the nonionic surfactant is low molecular weight substance and its protection ability is less than that of PVA.

The solubility of cetyl alcohol in styrene droplet is better than PVA which is a suspending agent used in this work. Therefore, it would be adsorbed faster on the styrene/water interface. As a result, the coalescence resistance from PVA would decrease, leading to large particle size formed with an increase in the amount of cetyl

alcohol. The results reported by Tseng et.al. also indicated that the presence of cetyl alcohol led to the production of large particle size. [65]

Figures 4.23-4.24 show SEM micrographs of polymer bead prepared without and with cetyl alcohol. It can be seen that the roughness of the of polymer bead surface become more regular as cetyl alcohol was added. This may be because the head group of cetyl alcohol increase the hydrophilicity between oil phase (styrene droplet) and the aqueous phase. Adsorption of surfactant results in an increase in the hydrophilic character of the surface. [66]

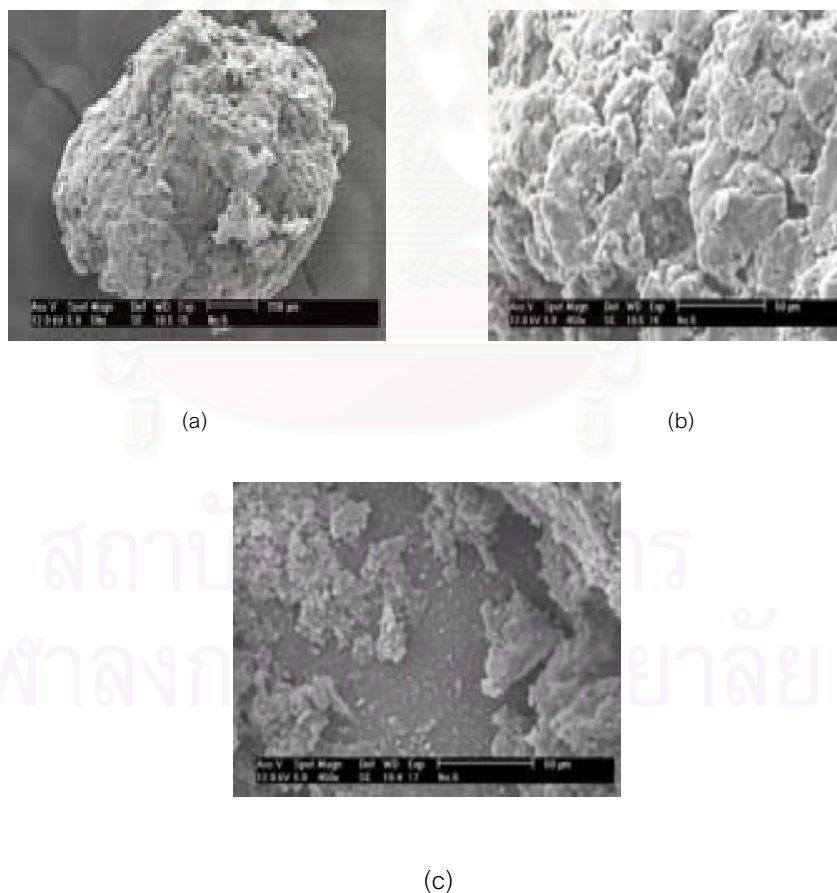


Figure 4.23 SEM micrographs of polymer bead in the absence of cetyl alcohol.

(a) magnification 59X (b) magnification 450X (c) magnification 450X

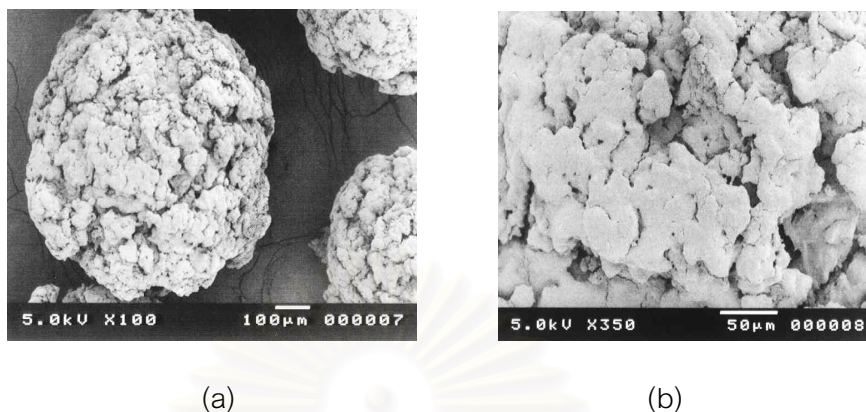


Figure 4.24 SEM micrographs of polymer bead at cetyl alcohol content 0.01 g.

(a) magnification 100X (b) magnification 350X

#### 4.2.6.2 Effect of Cationic Surfactants

In the field of dye adsorbents, large particle size is not desirable due to small surface area that consequently, reduces dye adsorption capability. In order to achieve better control of particle size, cationic surfactant (CTAB) was used to replace cetyl alcohol since this type of surfactants is more capable of decreasing surface tension between styrene phase and water phase. [67] The amounts of CTAB were vary from 0 wt%-0.12 wt% (based on styrene). Tables 4.13-4.14 and Figure 4.15 show the effects of CTAB on polymer particle.

Table 4.13 The relationship between the CTAB content and percent yield

| CTAB content (g) | % Yield |
|------------------|---------|
| 0                | 45.51   |
| 0.002            | 44.14   |
| 0.003            | 46.95   |
| 0.004            | 40.97   |
| 0.005            | 38.27   |

Table 4.14 Effect of CTAB on particle size and particle size distribution

| Particle size ( $\mu\text{m}$ ) | Product weight distribution(%) |       |       |       |       |
|---------------------------------|--------------------------------|-------|-------|-------|-------|
|                                 | CTAB content (g)               |       |       |       |       |
|                                 | 0                              | 0.002 | 0.003 | 0.004 | 0.005 |
| 106                             | 0                              | 0     | 0.97  | 3.95  | 6.52  |
| 125                             | 0                              | 1.20  | 0.72  | 1.08  | 6.45  |
| 150                             | 1.78                           | 8.06  | 9.51  | 22.96 | 67.66 |
| 300                             | 2.59                           | 39.69 | 48.69 | 57.28 | 16.65 |
| 500                             | 81.04                          | 44.99 | 33.97 | 12.18 | 2.71  |
| 1000-1800                       | 14.59                          | 6.06  | 6.14  | 2.55  | 0     |
| 3000-3500                       | 0                              | 0     | 0     | 0     | 0     |



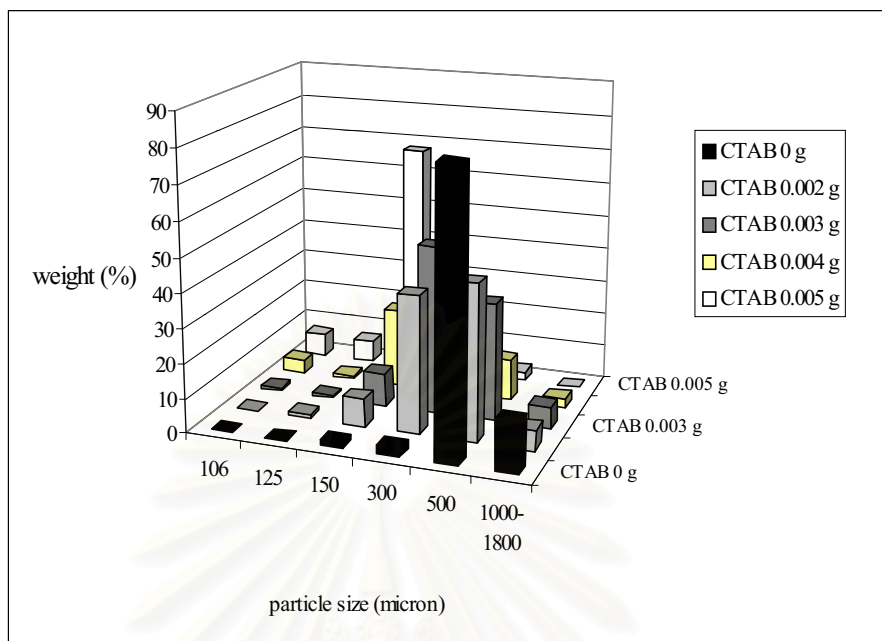


Figure 4.25 Particle size and distribution at different CTAB content.

As can be seen, the particle size obtained using CTAB is smaller than that of cetyl alcohol under the same condition. Mean bead size decreases gradually from 500  $\mu\text{m}$  to 150  $\mu\text{m}$  when the amounts of CTAB increases from 0wt %-0.12 wt%. According to Liu et.al. [21] report, the quaternary ammonium group of a surfactant strongly affected the particle size by means of the electrostatic stabilizer. In this case, the quaternary ammonium group of PMAPTAC radicals was anticipated to further enhance the stabilization of droplet phase. This combination could effectively prevent the coalescence of styrene droplets, leading to a decrease in the final particle size with an increase in amount of surfactant. As the concentration of surfactant further increased,

the stable emulsion was formed. A very fine small particle with irregular shape described as powder was produced.

Scanning electron microscope equipped with X-ray microanalysis was used to determine the elements present on the surface of polymer particle. The results obtained are shown in Table 4.15.

Table 4.15 Elements on polymer particle

| CTAB content (g) | Element (wt %) |          |          |        |        |
|------------------|----------------|----------|----------|--------|--------|
|                  | carbon         | chlorine | nitrogen | oxygen | sulfur |
| PMAPTAC          | 63.96          | 7.91     | 18.13    | 9.35   | 0.66   |
| polystyrene      | 100            | -        | -        | -      | -      |
| 0.002            | 96.57          | 0.02     | -        | 3.37   | 0.04   |
| 0.004            | 95.87          | 0.04     | -        | 4.00   | 0.08   |
| 0.005            | 96.09          | 0.13     | -        | 3.63   | 0.15   |

The result shows that X-ray analysis did not give nitrogen signal. However, it does not mean that nitrogen element is not present on the bead surface due to its trace availability. The presence of nitrogen element was proven by FTIR analysis as shown in Figure 4.26-4.27. From Figure 4.27, the adsorption bands at  $3400\text{ cm}^{-1}$  was the absorbance of NH functional group.

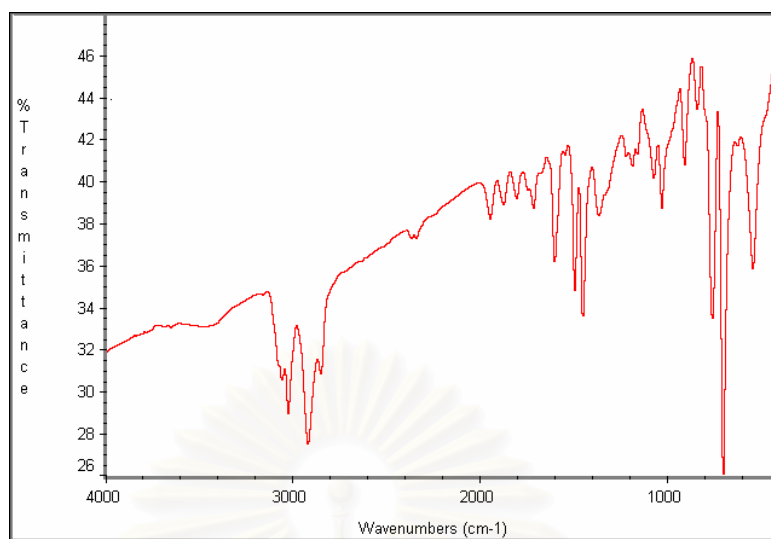


Figure 4.26 FTIR spectrum of polystyrene bead.

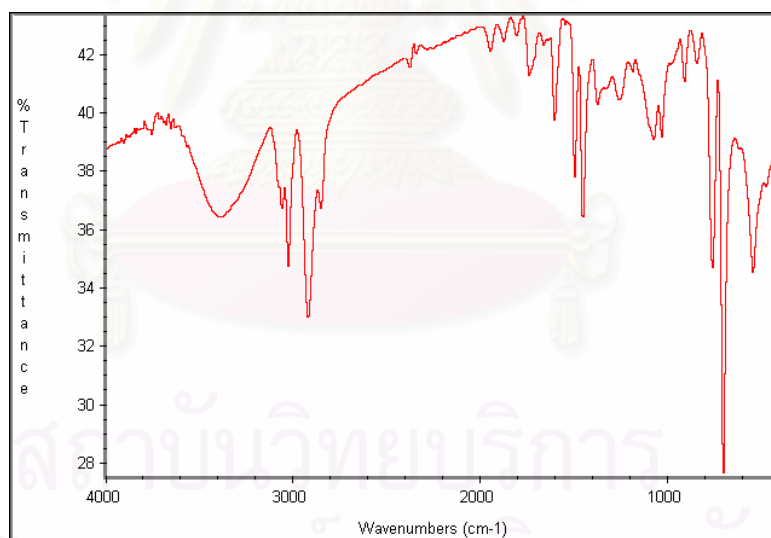


Figure 4.27 FTIR spectrum of polymer bead at CTAB contents of 0.002 g.

Morphology of the final particle revealed by SEM analysis (Figure 4.28) exhibits different shapes. It is believed that outer layer represents the poly(MAPTAC-co-styrene) copolymer, rendering the positive charge to the bead surface. It could be concluded that cationic surfactant of certain range of concentrations is crucial to achieve the desirable bead size with optimum surface charge density.



สถาบันวิทยบริการ  
จุฬาลงกรณ์มหาวิทยาลัย

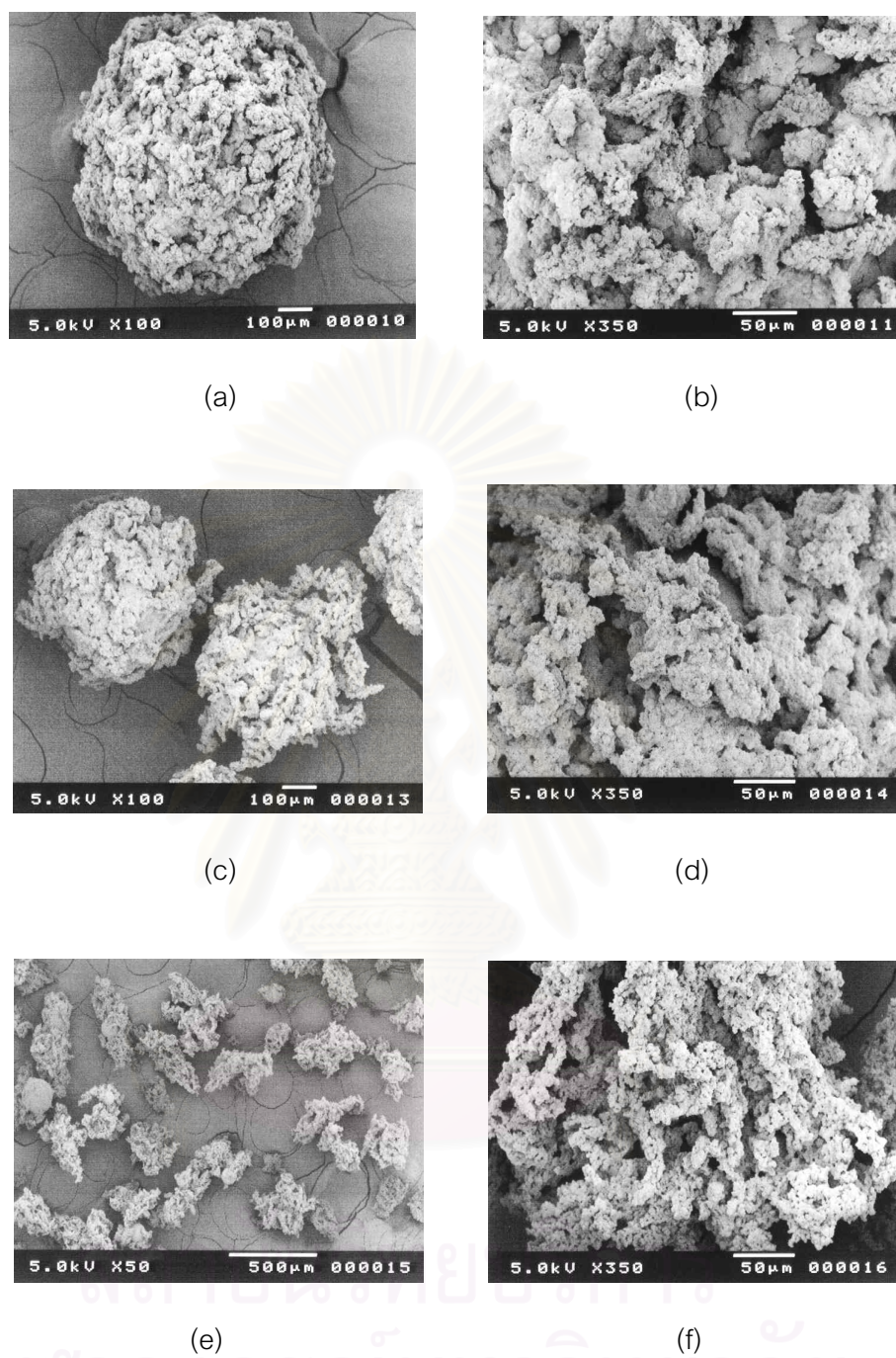


Figure 4.28 SEM micrographs of polymer bead with different amount of CTAB.

(a), (b) CTAB content of 0.002 g ; (c),(d) CTAB content of 0.004 g

(e), (f) CTAB content of 0.005 g

Effect of CTAB content and particle size of polymer bead on dye adsorption were investigated by varying CTAB contents from 0-0.005 g. The result obtained were shown in Table 4.16

Table 4.16 Effect of CTAB content and particle size on dye adsorption

| CTAB content (g) | Particle size ( $\mu\text{m}$ ) | Dye adsorption by bead (mg dye/g adsorbent) |
|------------------|---------------------------------|---|
| Polystyrene bead | 150-1000                        | 0.03  |
| 0                | 150-1000                        | 4.13  |
| 0.002            | 150                             | 7.44  |
|                  | 300                             | 6.77  |
|                  | 500                             | 5.76  |
| 0.004            | 150                             | 7.17  |
|                  | 300                             | 6.33  |
|                  | 500                             | 5.29  |
| 0.005            | 150                             | 7.19  |
|                  | 300                             | 6.21  |
|                  | 500                             | 5.09  |

The dye adsorption of polymer beads were about 5-7 mg/g at different amount of CTAB and particle size. The polymer bead had high dye adsorption when CTAB was used. It indicated that the reaction between PMAPTAC and styrene increased when CTAB was added in polymerization system. The dye adsorption increased when particle size decreased. This was due to the high surface area of particle to absorb dye.

For further experiment, such as the study of adsorption isotherm of polymer bead in reactive dyes, CTAB was chosen for preparation of polymer bead. It was used to reduce the interfacial tension between styrene phase and aqueous phase and to control the particle size of polymer bead better than cetyl alcohol.

#### 4.3 Dye Adsorption Study of the Prepared Bead

The synthetic polymer bead bearing cationic group on the surface was designed to be a color adsorbent for anionic dyes removal from textile wastewater. In this section, dye adsorption isotherm investigation including Langmuir and Freundlich models was carried out. Effects of particle sizes and contact time were also examined.



#### 4.3.1 Determination of Contact Time

Dye adsorption equilibrium experiments of three reactive dyes (C.I. Reactive Blue 171, C.I. Reactive Red 195, and C.I. Reactive yellow 84) were performed at the room temperature and at 80°C. The contact time was determined by mixing of polymer beads with reactive dye solution and shaking at the constant temperature. Measurement of dye adsorption by UV/VIS spectrophotometer at 10-120 minutes was conducted. The relation between time of adsorption and ratio of concentration of dye at time t and original dye concentration ( $C_t / C_o$ ) are shown in Tables 4.17-4.19 and Figures 4.29-4.31.

Table 4.17 Effect of contact time on the adsorption of C.I. Reactive Blue 171 by the polymer bead

| Time (minutes) | $C_t / C_o$                        |                                    |
|----------------|------------------------------------|------------------------------------|
|                | Particle size of 150 $\mu\text{m}$ | Particle size of 500 $\mu\text{m}$ |
| 0              | 1.00                               | 1.00                               |
| 10             | 0.62                               | 0.84                               |
| 20             | 0.59                               | 0.78                               |
| 30             | 0.65                               | 0.80                               |
| 60             | 0.61                               | 0.80                               |
| 90             | 0.61                               | 0.80                               |
| 120            | 0.61                               | 0.80                               |



Table 4.18 Effect of contact time on the adsorption of C.I. Reactive Red 195 by the polymer bead

| Time (minutes) | $C_t / C_o$                        |                                    |
|----------------|------------------------------------|------------------------------------|
|                | Particle size of 150 $\mu\text{m}$ | Particle size of 500 $\mu\text{m}$ |
| 0              | 1.00                               | 1.00                               |
| 10             | 0.76                               | 0.89                               |
| 20             | 0.67                               | 0.86                               |
| 30             | 0.76                               | 0.89                               |
| 60             | 0.74                               | 0.89                               |
| 90             | 0.74                               | 0.89                               |
| 120            | 0.74                               | 0.89                               |

Table 4.19 Effect of contact time on the adsorption of C.I. Reactive Yellow 84 by the polymer bead

| Time (minutes) | $C_t / C_o$                        |                                    |
|----------------|------------------------------------|------------------------------------|
|                | Particle size of 150 $\mu\text{m}$ | Particle size of 500 $\mu\text{m}$ |
| 0              | 1.00                               | 1.00                               |
| 10             | 0.58                               | 0.73                               |
| 20             | 0.57                               | 0.73                               |
| 30             | 0.58                               | 0.73                               |

Table 4.19 Effect of contact time on the adsorption of C.I. Reactive Yellow 84 by the polymer bead (continued)

| Time (minutes) | $C_t / C_o$                        |                                    |
|----------------|------------------------------------|------------------------------------|
|                | Particle size of 150 $\mu\text{m}$ | Particle size of 500 $\mu\text{m}$ |
| 20             | 0.57                               | 0.73                               |
| 30             | 0.58                               | 0.73                               |
| 60             | 0.57                               | 0.73                               |
| 90             | 0.57                               | 0.73                               |
| 120            | 0.57                               | 0.73                               |

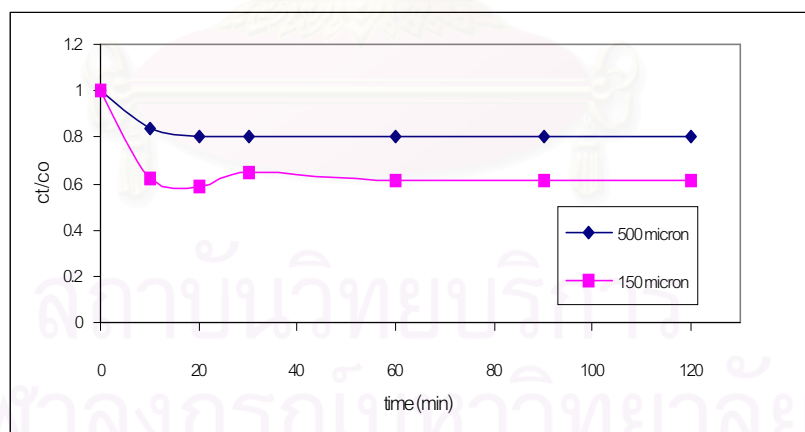


Figure 4.29 Effect of contact time on the adsorption of reactive blue by the polymer bead at temperature of 80°C.

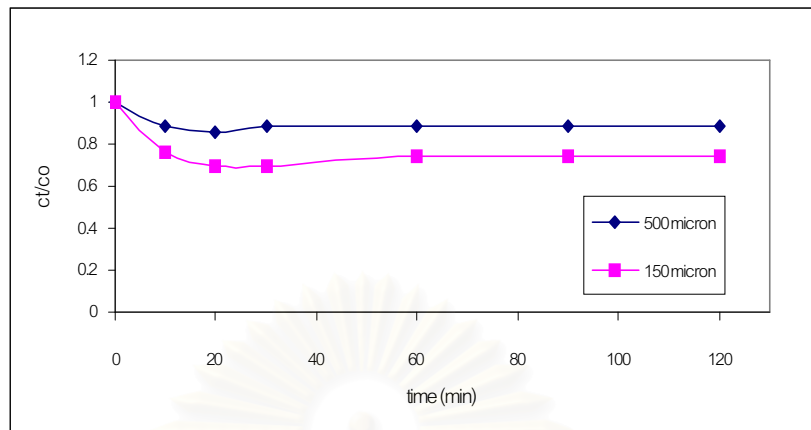


Figure 4.30 Effect of contact time on the adsorption of reactive red by the polymer bead at temperature of 80°C.

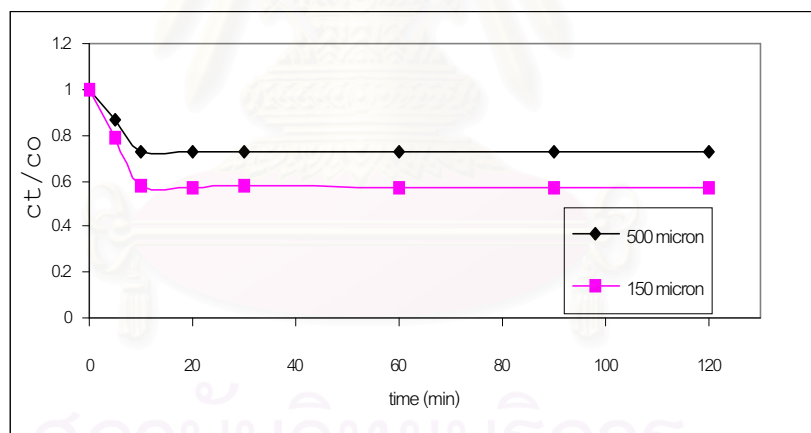


Figure 4.31 Effect of contact time on the adsorption of reactive yellow by the polymer bead at temperature of 80°C.

The results show that the dye adsorption rate is high at the initial period of contact time that reflects the strong attraction force between anionic dye molecule and cationic surface of the polymer bead. The adsorption reaches equilibrium rate at the contact time of 20 minute. In addition, an increase in adsorption with decreasing particle size suggests that anionic dyes did not seem to penetrate the whole particle but rather adsorb on the surface of the polymer bead. Therefore, adsorption performance would rely on the surface area; the higher the surface area (the smaller particle size), the higher the adsorption capacity.

#### 4.3.2 Adsorption Isotherm

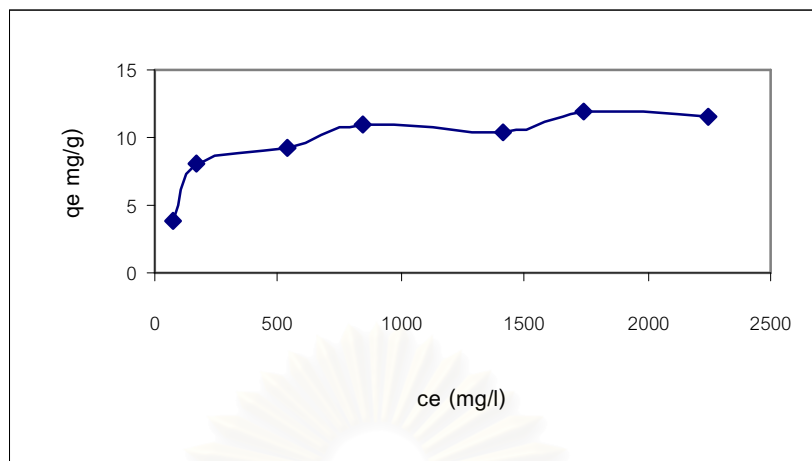
When a solution is contacted with a solid adsorbent, the molecule of adsorbate transfer from the fluid to the solid until the concentration of adsorbate in solution is in equilibrium with the adsorbate on the solid. The equilibrium data at a given temperature are usually described by an adsorption isotherm, which is the relationship between the quantity adsorbed per unit mass of solid and the concentration of adsorbate in solution. To measure an adsorption isotherm, known quantities of solid adsorbent and solution are contacted at constant temperature until the solution does not change in composition with time. The adsorption isotherm can be calculated from the measured concentrations of adsorbate in solution at the start and at equilibrium.

A reactive dye solution of known concentration  $C_0$  was added to the container of polymer bead, which was continuously shaken to allow the adsorption equilibrium. The amount of adsorbed dye ( $q_e$ ) was calculated using the equation of  $q_e = (C_0 - C_e) V / W$  where  $C_0$  = initial dye concentration,  $C_e$  = equilibrium concentration of dye in solution,  $V$  is volume of dye solution and  $W$  is the weight of polymer bead.

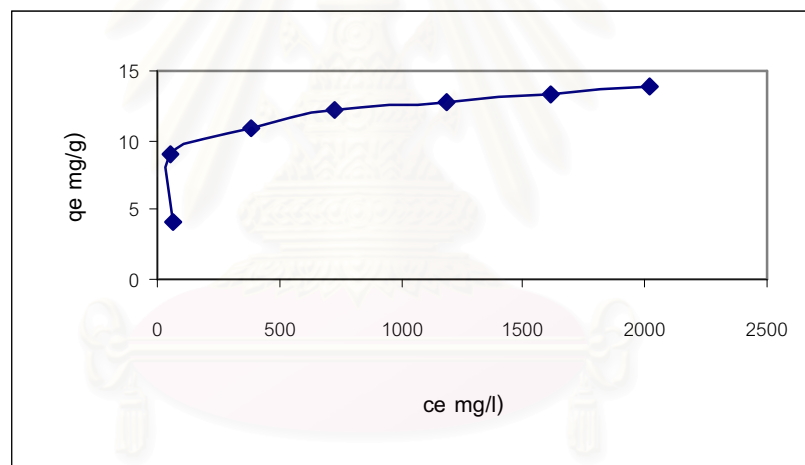
The initial dye concentration ( $C_0$ ) was about 500-3500 mg/l. The polymer beads with the particle sizes ranging from 150-500  $\mu\text{m}$  were employed and the adsorption experiment was carried out at the room temperature and the temperature of 80°C. The typical adsorption isotherms of polymer bead for three reactive dyes are shown in Figures 4.32-4.34 and experimental data in Appendix C and D.



สถาบันวิทยบริการ  
จุฬาลงกรณ์มหาวิทยาลัย



(a)

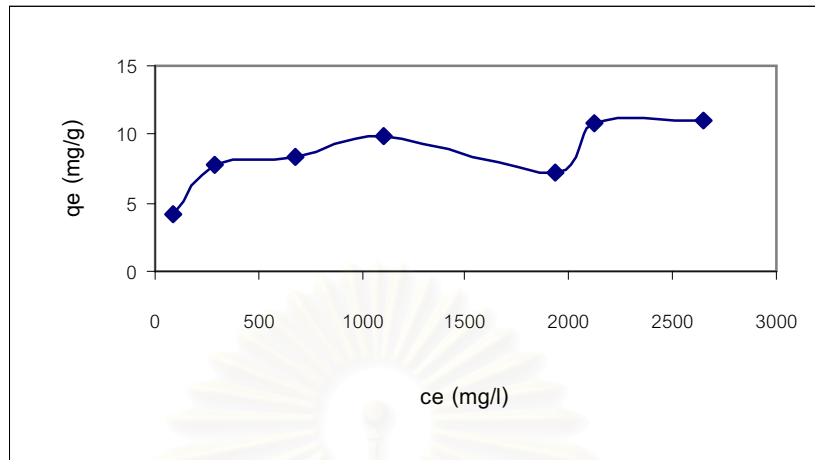


(b)

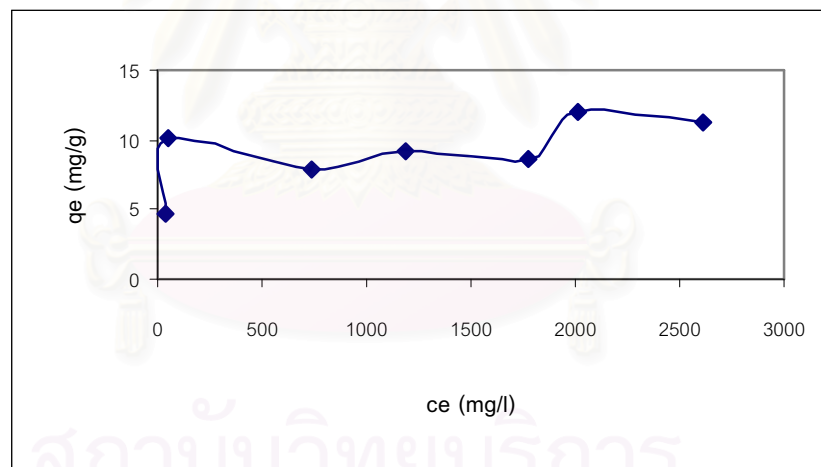
Figure 4.32 Equilibrium adsorption isotherms of reactive blue on polymer bead at particle of 150  $\mu\text{m}$ .

(a) at room temperature

(b) at temperature of 80°C



(a)

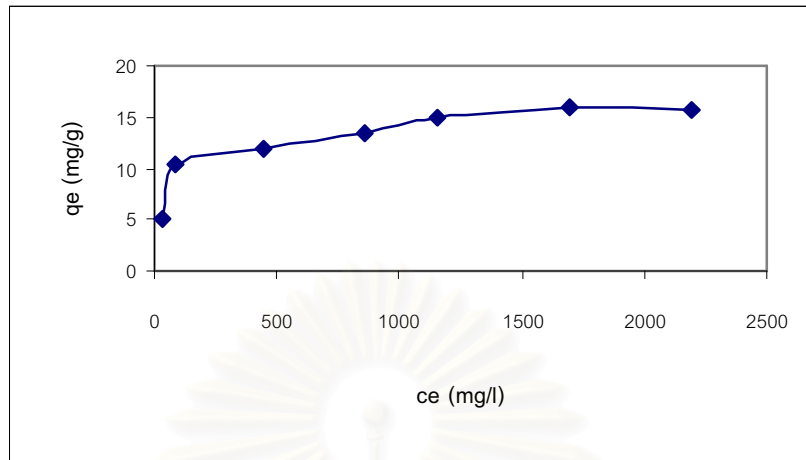


(b)

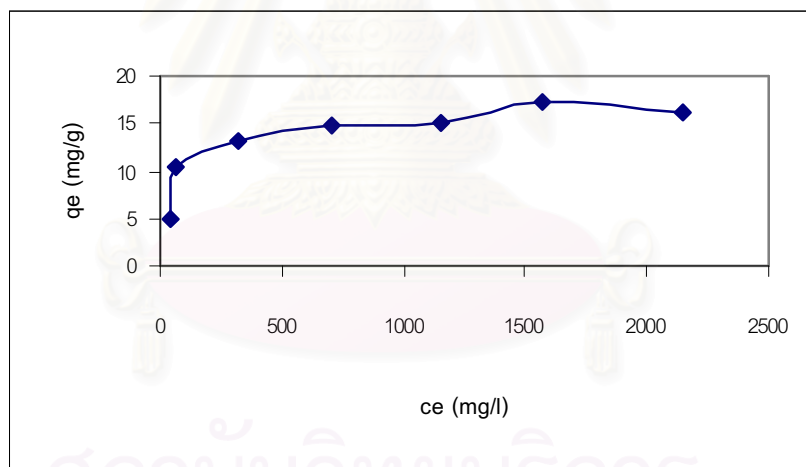
Figure 4.33 Equilibrium adsorption isotherms of reactive red on polymer bead at particle of 150  $\mu\text{m}$ .

(a) at room temperature

(b) at temperature of 80°C



(a)



(b)

Figure 4.34 Equilibrium adsorption isotherms of reactive red on polymer bead at particle of 150  $\mu\text{m}$ .

(a) at room temperature

(b) at temperature of 80°C



The adsorption of reactive dye on polymer beads was due to the ionic interaction between the negative charge on dyestuff and the positive charge on polymer bead. The results obtained show that the adsorption isotherm had a shape corresponding to the classification by Giles et.al.. [40] The dye adsorption is high at initial and then level off. This represents a monolayer adsorption of reactive dyes, which is found in good agreement with the report of Kipling. [68]

#### 4.3.2.1 Effect of Particle Size on Adsorption Isotherm

Concerning the adsorption, the particle surface area plays a dominant role in the adsorption capacity. Therefore, the effect of particle size on adsorption isotherm was investigated. Polymer beads of three particle sizes (150, 300, and 500  $\mu\text{m}$ ) were used to study the adsorption isotherm of three reactive dyes (blue, red, and yellow). The influence of particle size represented by the  $C_e$  VS  $q_e$  curve is graphically illustrated in Figures 4.35-4.40.

สถาบันวิทยบริการ  
จุฬาลงกรณ์มหาวิทยาลัย

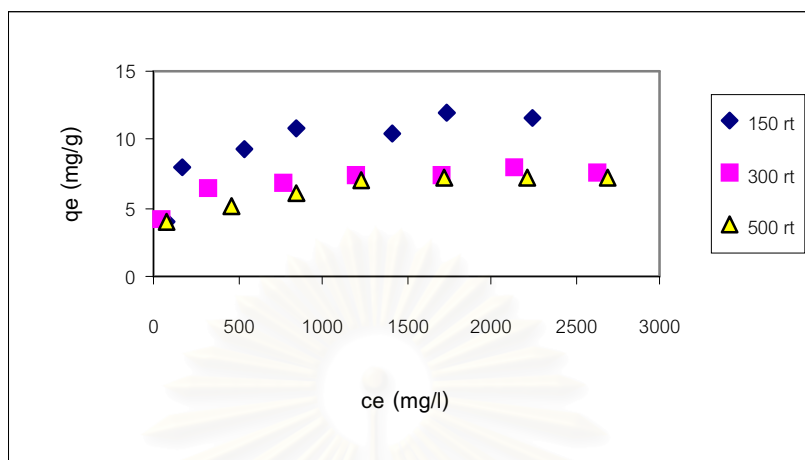


Figure 4.35 Effect of particle size on the equilibrium adsorption isotherm of reactive blue at room temperature.

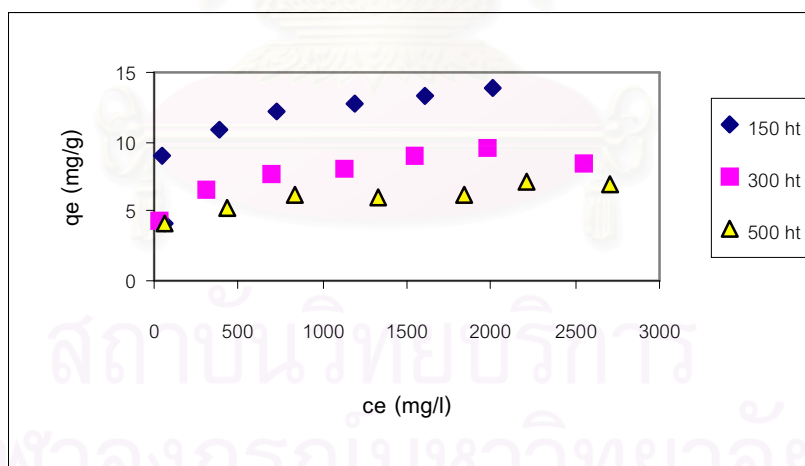


Figure 4.36 Effect of particle size on the equilibrium adsorption isotherm of reactive blue at temperature of 80°C.

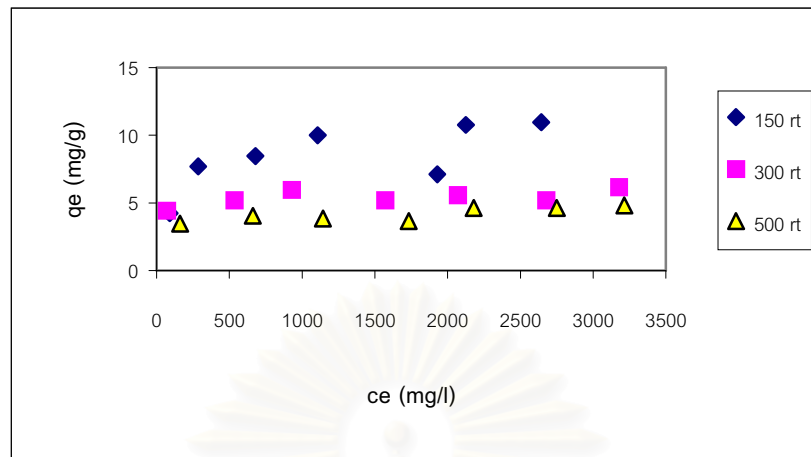


Figure 4.37 Effect of particle size on the equilibrium adsorption isotherm of reactive red at room temperature.

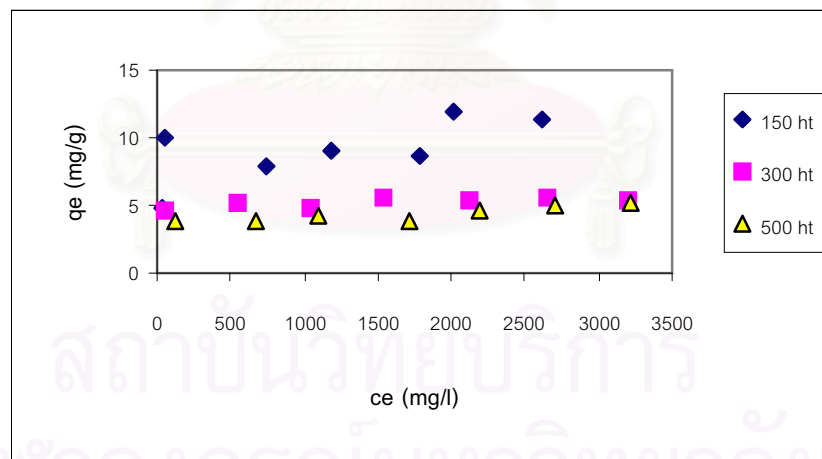


Figure 4.38 Effect of particle size on the equilibrium adsorption isotherm of reactive red at temperature of 80°C.

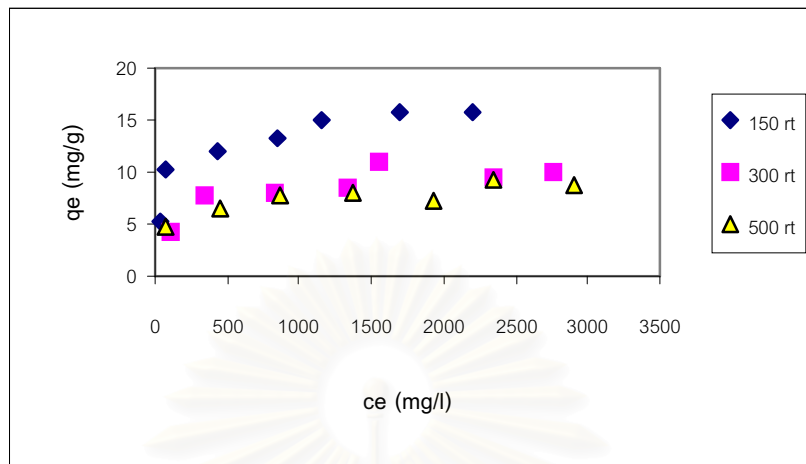


Figure 4.39 Effect of particle size on the equilibrium adsorption isotherm of reactive yellow at room temperature.

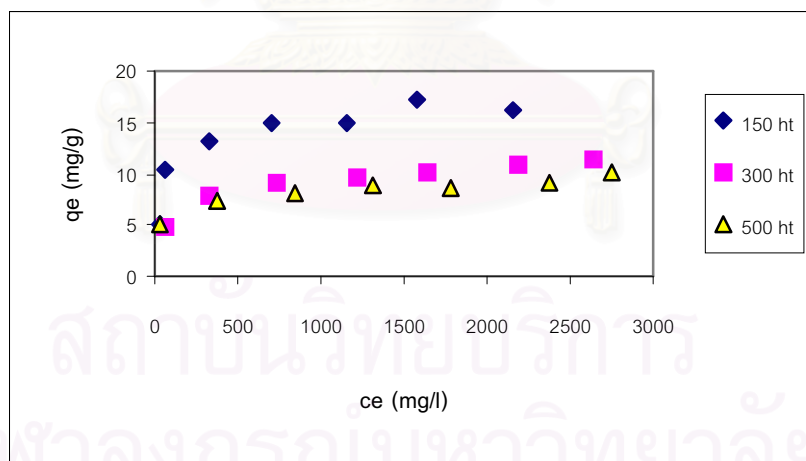


Figure 4.40 Effect of particle size on the equilibrium adsorption isotherm of reactive yellow at temperature of 80°C.

As can be seen, the adsorption capacity of the three reactive dyes is related to the particle size of the polymer bead; the smaller the particle size, the higher the adsorb capacity. The results indicate that total surface area governs the amount of dye uptake.

#### 4.3.2.2 Effect of Temperature on Adsorption Isotherm

The effect of adsorption temperature on adsorption isotherm was investigated. Figures 4.41-4.43 and Appendix E show the adsorption isotherm for blue, red, and yellow dyes at a constant temperature (room temperature and 80°C), which are the relationships between the amount of dye adsorbed per unit mass of adsorbent ( $q_e$ ) and residue dye concentration ( $C_e$ ). The typical shape of the isotherms indicates the formation of a monolayer on the polymer bead surface which exhibits a steep slope at the low concentration range. [68]

In all cases of studied dyes, it could be said that adsorption temperature played an indifferent role in controlling the dye adsorption. It is, therefore, difficult to claim that the adsorption phenomenon was exothermic or endothermic mechanism (eg. In the case of endothermic, adsorption increases with the increased temperature). It was likelihood to observe the tendency in the increased dye sorption with the rise in the temperature. It was also probable that the binding force between cationic charge surface and the anionic dye molecules were very strong due to their high molecular

weight with a number of sulphonate groups. Consequently, the effect of temperature on dye adsorption performance seemed to be negligible.

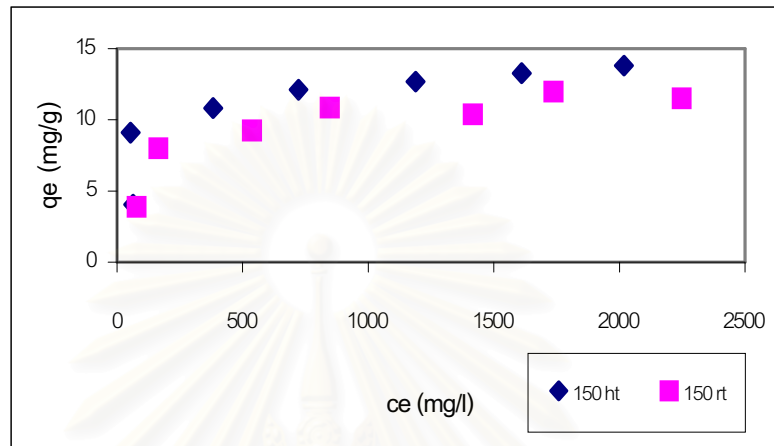


Figure 4.41 Effect of temperature on the equilibrium adsorption isotherm of reactive blue on polymer bead at particle size of 150  $\mu\text{m}$ .

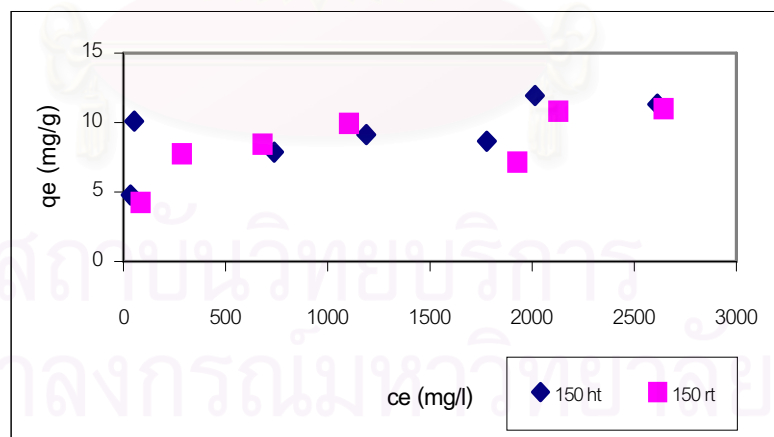


Figure 4.42 Effect of temperature on the equilibrium adsorption isotherm of reactive red on polymer bead at particle size of 150  $\mu\text{m}$ .

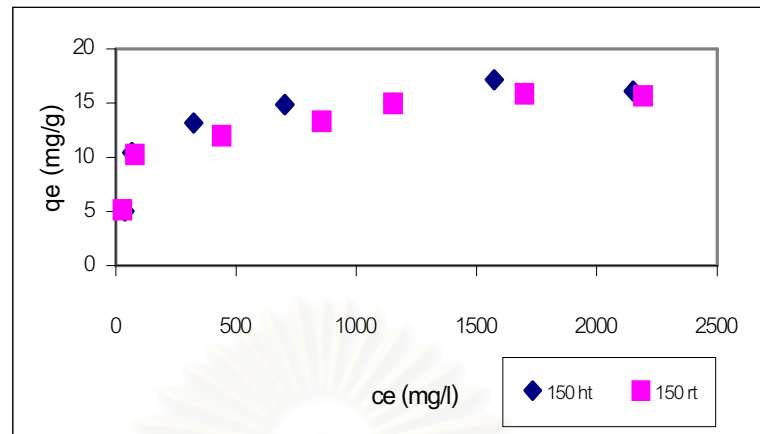


Figure 4.43 Effect of temperature on the equilibrium adsorption isotherm of reactive yellow on polymer bead at particle size of 150  $\mu\text{m}$ .

### 4.3.3 Analysis of Adsorption Isotherm

The Freundlich and Langmuir isotherms of the adsorbed dyes were investigated as follows.

#### 4.3.3.1 Analysis Through Freundlich Isotherm

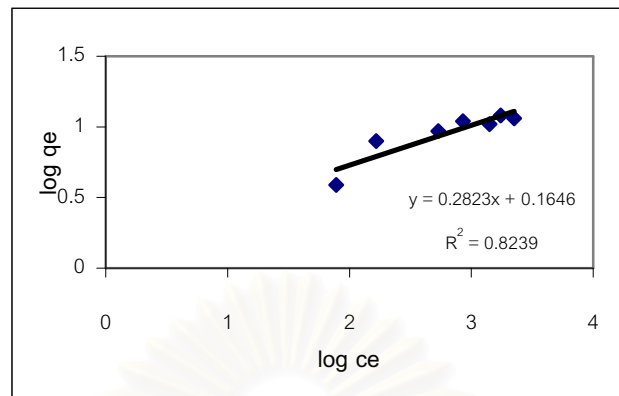
Freundlich Isotherm was utilized in analyzing the adsorption of reactive dyes on polymer bead. The Freundlich equation for a linear plot is expressed as.

$$\log q_e = \log k + 1/n \log C_e$$

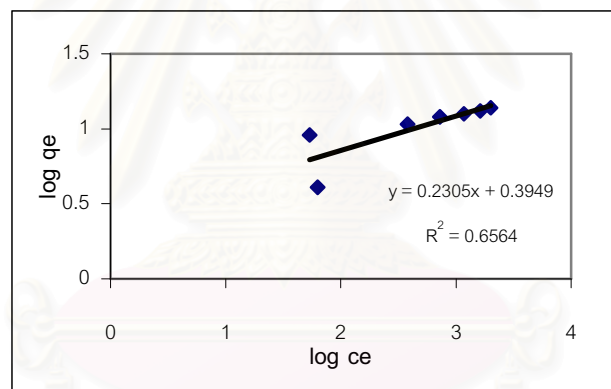
where  $q_e = (C_o - C_e) v / W$ ;  $C_o$  and  $C_e$  are the initial and equilibrium concentration of dye in solution, respectively (mg/l);  $q_e$  is the milligram of adsorbed dye per gram of adsorbent (mg/g);  $v$  is the volume of dye solution (ml);  $W$  is the amount of adsorbent required to adsorb dye (g). The  $n$  values calculate from the slope of Freundlich plot.

Figures 4.44-4.46 and Appendix F show the isotherms of three reactive dyes on 150-500  $\mu\text{m}$  of polymer bead at room temperature and at 80°C. Tables 4.20-4.21 summarizes the linear equation and Freundlich constants obtained from the plots shown in Figures 4.44-4.46 and Appendix F. In all cases,  $n$  value are above 1. However, the  $R^2$  from the linear equation were quite low, especially in reactive red, which indicates that the isotherms were not fitted well with Freundlich isotherm.





(a)

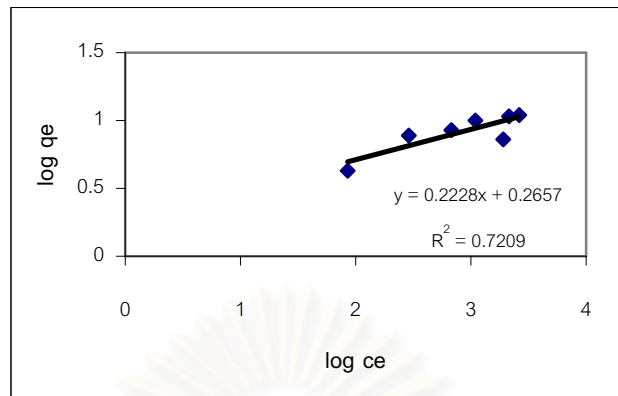


(b)

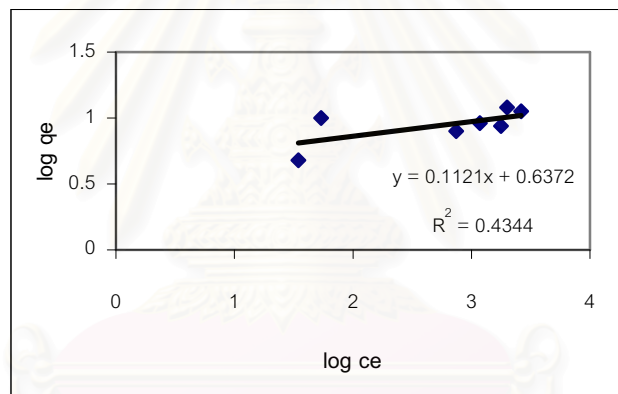
Figure 4.44 Freundlich plots for the adsorption of reactive blue on bead 150  $\mu\text{m}$ .

(a) at room temperature

(b) at 80°C



(a)

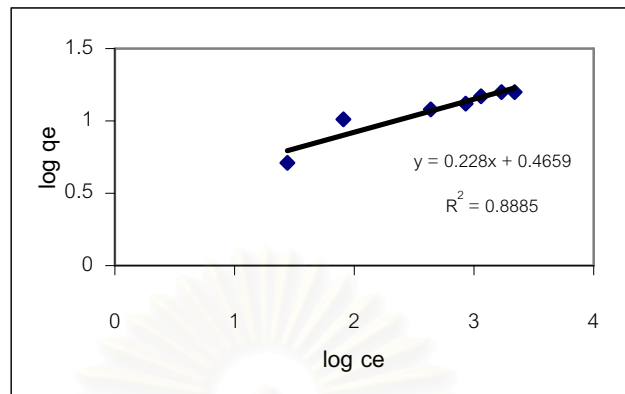


(b)

Figure 4.45 Freundlich plots for the adsorption of reactive red on bead 150  $\mu\text{m}$ .

(a) at room temperature

(b) at 80°C



(a)



(b)

Figure 4.46 Freundlich plots for the adsorption of reactive yellow on bead 150  $\mu\text{m}$ .

(a) at room temperature

(b) at 80°C

Table 4.20 Linear equation from Freundlich plots

| Type of dyes | Particle size ( $\mu\text{m}$ ) | Condition        | Linear equation        | $R^2$  |
|--------------|---------------------------------|------------------|------------------------|--------|
| Blue         | 150                             | room temperature | $y = 0.2823x + 0.1646$ | 0.8239 |
|              |                                 | 80°C             | $y = 0.2305x + 0.3949$ | 0.6564 |
|              | 300                             | room temperature | $y = 0.1537x + 0.3830$ | 0.9320 |
|              |                                 | 80°C             | $y = 0.1712x + 0.3890$ | 0.9584 |
|              | 500                             | room temperature | $y = 0.1790x + 0.2610$ | 0.9583 |
|              |                                 | 80°C             | $y = 0.1369x + 0.3722$ | 0.9283 |
| Red          | 150                             | room temperature | $y = 0.2228x + 0.2657$ | 0.7209 |
|              |                                 | 80°C             | $y = 0.1121x + 0.6372$ | 0.4344 |
|              | 300                             | room temperature | $y = 0.0706x + 0.5213$ | 0.6063 |
|              |                                 | 80°C             | $y = 0.0384x + 0.6012$ | 0.6081 |
|              | 500                             | room temperature | $y = 0.1132x + 0.2731$ | 0.5909 |
|              |                                 | 80°C             | $y = 0.0784x + 0.4029$ | 0.4713 |
| Yellow       | 150                             | room temperature | $y = 0.2280x + 0.4659$ | 0.8885 |
|              |                                 | 80°C             | $y = 0.2416x + 0.4569$ | 0.8038 |
|              | 300                             | room temperature | $y = 0.2378x + 0.2117$ | 0.8443 |
|              |                                 | 80°C             | $y = 0.2213x + 0.3072$ | 0.9811 |
|              | 500                             | room temperature | $y = 0.1624x + 0.3861$ | 0.8954 |
|              |                                 | 80°C             | $y = 0.1439x + 0.4883$ | 0.9748 |

Table 4.21 Linear equation from Freundlich plots

| Type of dyes | Particle size ( $\mu\text{m}$ ) | Condition        | Freundlich constant |       |
|--------------|---------------------------------|------------------|---------------------|-------|
|              |                                 |                  | 1/n                 | n     |
| Blue         | 150                             | room temperature | 0.2823              | 3.54  |
|              |                                 | 80°C             | 0.2305              | 4.34  |
|              | 300                             | room temperature | 0.1537              | 6.51  |
|              |                                 | 80°C             | 0.1712              | 5.84  |
|              | 500                             | room temperature | 0.1790              | 5.59  |
|              |                                 | 80°C             | 0.1369              | 7.30  |
| Red          | 150                             | room temperature | 0.2228              | 4.49  |
|              |                                 | 80°C             | 0.1121              | 8.92  |
|              | 300                             | room temperature | 0.0706              | 14.16 |
|              |                                 | 80°C             | 0.0384              | 26.04 |
|              | 500                             | room temperature | 0.1132              | 8.83  |
|              |                                 | 80°C             | 0.0784              | 12.76 |
| Yellow       | 150                             | room temperature | 0.2280              | 4.39  |
|              |                                 | 80°C             | 0.2416              | 4.14  |
|              | 300                             | room temperature | 0.2378              | 4.21  |
|              |                                 | 80°C             | 0.2213              | 4.52  |
|              | 500                             | room temperature | 0.1624              | 6.16  |
|              |                                 | 80°C             | 0.1439              | 6.95  |

#### 4.3.3.2 Analysis Through Langmuir Isotherm

The linear representation of the Langmuir isotherm can be expressed as.

$$C_e / q_e = 1/Q_0b + C_e/Q_0$$

A plot of  $C_e / q_e$  versus  $C_e$  should yield a straight line having a slope  $1/Q_0$ . The Langmuir adsorption isotherms are shown in Figures 4.47-4.49. The linear equation and Langmuir constant are shown in Tables 4.22-4.23. Utilizing the Langmuir isotherm to analyze the equilibrium isotherms of the three reactive dyes gave the linear plots. The value of  $Q_0$  represents the maximum adsorption capacity of the polymer bead to the reactive dyes. The maximum adsorption capacities were in the range of 7.11-14.33 mg/g, 5.30-11.28 mg/g, and 9.00-16.92 mg/g for reactive blue, red, and yellow, respectively. Therefore, the reactive yellow had the highest adsorption capacity and the lowest was reactive red.

From  $Q_0$ , the small size of the polymer bead increased adsorption of reactive dyes. This was due to the small size of particles have higher surface area than the large sizes.

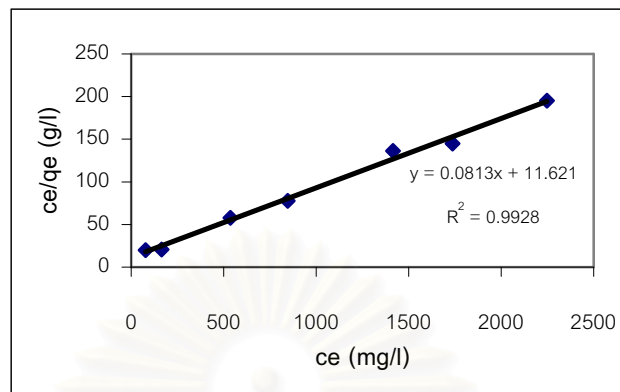
The effect of temperature on the maximum adsorption capacity of the polymer bead for these reactive dyes showed that  $Q_0$  tend to increase with increasing temperature. This may be because the mobility of dye increases with temperature. [54]

The maximum adsorption capacity was related to the structure of polymer bead. The bead consists of the inner core and outer shell. The inner core is polystyrene that does not have the functional group to adsorb the molecule of dye. The outer shell has some functional group of PMAPTAC that can adsorb the reactive dyes. From this structure, it induced the quite low of maximum adsorption capacity.

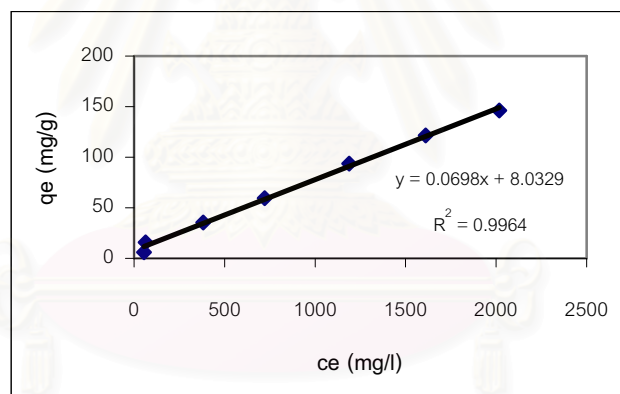
From linear equation,  $R^2$  indicate the linear relationship between x and y. In Langmuir isotherm, the value of  $R^2$  is quite high, indicating a strong linear relationship. This implies that the adsorption isotherms of reactive dyes are fitted well by a Langmuir isotherm than by a Freundlich isotherm.



สถาบันวิทยบริการ  
จุฬาลงกรณ์มหาวิทยาลัย



(a)



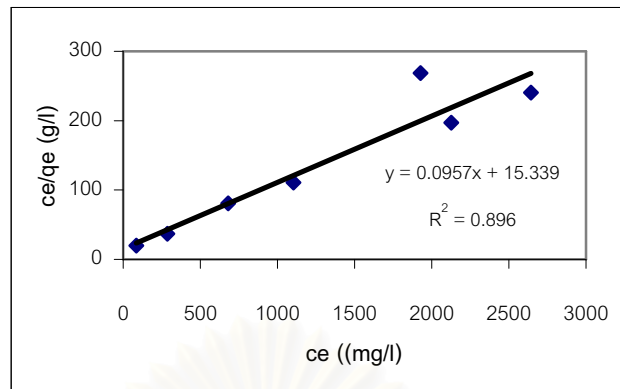
(b)

Figure 4.47 Langmuir plots for the adsorption of reactive blue on bead at particle size of 150  $\mu\text{m}$ .

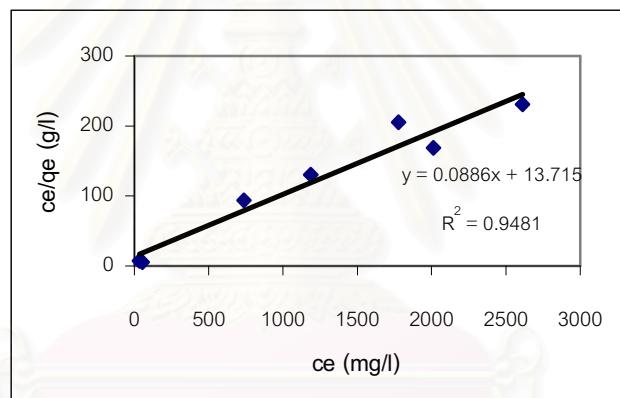
(a) at room temperature

(b) at 80°C





(a)

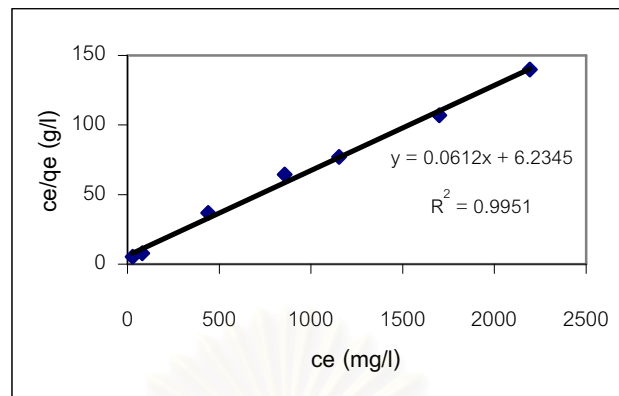


(b)

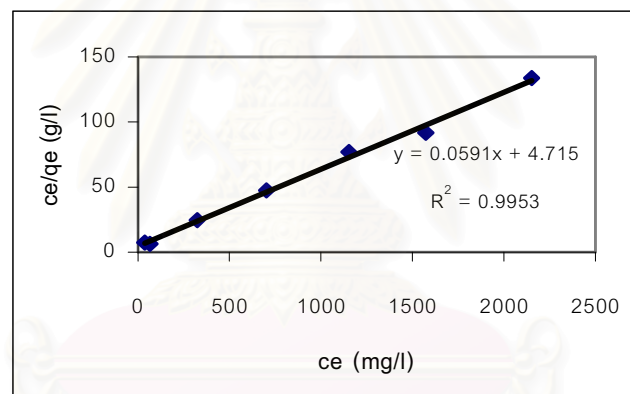
Figure 4.48 Langmuir plots for the adsorption of reactive red on bead at particle size of  $150 \mu\text{m}$ .

(a) at room temperature

(b) at  $80^\circ\text{C}$



(a)



(b)

Figure 4.49 Langmuir plots for the adsorption of reactive yellow on bead at particle size of 150  $\mu\text{m}$ .

(a) at room temperature      (b) at 80°C

Table 4.22 Linear equation from Langmuir plots

| Type of dyes | Particle size ( $\mu\text{m}$ ) | Condition        | Linear equation         | $R^2$  |
|--------------|---------------------------------|------------------|-------------------------|--------|
| Blue         | 150                             | room temperature | $y = 0.0813x + 11.6210$ | 0.9928 |
|              |                                 | 80°C             | $y = 0.0698x + 8.0329$  | 0.9964 |
|              | 300                             | room temperature | $y = 0.1251x + 10.1870$ | 0.9975 |
|              |                                 | 80°C             | $y = 0.1095x + 8.9160$  | 0.9871 |
|              | 500                             | room temperature | $y = 0.1314x + 18.5660$ | 0.9957 |
|              |                                 | 80°C             | $y = 0.1407x + 18.1690$ | 0.9863 |
| Red          | 150                             | room temperature | $y = 0.0957x + 15.3390$ | 0.8960 |
|              |                                 | 80°C             | $y = 0.0886x + 13.7150$ | 0.9481 |
|              | 300                             | room temperature | $y = 0.1703x + 11.1740$ | 0.9810 |
|              |                                 | 80°C             | $y = 0.1804x + 9.5650$  | 0.9966 |
|              | 500                             | room temperature | $y = 0.1887x + 59.0050$ | 0.9494 |
|              |                                 | 80°C             | $y = 0.1883x + 46.5170$ | 0.9663 |
| Yellow       | 150                             | room temperature | $y = 0.0612x + 6.2345$  | 0.9951 |
|              |                                 | 80°C             | $y = 0.0591x + 4.7150$  | 0.9953 |
|              | 300                             | room temperature | $y = 0.0958x + 15.1930$ | 0.9856 |
|              |                                 | 80°C             | $y = 0.0853x + 14.8390$ | 0.9950 |
|              | 500                             | room temperature | $y = 0.1111x + 16.2570$ | 0.9750 |
|              |                                 | 80°C             | $y = 0.0999x + 14.5780$ | 0.9870 |

Table 4.23 Linear equation from Langmuir plots

| Type of dyes | Particle size ( $\mu\text{m}$ ) | Condition        | Langmuir constant |       |
|--------------|---------------------------------|------------------|-------------------|-------|
|              |                                 |                  | $1/Q_0$           | $Q_0$ |
| Blue         | 150                             | room temperature | 0.0813            | 12.30 |
|              |                                 | 80°C             | 0.0698            | 14.33 |
|              | 300                             | room temperature | 0.1251            | 7.99  |
|              |                                 | 80°C             | 0.1095            | 9.13  |
|              | 500                             | room temperature | 0.1314            | 7.61  |
|              |                                 | 80°C             | 0.1407            | 7.11  |
| Red          | 150                             | room temperature | 0.0957            | 10.45 |
|              |                                 | 80°C             | 0.0886            | 11.28 |
|              | 300                             | room temperature | 0.1703            | 5.87  |
|              |                                 | 80°C             | 0.1804            | 5.54  |
|              | 500                             | room temperature | 0.1887            | 5.30  |
|              |                                 | 80°C             | 0.1883            | 5.31  |
| Yellow       | 150                             | room temperature | 0.0612            | 16.34 |
|              |                                 | 80°C             | 0.0591            | 16.92 |
|              | 300                             | room temperature | 0.0958            | 10.44 |
|              |                                 | 80°C             | 0.0853            | 11.72 |
|              | 500                             | room temperature | 0.1111            | 9.00  |
|              |                                 | 80°C             | 0.0999            | 10.01 |

## CHAPTER V

### CONCLUSIONS

This experiment concerned with the preparation of polystyrene beads bearing cationic surface charge. The bead synthesis was conducted using one-pot suspension polymerization of styrene and divinylbenzene in the presence of cationic functional monomer, MAPTAC. Two initiators,  $K_2S_2O_8$  (water soluble) and AIBN (oil soluble) were employed in order to achieve the final bead particle containing surface charged. Several synthesis parameters affecting bead formation were summarized as follows:

1. Polymerization time of MAPTAC (carried out at the first stage) was not found to affect the particle size. This was attributed to the insignificant difference of PMAPTAC chain length with various polymerization time of MAPTAC. Polymerization time carried out in the second stage (between PMAPTAC radical, styrene, and DVB) was also found having an effect on the final bead size.

2. The increase in the polymerization temperature resulted in an increase in the particle size of the polymer beads due to the coalescence of styrene-DVB droplets, faster polymerization rate between PMAPTAC radical, styrene, and DVB, and the increase in the agglomerate of outer layer.

3. An increase in the stirring speed tended to produce polymer beads with smaller size due to the breakage of monomer droplets.

4. An increase in the content of DVB did not change the final particle size but the surface irregularity and surface functionality decreased with increasing DVB content.

5. In the case of cetyl alcohol (nonionic surfactant) , the high amount used tended to produce large particle size due to the fact that the coalescence of monomer droplets rose.

6. In the case of replacement of cetyl alcohol with a cationic surfactant (CTAB), the particle size obtained using CTAB was smaller than that of cetyl alcohol under the same condition due to the electrostatic effect of the quaternary ammonium groups of the surfactant. Moreover, the use of cationic surfactant with the certain concentration range could produce the final particles with desirable bead size.

7. Finally, the dye adsorption study of the prepared beads was carried out to evaluate its performance as an ion exchange. The results showed that adsorption mechanism involved the opposite charge interaction between the bead cationic group and the dye anionic group. The adsorption capacity of polymer beads with reactive dyes was depended on the particle size. The adsorption data was fit with the Langmuir adsorption isotherm when compared with a Freundlich adsorption isotherm.

### Recommendations for future work

1. Polymer beads of PMAPTAC should be synthesized by suspension polymerization using water in oil condition.
2. To improve the characteristic of final bead particle, the comonomer should be more hydrophilic than styrene.
3. Adsorption capacity of other dyes such as acid dyes and disperse dyes should be investigated.



สถาบันวิทยบริการ  
จุฬาลงกรณ์มหาวิทยาลัย

## REFERENCES

1. Nemerow, N. L. Treatment of Textile Wastes Industrial Water Pollution : Origins, Characteristics and Treatment. New York: Addison-Wesley, 1978.
2. Chandran, C.B.; Singh, D.; and Nigam, P. Remedation of Textile Effluent Using Agricultural Residues. Appl Biochem Biotech. 102 (2002): 207-212.
3. Robinson, T.; Chandran, B.; and Nigam, P. Effect of Pretreatments of Three Waste Residues, Wheat Straw, Corncobs and Barley Husks on Dye Adsorption. Bioresource Technol. 85 (2002): 119-124.
4. Low, K.S.; Lee, C. K.; and Tan, B.F. Quaternized Wood as Sorbent for Reactive Dye. Appl Biochem Biotech. 87 (2000): 233-245.
5. Graham, N.; Chen, X.G.; and Jayaseelan, S. The Potential Application of Activated Carbon from Sewage Sludge to Organic Dyes Removal. Water Sci Technol. 43 (2001): 245-252.
6. Lee, C. K.; Low, K. S.; and Chow, S. W. Chrome Sludge as an Adsorbent for Colour Removal. Environ Technol. 17 (1996): 1023-1028.
7. Nicolet, L.; and Rott, U. Recirculation of Powdered Activated Carbon for the Adsorption of Dyes in Municipal Wastewater Treatment Plants. Water Sci Technol. 40 (1999): 191-198.



8. Chu, W. Dye Removal from Textile Dye Wastewater Using Recycled Alum Sludge.  
Water Res. 35 (2001): 3147-3153.
9. Coutinho, F.M.B.; and Wima, C.T. The Influence of Diluents on the Formation of Porous Structure in Ion Exchange Resins Based on 2-Vinylpyridine and Divinylbenzene. Eur Polym J. 29(8) (1993): 1119-1123.
10. Paterson, R. An Introduction to Ion Exchange. Great Britain: Heyden & Son, 1970.
11. Ibrahim, N. A.; Hashem, A.; and Abou Shosha M. H. Amination of Wood Sawdust for Removing Anionic Dyes from Aqueous Solutions. Poly-Plast Technol. 36 (1997): 963-971.
12. Yu, P. L.; Dunn, N. W.; and Kim, W. S. Lactate Removal by Anionic-Exchange Resin Improve Nisin Production by *Lactococcus Lactis*. Biotechnol. 24 (2002): 59-64.
13. Simon, G. P. Ion Exchange Training Manual. New York: Van Nostrand Reinhold, 1991.
14. Moustafa, A.B. and Faizalla, A. Synthesis and Characterization of Highly Porous Poly(methacrylic-co-triethylene glycol dimethacrylate) by Suspension Polymerization. J Appl Poly Sci. 73 (1999): 149-159.
15. Santos, A.F.; Lima, E.L.; and Pinto, J.C. In-Line Evaluation of Average Particle Size in Styrene Suspension Polymerizations Using Near-Infrared Spectroscopy. J Appl Poly Sci. 70 (1998): 1737-1745.

16. Shinzo Omi. Et.al. Morphology Development of 10 um Scale Polymer Particles Prepared by SPG Emulsification and Suspension Polymerization. J Appl Poly Sci. 79 (2001): 2200-2220.
17. Jayaswal, N.; Sinha, S.; and Kumar, A. Effect of Chemical Modifications upon Exchange Capacity of Aminated Macroporous Styrene-Divinyl Benzene (PS-DVB) Copolymer Anion Exchange Resin. J Appl Polym Sci. 79 (2001): 1735-1748.
18. Reza, A. Review Beaded Polymer Supports and Crels I. Manufacturing Techniques. J Chromatography. 586 (1991): 181-197.
19. Stefan, A.F. et.al. Emulsion-Free Synthesis of Monodisperse Core-Shell Polymer Colloids Containing Chloromethyl Group. J Appl Poly Sci. 58 (1995): 19-29.
20. Kemmere, M.F. et.al. Emulsification in Batch Emulsion Polymerization. J Appl Poly Sci. 74 (1999): 3225-3241.
21. Liu, Z.; Xio, H.; and Wiseman, N. Emulsifier-Free Emulsion Copolymerization of Styrene with Quaternary Ammonium Cationic Monomers. J Appl Poly Sci. 74 (2000): 1129-1140.
22. Santas, A.F.; Lima, E.L.; and Pinto, J.C. Control and Design of Average Particle Size in Styrene Suspension Polymerization Using NIRS. J Appl Poly Sci. 77 (2000): 453-462.

23. Christopher, K. et.al. Monodispersed, Micron-Sized Polystyrene Particles by Dispersion Polymerization. J Polym Sci : Polym Letters Edition. 23 (1985): 103-108.
24. Tseng, C.M. et.el. Uniform Polymer Particle by Dispersion Polymerization. J Polym Sci : Part A : Polym Chem. 24 (1986): 2995-3007.
25. Christopher, K.; Ober and Kar, P. Lok. Formation of Large Monodisperse Copolymer Particles by Dispersion Polymerization. Macromolecules. 20 (1987): 268-273.
26. Shen, S.; Sudol, E.D.; and El-Aasser M.S. Dispersion Polymerization of Methyl Methacrylate: Mechanism of Particle Formation. J Polym Sci: Part A: Polym Chem. 32 (1994): 1087-1100.
27. Yaacov, A. and Mosle, L. Effect of Initiator on the Molecular Weight Distribution in Dispersion Polymerization of Styrene. J Poly Sci: Polymer Chemistry Edition. 18 (1980): 1-11.
28. Joseph, C.S. Polymeric Materials Encyclopedia. volume 1. United States of America: CRC Press, 1996.
29. Yuan, H. G.; Kalfas, G.; and Ray, W. H. Suspension Polymerization. J M S -Rev. Macromol Chem Phys. C 31 283 (1991): 215-299.
30. Balakrishman, T.; and Warren. T.F. Particle Size Control in Suspension Copolymerization of Styrene, Chloromethylstyrene and Divinylbenzene. J Appl Poly Sci. 27 (1982): 133-138.

31. Shen, S.; Sudol E.D.; and El-Aasser M.S. Dispersion Polymerization of Methyl Methacrylate. J Polym Sci: Part A: Polym Chem. 31 (1993): 1393-1402.
32. Chi-Hao and Wen-Chien Lee. Preparation of Methyl Methacrylate and Glycidyl Methacrylate Copolymerized Nonporous Particles. J of Polym Sci : Part A : Polym Chem. 37 (1999): 1457-1463.
33. Carles, M. et.al. Development of a Suspension Copolymerization Process for Bone Cement Production. J Appl Poly Sci. 76 (2000): 814-823.
34. Jyongsik, J, ; and Beom-Seok-Kim. Studied of Crosslinked Styrene-Alkyl Acrylate Copolymers for Oil Absorbency Application I. Synthesis and Characterization. J Appl Poly Sci. 76 (2000): 814-823.
35. Rabelo, D. and Coutinho, F.M.B. Cosolvency effects of Benzyl Alcohol and Heptane on the Formation of Macroporous Styrene-Divinylbenzene Copolymers. Polymer Bulletin. 31 (1993): 585-592.
36. W.-H. Li.; Stoven, H.D.H.; and Hamiele, A.E. Novel Polystyryl Resins for Size Exclusion Chromatography. J Polym Sci : Part A : Polym Chem. 32 (1994): 2029-2038.
37. Ganachaud,F.; Sauzedde,F.; Elaissri, A.; and Pichat, C. Emulsifier-Free Emulsion Copolymerization of Styrene with Two Different Amino-Containing Cationic Monomers I. Kinetic Studies. J Appl Poly Sci. 65 (1997): 2315-2330.

38. Koji, I.; Suunwook, K.; and Ayako, I. Microspher Synthesis by Emulsion Copolymerization of Styrene with Poly (Methacrylic Acid) Macromonomers. J Appl Poly Sci. 85 (2002): 900-905.
39. Friberg, S.; Mandell, L.; and Larson, M. J of Coll Interface Sci. 29 (1969) p.155 cited in Martin, J.S. Nonionic Surfactants Physical Chemistry. New York: Marcel Dekker, 1987.
40. Giles, C.H. et. al. Studies in Adsorption. Part XI A System of Classification of Solution Adsorption Isotherms, and its Use in Diagonis of Adsorption Mechanisms and in Measurement of Specific Surface Area of Solids J of the Chemical Society. October (1960): 3973-3993.
41. Hollowa, P.W.; Popjok, G.; Bond, R.P.; and Robert, M. Chem J. 111 (1990): 33 cited in Friberg, S.; Mandell, L.; and Larson, M. J of Coll Interface Sci. 29 (1969) p.155 cited in Martin, J.S. Nonionic Surfactants Physical Chemistry. New York: Marcel Dekker, 1987.
42. Marina, G.; Frantisek, S. ;and Jean, M.J.F. J Polym Sci: Part A: Polymer Chemistry. 32 (1994): 2169-2175.
43. Ching, O.W.; Frantisek, S.; and Jean, M.J.F. J Polym Sci: Part A: Polymer Chemistry. 32 (1994): 2577-2588.
44. Godjevargova, T.; Simeonova, A. and Dimov. Adsorption of Lead and Copper on Modified Polyacrylonitril Bead. J Appl Poly Sci. 79 (2001): 283-288.

45. Ogawa, N. et.al. Preparation of Spherical Polymer Beads of Maleic Anhydride-Styrene-Divinylbenzene and Metal Sorption of Its Derivative. J Appl Poly Sci. 78 (2000): 171-183.
46. Russell, P. An Introduction to Ion Exchange. Great Britain: Heyden & Son, 1970.
47. Geoge, P.S. Ion Exchange Training Manual. New York: Van Nostrand, 1991.
48. Harland, C.E. Ion Exchange: Theory and Practice. Second edition. New York: Royal Society of Chemistry, 1994.
49. Mohamed, H. et al. Immobilization Residual Dye onto Ion-Exchange Cellulosic Materials. J Appl Poly Sci. 77 (2000): 171-183.
50. Minghua, L. et al. Adsorption and Desorption of Copper (II) from Solution on New Spherical Cellulose Adsorbent. J Appl Poly Sci. 84 (2002): 478-485.
51. Hwang, M. C., and Chen, K. M. The Removal of Color from Effluents Using Polyamide-Epichlorohydrin-Cellulose Polymer. III Use in Anionic Dye Removal in a Batch Process. J Appl Poly Sci. 50 (1993): 735-744.
52. Ahmed, M.N.; and Ram, R. N. Removal of Basic Dye from Waste-Water Using Silica as Adsorbent. Environ Pollut. 77 (1992): 79-86.
53. Walken, G.M. and Weatherley, L.R. Kinetics of Acid Dye Adsorption. Wat Res. 33(8) (1997): 1895-1899.

54. Hwang, M.C. and Chen, K.M. The Removal of Color from Effluents Using Polyamide-Epichlorohydrin-Cellulose Polymer. III Use in Anionic Dye Removal in a Batch Process. J Appl Poly Sci. 50 (1993): 735-744.
55. Morais, L.C. et al. Reactive Dyes Removal from Wastewaters by Adsorption on Eucalyptus Bark: Variable That Define the Process. Wat Res. 34(3) (1999): 979-988.
56. Joseph, A. L. Preparing an Ion Exchange Resin from Sugacane Bagasse to Remove Reactive Dye from Wastewater. Textile Chemist and Colorist. 28 (May 1996): 13-17.
57. Namasivayam, C. and Yamuna, R.T. Adsorption of Direct Red 12 B by Biogas Residual Slurry: Equilibrium and Rate Processes. Environ Pollut. 89(1995): 1-7.
58. Flores, A. et al. Imprinted Polymers Prepared by Aqueous Suspension Polymerization. J Appl Polym Sci. 77(2000): 1841-1850.
59. van Streun, K.H. et al. Eur Polym J. 27(1991): 931-938.
60. Shen, S.; Sudol, E. D.; and El-Aasser. M. S. Dispersion Polymerization of Acrylamide in Aqueous Solution of Ammonium Sulfate : Synthesis and Characterzation. J Polym Sci Part A : Polym Chem. 31(1993): 1393-1402.
61. Olayo, R. et al. Poly (vinyl alcohol) as a Stabilizer in the suspension Polymerization of Styrene : The Effect of the Molecular Weight. J Appl Pol Sci. 67(1998): 71-77.

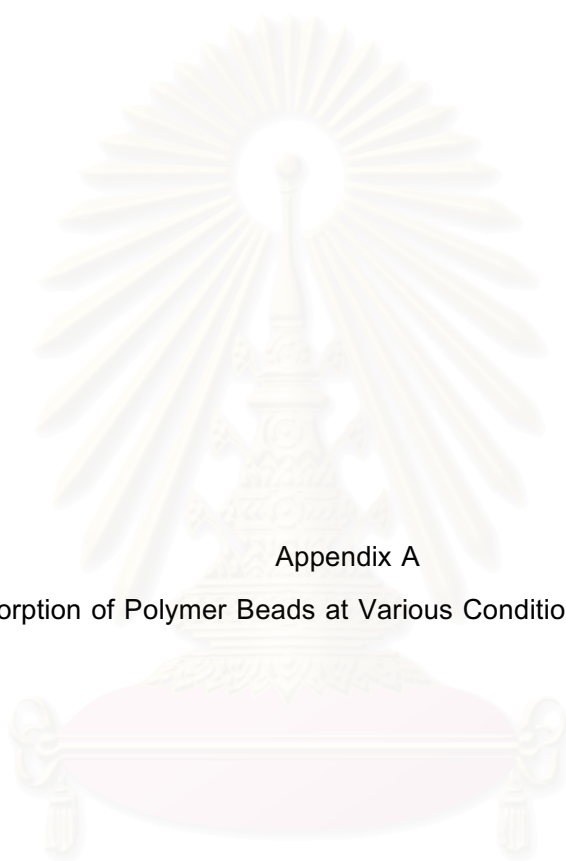
62. Kangwansupamonkon, W.; Damronglerd, S.; Kiatkamjornwong, S. Effects of the Crosslinking Agent and Diluents on Bead Properties of Styrene – Divinylbenzene Copolymers J Appl Poly Sci. 85 (2002): 654-669.
63. Salamone, J. C. Polymeric Material Encyclopedia. vol 10 ; United States of America : CRC Press, 1996.
64. Bao, Y.Z.; Brooks, B.W. Influences of Some Polymerization Conditions on Particle Properties of Suspension Poly(vinyl chloride) Resin. J Appl Poly Sci. 85 (2002): 1544-1552.
65. Tseng, C. W. et. al.; Uniform Polymer Particles by Dispersion Polymerization in Alcohol. J Polym Sci Polym Chem Ed. 24 (1986): 2995-3007.
66. Meyer, D. Surfactant Science and Technology. second edition. United State of America: VCH Publisher: 1992.
67. Sangsirimongkolying, R.; Kiatkamjornwong, S.; Damronglerd, S. Multilayer Polymer Particles. I. Synthesis of Hydrophilic Poly (dimethyl aminoethyl methacrylate) Core Particles. J Appl Poly Sci. 86 (2002): 1057-1070.
68. Kipling, J.J. Adsorption from Solutions of Non-Electrolytes. London: Academic Press: 1965.





Appendices

สถาบันวิทยบริการ  
จุฬาลงกรณ์มหาวิทยาลัย



Appendix A

Dye Adsorption of Polymer Beads at Various Condition of Polymerization

สถาบันวิทยบริการ  
จุฬาลงกรณ์มหาวิทยาลัย

### 1. Dye Adsorption by Polystyrene Bead

Table 1 Initial dye concentration of reactive red

| Initial dye concentration : $C_0$ (mg/l) |         |         |            | SD |
|--|---------|---------|------------|----|
| 1  | 2       | 3       | Mean value |    |
| 1009.38                                  | 1009.38 | 1009.38 | 1009.38    | 0  |

Table 2 Equilibrium concentration of reactive red in solution after adsorption by polymer bead

| Equilibrium dye concentration in solution: $C_e$ (mg/l) |         |         |            | SD |
|---|---------|---------|------------|----|
| 1   | 2       | 3       | Mean value |    |
| 1006.25   | 1006.25 | 1006.25 | 1006.25    | 0  |

Table 3 Experimental data for equilibrium adsorption of reactive red by polymer bead

| $C_0$ (mg/l) | $C_e$ (mg/l) | Weight of bead : $W$ (g) | Dye adsorbed by bead : $q_e$ (mg/g) |
|--------------|--------------|--------------------------|-------------------------------------|
| 1009.38      | 1006.25      | 1.0000                   | 0.03                                |

สถาบันวิทยบริการ  
จุฬาลงกรณ์มหาวิทยาลัย

## 2. Effect of Polymerization Time of MAPTAC on Dye Adsorption of Polymer Bead

Table 4 Initial dye concentration of reactive red

| Initial dye concentration : $C_0$ (mg/l) |         |         |            | SD |
|--|---------|---------|------------|----|
| 1  | 2       | 3       | Mean value |    |
| 1091.00                                  | 1091.00 | 1091.00 | 1091.00    | 0  |

Table 5 Equilibrium concentration of reactive red in solution after adsorption by polymer bead

| Polymerization time of MAPTAC (min) | Equilibrium dye concentration in solution: $C_e$ (mg/l) |        |        |            | SD |
|-------------------------------------|---|--------|--------|------------|----|
|                                     | 1   | 2      | 3      | Mean value |    |
| 15                                  | 700.00  | 700.00 | 700.00 | 700.00     | 0  |
| 30                                  | 637.00  | 637.00 | 637.00 | 637.00     | 0  |
| 45                                  | 686.00  | 686.00 | 686.00 | 686.00     | 0  |

Table 6 Experimental data for equilibrium adsorption of reactive red by polymer bead

| Polymerization time of MAPTAC (min) | $C_0$ (mg/l) | $C_e$ (mg/l) | Weight of bead :<br>W (g) | Dye adsorbed by bead : $q_e$ (mg/g) |
|-------------------------------------|--------------|--------------|---------------------------|-------------------------------------|
| 15                                  | 1091.00      | 700.00       | 1.0015                    | 3.90                                |
| 30                                  | 1091.00      | 637.00       | 1.0024                    | 4.53                                |
| 45                                  | 1091.00      | 686.00       | 1.0025                    | 4.04                                |

### 3. Effect of Polymerization Temperature on Dye Adsorption of Polymer Bead

Table 7 Initial dye concentration of reactive red

| Initial dye concentration : $C_0$ (mg/l) |         |         |            | SD |
|--|---------|---------|------------|----|
| 1  | 2       | 3       | Mean value |    |
| 1091.00                                  | 1091.00 | 1091.00 | 1091.00    | 0  |

Table 8 Equilibrium concentration of reactive red in solution after adsorption by polymer bead

| Polymerization temperature ( $^{\circ}\text{C}$ ) | Equilibrium dye concentration in solution: $C_e$ (mg/l) |        |        |            | SD |
|---|---|--------|--------|------------|----|
|   | 1   | 2      | 3      | Mean value |    |
| 60  | 956.00  | 957.00 | 956.00 | 956.33     | 0  |
| 70  | 581.00  | 581.00 | 581.00 | 581.00     | 0  |
| 80  | 759.00  | 759.00 | 759.00 | 759.00     | 0  |

Table 9 Experimental data for equilibrium adsorption of reactive red by polymer bead

| Polymerization temperature ( $^{\circ}\text{C}$ ) | $C_0$ (mg/l) | $C_e$ (mg/l) | Weight of bead :<br>W (g) | Dye adsorbed by bead : $q_e$ (mg/g) |
|---|--------------|--------------|---------------------------|-------------------------------------|
| 60  | 1091.00      | 956.33       | 1.0019                    | 1.34                                |
| 70  | 1091.00      | 581.00       | 1.0020                    | 5.09                                |
| 80  | 1091.00      | 759.00       | 1.0001                    | 3.32                                |

#### 4. Effect of CTAB on Dye Adsorption of Polymer Bead

Table 10 Initial dye concentration of reactive red

| Initial dye concentration : $C_0$ (mg/l) |        |        |            | SD |
|--|--------|--------|------------|----|
| 1  | 2      | 3      | Mean value |    |
| 864.00                                   | 864.00 | 864.00 | 864.00     | 0  |

Table 11 Equilibrium concentration of reactive red in solution after adsorption by polymer bead

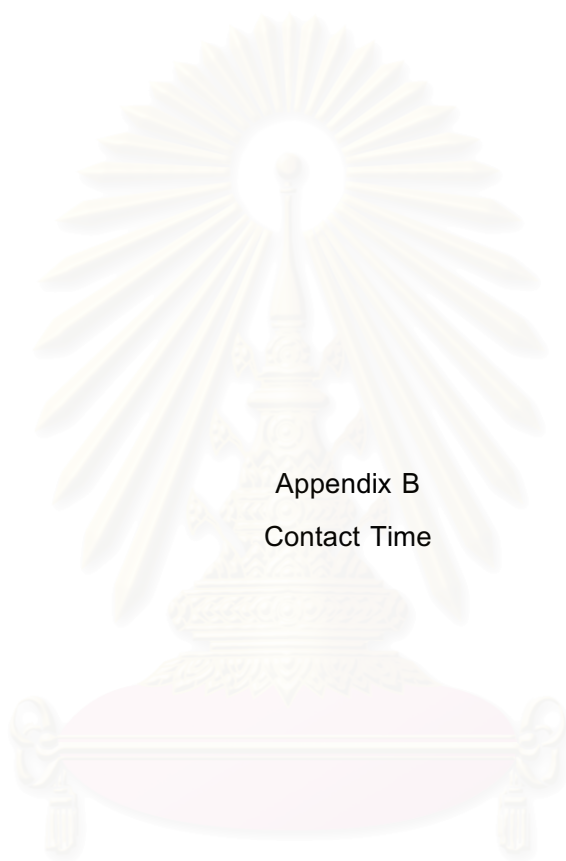
| CTAB content (g) | Particle size ( $\mu\text{m}$ ) | Equilibrium dye concentration in solution: $C_e$ (mg/l) |        |        |            | SD |
|------------------|---------------------------------|---|--------|--------|------------|----|
|                  |                                 | 1   | 2      | 3      | Mean value |    |
| 0.002            | 150                             | 106.00  | 106.00 | 106.00 | 106.00     | 0  |
|                  | 300                             | 319.00  | 319.00 | 319.00 | 319.00     | 0  |
|                  | 500                             | 398.00  | 398.00 | 398.00 | 398.00     | 0  |
| 0.004            | 150                             | 283.00  | 283.00 | 283.00 | 202.00     | 0  |
|                  | 300                             | 355.00  | 356.00 | 355.00 | 355.33     | 0  |
|                  | 500                             | 436.00  | 436.00 | 436.00 | 436.33     | 0  |
| 0.005            | 150                             | 286.00  | 288.00 | 287.00 | 287.00     | 0  |
|                  | 300                             | 366.00  | 367.00 | 367.00 | 366.67     | 0  |
|                  | 500                             | 455.00  | 455.00 | 455.00 | 455.00     | 0  |

สถาบันวิทยบริการ  
จุฬาลงกรณ์มหาวิทยาลัย

Table 12 Experimental data for equilibrium adsorption of reactive red by polymer bead

| CTAB content (g) | Particle size ( $\mu\text{m}$ ) | $C_o$ (mg/l) | $C_e$ (mg/l) | Weight of bead :<br>W (g) | Dye adsorbed by bead : $q_e$ (mg/g) |
|------------------|---------------------------------|--------------|--------------|---------------------------|-------------------------------------|
| 0.002            | 150                             | 864.00       | 106.00       | 0.5094                    | 7.44                                |
|                  | 300                             | 864.00       | 319.00       | 0.4025                    | 6.77                                |
|                  | 500                             | 864.00       | 398.00       | 0.4045                    | 5.76                                |
| 0.004            | 150                             | 864.00       | 283.00       | 0.4051                    | 7.17                                |
|                  | 300                             | 864.00       | 355.33       | 0.4021                    | 6.33                                |
|                  | 500                             | 864.00       | 436.00       | 0.4044                    | 5.29                                |
| 0.005            | 150                             | 864.00       | 287.00       | 0.4013                    | 7.19                                |
|                  | 300                             | 864.00       | 366.67       | 0.4002                    | 6.21                                |
|                  | 500                             | 864.00       | 455.00       | 0.4018                    | 5.09                                |

สถาบันวิทยบริการ  
จุฬาลงกรณ์มหาวิทยาลัย



Appendix B  
Contact Time

สถาบันวิทยบริการ  
จุฬาลงกรณ์มหาวิทยาลัย



### 1. Contact Time of Reactive Blue

Table 1 Initial dye concentration of reactive blue

| Initial dye concentration : $C_0$ (mg/l) |         |         |            | SD   |
|--|---------|---------|------------|------|
| 1  | 2       | 3       | Mean value |      |
| 3401.63                                  | 3400.75 | 3399.38 | 3400.59    | 1.13 |

Table 2 Concentration of reactive blue in solution after adsorption on bead 150  $\mu\text{m}$  at different time interval

| Time (min) | Concentration of dye in solution at time t : $C_t$ (mg/l) |         |         |            | SD   |
|------------|---|---------|---------|------------|------|
|            | 1   | 2       | 3       | Mean value |      |
| 10         | 2100.53   | 2100.35 | 2100.53 | 2100.47    | 0.10 |
| 20         | 2017.83   | 2018.16 | 2017.24 | 2017.74    | 0.47 |
| 30         | 2208.15   | 2208.15 | 2207.94 | 2208.08    | 0.12 |
| 60         | 2086.71   | 2086.71 | 2086.18 | 2086.53    | 0.31 |
| 90         | 2082.29   | 2082.10 | 2083.21 | 2082.53    | 0.59 |
| 120        | 2084.61   | 2083.66 | 2083.79 | 2084.02    | 0.52 |

Table 3 Adsorption rate of reactive blue on bead 150  $\mu\text{m}$

| Time (min) | Concentration of dye in solution at time t : $C_t$ (mg/l) | Initial dye concentration : $C_0$ (mg/l) | $C_t / C_0$ |
|------------|---|--|-------------|
| 0          | 3400.59   | 3400.59                                  | 1.00        |
| 10         | 2100.47   | 3400.59                                  | 0.62        |
| 20         | 2017.74   | 3400.59                                  | 0.59        |
| 30         | 2208.08   | 3400.59                                  | 0.65        |
| 60         | 2086.53   | 3400.59                                  | 0.61        |
| 90         | 2082.53   | 3400.59                                  | 0.61        |
| 120        | 2084.02   | 3400.59                                  | 0.61        |

Table 4 Concentration of reactive blue in solution after adsorption on bead 500  $\mu\text{m}$  at different time interval

| Time (min) | Concentration of dye in solution at time t : $C_t$ (mg/l) |         |         |            | SD   |
|------------|---|---------|---------|------------|------|
|            | 1   | 2       | 3       | Mean value |      |
| 10         | 2862.08   | 2861.35 | 2860.44 | 2861.29    | 0.82 |
| 20         | 2712.24   | 2712.24 | 2712.88 | 2712.45    | 0.37 |
| 30         | 2709.56   | 2709.56 | 2710.13 | 2709.75    | 0.33 |
| 60         | 2721.94   | 2721.94 | 2723.58 | 2722.49    | 0.95 |
| 90         | 2713.81   | 2713.81 | 2712.20 | 2713.27    | 0.93 |
| 120        | 2712.24   | 2711.56 | 2711.56 | 2711.79    | 0.39 |

Table 5 Adsorption rate of reactive blue on bead 500  $\mu\text{m}$

| Time (min) | Concentration of dye in solution at time t : $C_t$ (mg/l) | Initial dye concentration : $C_0$ (mg/l) | $C_t / C_0$ |
|------------|---|--|-------------|
| 0          | 3400.59   | 3400.59                                  | 1.00        |
| 10         | 2861.29   | 3400.59                                  | 0.84        |
| 20         | 2712.45   | 3400.59                                  | 0.80        |
| 30         | 2709.75   | 3400.59                                  | 0.80        |
| 60         | 2722.49   | 3400.59                                  | 0.80        |
| 90         | 2713.27   | 3400.59                                  | 0.80        |
| 120        | 2711.79   | 3400.59                                  | 0.80        |

จุฬาลงกรณ์มหาวิทยาลัย

## 2. Contact Time of Reactive Red

Table 6 Initial dye concentration of reactive red

| Initial dye concentration : $C_0$ (mg/l) |         |         |            | SD   |
|--|---------|---------|------------|------|
| 1  | 2       | 3       | Mean value |      |
| 3743.88                                  | 3740.75 | 3743.75 | 3742.79    | 1.77 |

Table 7 Concentration of reactive red in solution after adsorption on bead 150  $\mu\text{m}$  at different time interval

| Time (min) | Concentration of dye in solution at time t : $C_t$ (mg/l) |         |         |            | SD   |
|------------|---|---------|---------|------------|------|
|            | 1   | 2       | 3       | Mean value |      |
| 10         | 2848.38   | 2848.38 | 2849.38 | 2848.71    | 0.58 |
| 20         | 2611.38   | 2611.35 | 2611.31 | 2611.35    | 0.04 |
| 30         | 2632.38   | 2631.88 | 2632.00 | 2632.09    | 0.26 |
| 60         | 2778.50   | 2778.50 | 2777.63 | 2778.21    | 0.50 |
| 90         | 2779.00   | 2779.88 | 2779.50 | 2779.46    | 0.44 |
| 120        | 2779.25   | 2778.75 | 2779.50 | 2779.17    | 0.38 |

Table 8 Adsorption rate of reactive red on bead 150  $\mu\text{m}$

| Time (min) | Concentration of dye in solution at time t : $C_t$ (mg/l) | Initial dye concentration : $C_0$ (mg/l) | $C_t / C_0$ |
|------------|---|--|-------------|
| 0          | 3742.79   | 3742.79                                  | 1.00        |
| 10         | 2848.71   | 3742.79                                  | 0.76        |
| 20         | 2611.35   | 3742.79                                  | 0.70        |
| 30         | 2632.09   | 3742.79                                  | 0.70        |
| 60         | 2778.21   | 3742.79                                  | 0.74        |
| 90         | 2779.46   | 3742.79                                  | 0.74        |
| 120        | 2779.17   | 3742.79                                  | 0.74        |

Table 9 Concentration of reactive red in solution after adsorption on bead 500  $\mu\text{m}$  at different time interval

| Time (min) | Concentration of dye in solution at time t : $C_t$ (mg/l) |         |         |            | SD   |
|------------|---|---------|---------|------------|------|
|            | 1   | 2       | 3       | Mean value |      |
| 10         | 3316.25   | 3316.75 | 3317.63 | 3316.88    | 0.70 |
| 20         | 3223.38   | 3221.50 | 3221.75 | 3222.21    | 1.02 |
| 30         | 3314.63   | 3314.38 | 3315.25 | 3314.75    | 0.45 |
| 60         | 3348.25   | 3348.13 | 3346.63 | 3347.67    | 0.90 |
| 90         | 3323.13   | 3322.50 | 3322.75 | 3322.79    | 0.32 |
| 120        | 3321.75   | 3323.00 | 3322.34 | 3322.36    | 0.63 |

Table 10 Adsorption rate of reactive red on bead 500  $\mu\text{m}$

| Time (min) | Concentration of dye in solution at time t : $C_t$ (mg/l) | Initial dye concentration : $C_0$ (mg/l) | $C_t / C_0$ |
|------------|---|--|-------------|
| 0          | 3742.79   | 3742.79                                  | 1.00        |
| 10         | 3316.88   | 3742.79                                  | 0.89        |
| 20         | 3222.21   | 3742.79                                  | 0.86        |
| 30         | 3314.75   | 3742.79                                  | 0.89        |
| 60         | 3347.67   | 3742.79                                  | 0.89        |
| 90         | 3322.79   | 3742.79                                  | 0.89        |
| 120        | 3322.36   | 3742.79                                  | 0.89        |

จุฬาลงกรณ์มหาวิทยาลัย

### 3. Contact Time of Reactive Yellow

Table 11 Initial dye concentration of reactive yellow

| Initial dye concentration : $C_0$ (mg/l) |         |         |            | SD   |
|--|---------|---------|------------|------|
| 1  | 2       | 3       | Mean value |      |
| 3762.89                                  | 3762.23 | 3761.70 | 3762.27    | 0.60 |

Table 12 Concentration of reactive yellow in solution after adsorption on bead 150  $\mu\text{m}$  at different time interval

| Time (min) | Concentration of dye in solution at time t : $C_t$ (mg/l) |         |         |            | SD   |
|------------|---|---------|---------|------------|------|
|            | 1   | 2       | 3       | Mean value |      |
| 10         | 2190.91   | 2190.91 | 2190.68 | 2190.83    | 0.13 |
| 20         | 2150.64   | 2150.74 | 2150.77 | 2150.72    | 0.07 |
| 30         | 2194.61   | 2194.61 | 2193.79 | 2194.34    | 0.47 |
| 60         | 2151.11   | 2151.11 | 2150.41 | 2150.88    | 0.40 |
| 90         | 2153.10   | 2153.10 | 2151.86 | 2152.69    | 0.72 |
| 120        | 2153.85   | 2153.85 | 2152.61 | 2153.44    | 0.72 |

Table 13 Adsorption rate of reactive blue on bead 150  $\mu\text{m}$

| Time (min) | Concentration of dye in solution at time t : $C_t$ (mg/l) | Initial dye concentration : $C_0$ (mg/l) | $C_t / C_0$ |
|------------|---|--|-------------|
| 0          | 3762.27   | 3762.27                                  | 1.00        |
| 10         | 2190.83   | 3762.27                                  | 0.58        |
| 20         | 2150.72   | 3762.27                                  | 0.57        |
| 30         | 2194.34   | 3762.27                                  | 0.58        |
| 60         | 2150.88   | 3762.27                                  | 0.57        |
| 90         | 2152.69   | 3762.27                                  | 0.57        |
| 120        | 2153.44   | 3762.27                                  | 0.57        |

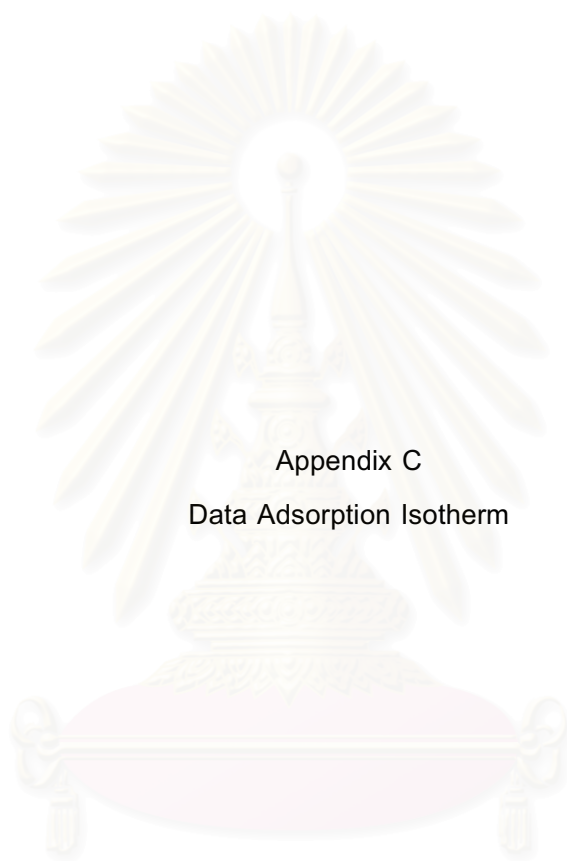
Table 14 Concentration of reactive yellow in solution after adsorption on bead 500  $\mu\text{m}$  at different time interval

| Time (min) | Concentration of dye in solution at time t : $C_t$ (mg/l) |         |         |            | SD   |
|------------|---|---------|---------|------------|------|
|            | 1   | 2       | 3       | Mean value |      |
| 10         | 2748.96   | 2748.61 | 2748.51 | 2748.69    | 0.24 |
| 20         | 2742.70   | 2742.70 | 2742.65 | 2742.68    | 0.03 |
| 30         | 2744.01   | 2744.38 | 2744.11 | 2744.17    | 0.19 |
| 60         | 2737.55   | 2736.24 | 2737.05 | 2736.95    | 0.66 |
| 90         | 2739.90   | 2739.90 | 2738.26 | 2739.35    | 0.95 |
| 120        | 2735.21   | 2735.21 | 2736.29 | 2735.57    | 0.62 |

Table 15 Adsorption rate of reactive blue on bead 500  $\mu\text{m}$

| Time (min) | Concentration of dye in solution at time t : $C_t$ (mg/l) | Initial dye concentration : $C_0$ (mg/l) | $C_t / C_0$ |
|------------|---|--|-------------|
| 0          | 3762.27   | 3762.27                                  | 1.00        |
| 10         | 2748.69   | 3762.27                                  | 0.73        |
| 20         | 2742.68   | 3762.27                                  | 0.73        |
| 30         | 2744.17   | 3762.27                                  | 0.73        |
| 60         | 2736.95   | 3762.27                                  | 0.73        |
| 90         | 2739.35   | 3762.27                                  | 0.73        |
| 120        | 2735.57   | 3762.27                                  | 0.73        |

จุฬาลงกรณ์มหาวิทยาลัย



Appendix C  
Data Adsorption Isotherm

สถาบันวิทยบริการ  
จุฬาลงกรณ์มหาวิทยาลัย

## 1. Reactive Blue at Room Temperature

### 1.1 Particle Size 150 $\mu\text{m}$

Table 1 Initial dye concentration of reactive blue

| Concentration number | Initial dye concentration : $C_0$ (mg/l) |         |         |            | SD   |
|----------------------|--|---------|---------|------------|------|
|                      | 1  | 2       | 3       | Mean value |      |
| 1                    | 468.15                                   | 467.70  | 468.15  | 468.00     | 0.26 |
| 2                    | 963.85                                   | 964.40  | 963.95  | 964.07     | 0.29 |
| 3                    | 1462.63                                  | 1463.94 | 1466.44 | 1464.34    | 1.94 |
| 4                    | 1933.25                                  | 1934.13 | 1934.00 | 1933.79    | 0.48 |
| 5                    | 2455.75                                  | 2454.00 | 2455.00 | 2454.92    | 0.88 |
| 6                    | 2938.75                                  | 2936.13 | 2939.38 | 2938.42    | 1.99 |
| 7                    | 3401.63                                  | 3400.75 | 3399.38 | 3400.59    | 1.13 |

Table 2 Equilibrium concentration of reactive blue in solution at room temperature on bead 150  $\mu\text{m}$

| Initial dye concentration (mg/l) | Equilibrium dye concentration in solution: $C_e$ (mg/l) |         |         |            | SD   |
|----------------------------------|---|---------|---------|------------|------|
|                                  | 1   | 2       | 3       | Mean value |      |
| 468.00                           | 77.83   | 77.78   | 77.85   | 77.82      | 0.04 |
| 964.07                           | 164.47  | 164.61  | 164.68  | 164.59     | 0.11 |
| 1464.34                          | 538.31  | 536.61  | 536.51  | 537.14     | 1.01 |
| 1933.79                          | 846.44  | 845.61  | 847.26  | 846.44     | 0.83 |
| 2454.92                          | 1416.15   | 1415.63 | 1416.15 | 1415.98    | 0.30 |
| 2938.42                          | 1737.85   | 1737.85 | 1738.17 | 1737.96    | 0.18 |
| 3400.59                          | 2248.68   | 2248.23 | 2247.59 | 2248.17    | 0.55 |



Table 3 Experimental data for equilibrium adsorption isotherm of reactive blue at room temperature on bead 150  $\mu\text{m}$

| $C_o$ (mg/l) | $C_e$ (mg/l) | Weight of bead : W (g) | Dye adsorbed by bead : $q_e$ (mg/g) |
|--------------|--------------|------------------------|-------------------------------------|
| 468.00       | 77.82        | 0.5002                 | 3.90                                |
| 964.07       | 164.59       | 0.5005                 | 7.99                                |
| 1464.34      | 537.14       | 0.5001                 | 9.27                                |
| 1933.79      | 846.44       | 0.5002                 | 10.87                               |
| 2454.92      | 1415.98      | 0.5003                 | 10.38                               |
| 2938.42      | 1737.96      | 0.5000                 | 12.00                               |
| 3400.59      | 2248.17      | 0.5001                 | 11.52                               |

Table 4 Experimental data for Langmuir isotherm of reactive blue at room temperature on bead 150  $\mu\text{m}$

| $C_e$ (mg/l) | $q_e$ (mg/g) | $C_e/q_e$ (g/l) |
|--------------|--------------|-----------------|
| 77.82        | 3.90         | 19.95           |
| 164.59       | 7.99         | 20.60           |
| 537.14       | 9.27         | 57.94           |
| 846.44       | 10.87        | 77.87           |
| 1415.98      | 10.38        | 136.41          |
| 1737.96      | 12.00        | 144.83          |
| 2248.17      | 11.52        | 195.15          |

Table 5 Experimental data for Freundlich isotherm of reactive blue at room temperature on bead 150  $\mu\text{m}$

| $C_e$ (mg/l) | $q_e$ (mg/g) | $\log C_e$ | $\log q_e$ |
|--------------|--------------|------------|------------|
| 77.82        | 3.90         | 1.89       | 0.59       |
| 164.59       | 7.99         | 2.22       | 0.90       |
| 537.14       | 9.27         | 2.73       | 0.97       |
| 846.44       | 10.87        | 2.93       | 1.04       |
| 1415.98      | 10.38        | 3.15       | 1.02       |
| 1737.96      | 12.00        | 3.24       | 1.08       |
| 2248.17      | 11.52        | 3.35       | 1.06       |



สถาบันวิทยบริการ  
จุฬาลงกรณ์มหาวิทยาลัย

### 1.2 Particle Size 300 $\mu\text{m}$

Table 6 Equilibrium concentration of reactive blue in solution at room temperature on bead 300  $\mu\text{m}$

| Initial dye concentration (mg/g) | Equilibrium dye concentration in solution: $C_e$ (mg/l) |         |         |            | SD   |
|----------------------------------|---|---------|---------|------------|------|
|                                  | 1   | 2       | 3       | Mean value |      |
| 468.00                           | 52.09   | 52.09   | 52.09   | 52.09      | 0    |
| 964.07                           | 317.28  | 317.45  | 318.34  | 317.69     | 0.57 |
| 1464.34                          | 772.60  | 772.50  | 772.41  | 772.50     | 0.10 |
| 1933.79                          | 1201.80   | 1201.44 | 1201.37 | 1201.54    | 0.23 |
| 2454.92                          | 1707.37   | 1706.18 | 1706.15 | 1706.57    | 0.70 |
| 2938.42                          | 2134.95   | 2133.64 | 2133.05 | 2133.88    | 0.97 |
| 3400.59                          | 2632.45   | 2632.45 | 2635.75 | 2633.55    | 1.91 |

Table 7 Experimental data for equilibrium adsorption isotherm of reactive blue at room temperature on bead 300  $\mu\text{m}$

| $C_o$ (mg/l) | $C_e$ (mg/l) | Weight of bead : W (g) | Dye adsorbed by bead : $q_e$ (mg/g) |
|--------------|--------------|------------------------|-------------------------------------|
| 468.00       | 52.09        | 0.5007                 | 4.33                                |
| 964.07       | 317.69       | 0.5009                 | 6.45                                |
| 1464.34      | 772.50       | 0.5000                 | 6.92                                |
| 1933.79      | 1201.54      | 0.5002                 | 7.32                                |
| 2454.92      | 1706.57      | 0.5000                 | 7.48                                |
| 2938.42      | 2133.88      | 0.5009                 | 8.03                                |
| 3400.59      | 2633.55      | 0.5002                 | 7.67                                |

Table 8 Experimental data for Langmuir isotherm of reactive blue at room temperature on bead 300  $\mu\text{m}$

| $C_e$ (mg/l) | $q_e$ (mg/g) | $C_e/q_e$ (g/l) |
|--------------|--------------|-----------------|
| 52.09        | 4.33         | 12.03           |
| 317.69       | 6.45         | 49.25           |
| 772.50       | 6.92         | 111.63          |
| 1201.54      | 7.32         | 164.14          |
| 1706.57      | 7.48         | 228.15          |
| 2133.88      | 8.03         | 265.74          |
| 2633.55      | 7.67         | 343.36          |

Table 9 Experimental data for Freundlich isotherm of reactive blue at room temperature on bead 300  $\mu\text{m}$

| $C_e$ (mg/l) | $q_e$ (mg/g) | $\log C_e$ | $\log q_e$ |
|--------------|--------------|------------|------------|
| 52.09        | 4.33         | 1.72       | 0.64       |
| 317.69       | 6.45         | 2.50       | 0.81       |
| 772.50       | 6.92         | 2.89       | 0.84       |
| 1201.54      | 7.32         | 3.08       | 0.86       |
| 1706.57      | 7.48         | 3.23       | 0.87       |
| 2133.88      | 8.03         | 3.33       | 0.90       |
| 2633.55      | 7.67         | 3.42       | 0.88       |

### 1.3 Particle Size 500 $\mu\text{m}$

Table 10 Equilibrium concentration of reactive blue in solution at room temperature on bead 500  $\mu\text{m}$

| Initial dye concentration (mg/g) | Equilibrium dye concentration in solution: $C_e$ (mg/l) |          |         |            | SD   |
|----------------------------------|---|----------|---------|------------|------|
|                                  | 1   | 2        | 3       | Mean value |      |
| 468.00                           | 73.83   | 73.82    | 73.78   | 73.81      | 0.03 |
| 964.07                           | 455.16  | 454.76   | 454.32  | 454.75     | 0.42 |
| 1464.34                          | 851.25  | 849.66   | 850.28  | 850.40     | 0.80 |
| 1933.79                          | 1235.76   | 1234.88  | 1234.81 | 1235.15    | 0.53 |
| 2454.92                          | 1725.31   | 1723.30  | 1723.98 | 1724.20    | 1.02 |
| 2938.42                          | 2218.83   | 2 219.33 | 2219.04 | 2219.07    | 0.25 |
| 3400.59                          | 2687.34   | 2684.38  | 2683.95 | 2685.22    | 1.85 |

Table 11 Experimental data for equilibrium adsorption isotherm of reactive blue at room temperature on bead 500  $\mu\text{m}$

| $C_o$ (mg/l) | $C_e$ (mg/l) | Weight of bead : W (g) | Dye adsorbed by bead : $q_e$ (mg/g) |
|--------------|--------------|------------------------|-------------------------------------|
| 468.00       | 73.81        | 0.5001                 | 3.94                                |
| 964.07       | 454.75       | 0.5006                 | 5.09                                |
| 1464.34      | 850.40       | 0.5005                 | 6.13                                |
| 1933.79      | 1235.15      | 0.5006                 | 6.98                                |
| 2454.92      | 1724.20      | 0.5006                 | 7.30                                |
| 2938.42      | 2219.07      | 0.5003                 | 7.19                                |
| 3400.59      | 2685.22      | 0.5008                 | 7.14                                |

Table 12 Experimental data for Langmuir isotherm of reactive blue at room temperature on bead 500  $\mu\text{m}$

| $C_e$ (mg/l) | $q_e$ (mg/g) | $C_e/q_e$ (g/l) |
|--------------|--------------|-----------------|
| 73.81        | 3.94         | 18.73           |
| 454.75       | 5.09         | 89.34           |
| 850.40       | 6.13         | 138.73          |
| 1235.15      | 6.98         | 176.96          |
| 1724.20      | 7.30         | 236.19          |
| 2219.07      | 7.19         | 308.63          |
| 2685.22      | 7.14         | 376.08          |

Table 13 Experimental data for Freundlich isotherm of reactive blue at room temperature on bead 500  $\mu\text{m}$

| $C_e$ (mg/l) | $q_e$ (mg/g) | $\log C_e$ | $\log q_e$ |
|--------------|--------------|------------|------------|
| 73.81        | 3.94         | 1.87       | 0.60       |
| 454.75       | 5.09         | 2.66       | 0.71       |
| 850.40       | 6.13         | 2.93       | 0.79       |
| 1235.15      | 6.98         | 3.09       | 0.84       |
| 1724.20      | 7.30         | 3.24       | 0.86       |
| 2219.07      | 7.19         | 3.35       | 0.86       |
| 2685.22      | 7.14         | 3.43       | 0.85       |

## 2. Reactive Blue at Temperature of 80°C

### 2.1 Particle Size 150 $\mu\text{m}$

Table 14 Equilibrium concentration of reactive blue in solution at 80°C on bead 150  $\mu\text{m}$

| Initial dye concentration (mg/g) | Equilibrium dye concentration in solution: $C_e$ (mg/l) |         |         |            | SD   |
|----------------------------------|---|---------|---------|------------|------|
|                                  | 1   | 2       | 3       | Mean value |      |
| 468.00                           | 63.59   | 63.61   | 63.61   | 63.60      | 0.01 |
| 964.07                           | 53.97   | 53.98   | 54.05   | 54.00      | 0.04 |
| 1464.34                          | 380.53  | 383.40  | 383.07  | 382.33     | 1.57 |
| 1933.79                          | 721.94  | 722.13  | 721.71  | 721.93     | 0.21 |
| 2454.92                          | 1188.01   | 1187.53 | 1188.19 | 1187.91    | 0.34 |
| 2938.40                          | 1610.93   | 1610.59 | 1611.42 | 1610.98    | 0.42 |
| 3400.59                          | 2017.83   | 2018.16 | 2017.24 | 2017.74    | 0.47 |

Table 15 Experimental data for equilibrium adsorption isotherm of reactive blue at 80°C on bead 150  $\mu\text{m}$

| $C_o$ (mg/l) | $C_e$ (mg/l) | Weight of bead : W (g) | Dye adsorbed by bead : $q_e$ (mg/g) |
|--------------|--------------|------------------------|-------------------------------------|
| 468.00       | 63.60        | 0.5001                 | 4.22                                |
| 964.07       | 54.00        | 0.5004                 | 9.09                                |
| 1464.34      | 382.33       | 0.5000                 | 10.82                               |
| 1933.79      | 721.93       | 0.5000                 | 12.12                               |
| 2454.92      | 1187.91      | 0.5000                 | 12.67                               |
| 2938.40      | 1610.98      | 0.5001                 | 13.27                               |
| 3400.59      | 2017.74      | 0.5008                 | 13.81                               |

Table 16 Experimental data for Langmuir isotherm of reactive blue at 80°C on bead 150  $\mu\text{m}$

| $C_e$ (mg/l) | $q_e$ (mg/g) | $C_e/q_e$ (g/l) |
|--------------|--------------|-----------------|
| 63.60        | 4.22         | 15.07           |
| 54.00        | 9.09         | 5.94            |
| 382.33       | 10.82        | 35.34           |
| 721.93       | 12.12        | 59.57           |
| 1187.91      | 12.67        | 93.76           |
| 1610.98      | 13.27        | 121.40          |
| 2017.74      | 13.81        | 146.11          |

Table 17 Experimental data for Freundlich isotherm of reactive blue at 80°C on bead 150  $\mu\text{m}$

| $C_e$ (mg/l) | $q_e$ (mg/g) | $\log C_e$ | $\log q_e$ |
|--------------|--------------|------------|------------|
| 63.60        | 4.22         | 1.80       | 0.63       |
| 54.00        | 9.09         | 1.73       | 0.96       |
| 382.33       | 10.82        | 2.58       | 1.03       |
| 721.93       | 12.12        | 2.86       | 1.08       |
| 1187.91      | 12.67        | 3.07       | 1.10       |
| 1610.98      | 13.27        | 3.21       | 1.12       |
| 2017.74      | 13.81        | 3.30       | 1.14       |



## 2.2 Particle Size 300 $\mu\text{m}$

Table 18 Equilibrium concentration of reactive blue in solution at 80°C on bead 300  $\mu\text{m}$

| Initial dye concentration (mg/g) | Equilibrium dye concentration in solution: $C_e$ (mg/l) |         |         |            | SD   |
|----------------------------------|---|---------|---------|------------|------|
|                                  | 1   | 2       | 3       | Mean value |      |
| 468.00                           | 31.33   | 31.04   | 31.02   | 31.13      | 0.17 |
| 964.07                           | 306.45  | 306.41  | 306.40  | 306.41     | 0.02 |
| 1464.34                          | 700.19  | 699.32  | 698.99  | 699.50     | 0.62 |
| 1933.79                          | 1130.11   | 1130.39 | 1129.94 | 1130.15    | 0.23 |
| 2454.92                          | 1552.19   | 1552.17 | 1552.99 | 1552.45    | 0.47 |
| 2938.40                          | 1974.76   | 1974.76 | 1975.16 | 1974.89    | 0.23 |
| 3400.59                          | 2556.94   | 2556.98 | 2556.95 | 2556.96    | 0.02 |

Table 19 Experimental data for equilibrium adsorption isotherm of reactive blue at 80°C on bead 300  $\mu\text{m}$

| $C_o$ (mg/l) | $C_e$ (mg/l) | Weight of bead : W (g) | Dye adsorbed by bead : $q_e$ (mg/g) |
|--------------|--------------|------------------------|-------------------------------------|
| 468.00       | 31.13        | 0.5001                 | 4.37                                |
| 964.07       | 306.41       | 0.5001                 | 6.58                                |
| 1464.34      | 699.50       | 0.5002                 | 7.65                                |
| 1933.79      | 1130.15      | 0.5005                 | 8.03                                |
| 2454.92      | 1552.45      | 0.5002                 | 9.02                                |
| 2938.40      | 1974.89      | 0.5007                 | 9.62                                |
| 3400.59      | 2556.96      | 0.5000                 | 8.44                                |

Table 20 Experimental data for Langmuir isotherm of reactive blue at 80°C on bead 300  $\mu\text{m}$

| $C_e$ (mg/l) | $q_e$ (mg/g) | $C_e/q_e$ (g/l) |
|--------------|--------------|-----------------|
| 31.13        | 4.37         | 7.12            |
| 306.41       | 6.58         | 46.57           |
| 699.50       | 7.65         | 91.44           |
| 1130.15      | 8.03         | 140.74          |
| 1552.45      | 9.02         | 172.11          |
| 1974.89      | 9.62         | 205.29          |
| 2556.96      | 8.44         | 302.96          |

Table 21 Experimental data for Freundlich isotherm of reactive blue at 80°C on bead 300  $\mu\text{m}$

| $C_e$ (mg/l) | $q_e$ (mg/g) | $\log C_e$ | $\log q_e$ |
|--------------|--------------|------------|------------|
| 31.13        | 4.37         | 1.50       | 0.64       |
| 306.41       | 6.58         | 2.49       | 0.82       |
| 699.50       | 7.65         | 2.84       | 0.88       |
| 1130.15      | 8.03         | 3.05       | 0.90       |
| 1552.45      | 9.02         | 3.19       | 0.96       |
| 1974.89      | 9.62         | 3.30       | 0.98       |
| 2556.96      | 8.44         | 3.41       | 0.93       |

### 2.3 Particle Size 500 $\mu\text{m}$

Table 22 Equilibrium concentration of reactive blue in solution at 80°C on bead 500  $\mu\text{m}$

| Initial dye concentration (mg/g) | Equilibrium dye concentration in solution: $C_e$ (mg/l) |         |         |            | SD   |
|----------------------------------|---|---------|---------|------------|------|
|                                  | 1   | 2       | 3       | Mean value |      |
| 468.00                           | 55.69   | 55.68   | 55.68   | 55.68      | 0.01 |
| 964.07                           | 431.18  | 432.41  | 432.07  | 431.89     | 0.64 |
| 1464.34                          | 836.98  | 836.99  | 836.74  | 836.90     | 0.14 |
| 1933.79                          | 1334.58   | 1334.58 | 1334.80 | 1334.65    | 0.13 |
| 2454.92                          | 1842.33   | 1843.13 | 1843.04 | 1842.83    | 0.44 |
| 2938.42                          | 2217.45   | 2216.78 | 2216.84 | 2217.02    | 0.37 |
| 3400.59                          | 2712.24   | 2712.24 | 2712.88 | 2712.45    | 0.37 |

Table 23 Experimental data for equilibrium adsorption isotherm of reactive blue at 80°C on bead 500  $\mu\text{m}$

| $C_o$ (mg/l) | $C_e$ (mg/l) | Weight of bead : W (g) | Dye adsorbed by bead : $q_e$ (mg/g) |
|--------------|--------------|------------------------|-------------------------------------|
| 468.00       | 55.60        | 0.5007                 | 4.12                                |
| 964.07       | 431.89       | 0.5001                 | 5.32                                |
| 1464.34      | 836.90       | 0.5009                 | 6.26                                |
| 1933.79      | 1334.65      | 0.5000                 | 5.99                                |
| 2454.92      | 1842.83      | 0.5003                 | 6.12                                |
| 2938.42      | 2217.02      | 0.5006                 | 7.21                                |
| 3400.59      | 2712.45      | 0.5008                 | 6.87                                |

Table 24 Experimental data for Langmuir isotherm of reactive blue at 80°C on bead  
500  $\mu\text{m}$

| $C_e$ (mg/l) | $q_e$ (mg/g) | $C_e / q_e$ (g/l) |
|--------------|--------------|-------------------|
| 55.60        | 4.12         | 13.50             |
| 431.89       | 5.32         | 81.18             |
| 836.90       | 6.26         | 133.69            |
| 1334.65      | 5.99         | 222.81            |
| 1842.83      | 6.12         | 301.12            |
| 2217.02      | 7.21         | 307.49            |
| 2712.45      | 6.87         | 394.83            |

Table 25 Experimental data for Freundlich isotherm of reactive blue at 80°C on bead  
500  $\mu\text{m}$

| $C_e$ (mg/l) | $q_e$ (mg/g) | $\log C_e$ | $\log q_e$ |
|--------------|--------------|------------|------------|
| 55.60        | 4.12         | 1.75       | 0.61       |
| 431.89       | 5.32         | 2.64       | 0.73       |
| 836.90       | 6.26         | 2.92       | 0.80       |
| 1334.65      | 5.99         | 3.13       | 0.78       |
| 1842.83      | 6.12         | 3.27       | 0.79       |
| 2217.02      | 7.21         | 3.35       | 0.86       |
| 2712.45      | 6.87         | 3.43       | 0.84       |

### 3. Reactive Red at Room Temperature

#### 3.1 Particle Size 150 $\mu\text{m}$

Table 26 Initial dye concentration of reactive red

| Concentration number | Initial dye concentration : $C_0$ (mg/l) |         |         |            | SD   |
|----------------------|--|---------|---------|------------|------|
|                      | 1  | 2       | 3       | Mean value |      |
| 1                    | 511.20                                   | 511.10  | 510.93  | 511.08     | 0.14 |
| 2                    | 1062.50                                  | 1061.95 | 1061.65 | 1062.03    | 0.43 |
| 3                    | 1524.63                                  | 1523.63 | 1525.25 | 1524.50    | 0.82 |
| 4                    | 2099.75                                  | 2100.38 | 2100.13 | 2100.09    | 0.32 |
| 5                    | 2644.88                                  | 2644.63 | 2645.00 | 2644.84    | 0.19 |
| 6                    | 3208.13                                  | 3207.88 | 3208.00 | 3208.00    | 0.13 |
| 7                    | 3743.88                                  | 3740.75 | 3743.75 | 3742.79    | 1.77 |

Table 27 Equilibrium concentration of reactive red in solution at room temperature on bead 150  $\mu\text{m}$

| Initial dye concentration (mg/g) | Equilibrium dye concentration in solution: $C_e$ (mg/l) |         |         |            | SD   |
|----------------------------------|---|---------|---------|------------|------|
|                                  | 1   | 2       | 3       | Mean value |      |
| 511.08                           | 84.09   | 84.16   | 84.18   | 84.14      | 0.05 |
| 1062.03                          | 285.93  | 285.60  | 285.88  | 285.80     | 0.18 |
| 1524.50                          | 681.30  | 680.88  | 680.58  | 680.92     | 0.36 |
| 2100.09                          | 1103.00   | 1103.44 | 1102.63 | 1103.02    | 0.41 |
| 2644.84                          | 1927.75   | 1927.56 | 1927.06 | 1927.46    | 0.36 |
| 3208.00                          | 2126.75   | 2127.63 | 2126.88 | 2127.09    | 0.48 |
| 3742.79                          | 2643.44   | 2643.40 | 2643.38 | 2643.41    | 0.03 |

Table 28 Experimental data for equilibrium adsorption isotherm of reactive red at room temperature on bead 150  $\mu\text{m}$

| $C_o$ (mg/l) | $C_e$ (mg/l) | Weight of bead : W (g) | Dye adsorbed by bead : $q_e$ (mg/g) |
|--------------|--------------|------------------------|-------------------------------------|
| 511.08       | 84.14        | 0.5007                 | 4.26                                |
| 1062.03      | 285.80       | 0.5004                 | 7.76                                |
| 1524.50      | 680.92       | 0.5006                 | 8.43                                |
| 2100.09      | 1103.02      | 0.5008                 | 9.95                                |
| 2644.84      | 1927.46      | 0.5002                 | 7.17                                |
| 3208.00      | 2127.09      | 0.5002                 | 10.80                               |
| 3742.79      | 2643.41      | 0.5001                 | 10.99                               |

Table 29 Experimental data for Langmuir isotherm of reactive red at room temperature on bead 150  $\mu\text{m}$

| $C_e$ (mg/l) | $q_e$ (mg/g) | $C_e/q_e$ (g/l) |
|--------------|--------------|-----------------|
| 84.14        | 4.26         | 19.75           |
| 285.80       | 7.76         | 36.83           |
| 680.92       | 8.43         | 80.77           |
| 1103.02      | 9.95         | 110.86          |
| 1927.46      | 7.17         | 268.82          |
| 2127.09      | 10.80        | 196.95          |
| 2643.41      | 10.99        | 240.53          |

Table 30 Experimental data for Freundlich isotherm of reactive red at room temperature on bead 150  $\mu\text{m}$

| $C_e$ (mg/l) | $q_e$ (mg/g) | $\log C_e$ | $\log q_e$ |
|--------------|--------------|------------|------------|
| 84.14        | 4.26         | 1.93       | 0.63       |
| 285.80       | 7.76         | 2.46       | 0.89       |
| 680.92       | 8.43         | 2.83       | 0.93       |
| 1103.02      | 9.95         | 3.04       | 1.00       |
| 1927.46      | 7.17         | 3.28       | 0.86       |
| 2127.09      | 10.80        | 3.33       | 1.03       |
| 2643.41      | 10.99        | 3.42       | 1.04       |



สถาบันวิทยบริการ  
จุฬาลงกรณ์มหาวิทยาลัย

### 3.2 Particle Size 300 $\mu\text{m}$

Table 31 Equilibrium concentration of reactive red in solution at room temperature on bead 300  $\mu\text{m}$

| Initial dye concentration (mg/g) | Equilibrium dye concentration in solution: $C_e$ (mg/l) |         |         |            | SD   |
|----------------------------------|---|---------|---------|------------|------|
|                                  | 1   | 2       | 3       | Mean value |      |
| 511.08                           | 70.78   | 70.78   | 70.73   | 70.76      | 0.03 |
| 1062.03                          | 540.78  | 540.65  | 540.63  | 540.69     | 0.08 |
| 1524.50                          | 922.50  | 922.25  | 921.31  | 922.02     | 0.63 |
| 2100.09                          | 1576.00   | 1576.63 | 1576.69 | 1576.44    | 0.38 |
| 2644.84                          | 2080.00   | 2080.13 | 2079.81 | 2079.98    | 0.16 |
| 3208.00                          | 2682.75   | 2680.63 | 2680.88 | 2681.42    | 1.16 |
| 3742.79                          | 3117.76   | 3117.75 | 3117.81 | 3117.77    | 0.03 |

Table 32 Experimental data for equilibrium adsorption isotherm of reactive red at room temperature on bead 300  $\mu\text{m}$

| $C_o$ (mg/l) | $C_e$ (mg/l) | Weight of bead : W (g) | Dye adsorbed by bead : $q_e$ (mg/g) |
|--------------|--------------|------------------------|-------------------------------------|
| 511.08       | 70.76        | 0.5003                 | 4.40                                |
| 1062.03      | 540.69       | 0.5001                 | 5.21                                |
| 1524.50      | 922.02       | 0.5000                 | 6.02                                |
| 2100.09      | 1576.44      | 0.5001                 | 5.24                                |
| 2644.84      | 2079.98      | 0.5000                 | 5.65                                |
| 3208.00      | 2681.42      | 0.5000                 | 5.27                                |
| 3742.79      | 3117.77      | 0.5000                 | 6.25                                |



Table 33 Experimental data for Langmuir isotherm of reactive red at room temperature on bead 300  $\mu\text{m}$

| $C_e$ (mg/l) | $q_e$ (mg/g) | $C_e/q_e$ (g/l) |
|--------------|--------------|-----------------|
| 70.76        | 4.40         | 16.08           |
| 540.69       | 5.21         | 103.78          |
| 922.02       | 6.02         | 153.16          |
| 1576.44      | 5.24         | 300.85          |
| 2079.98      | 5.65         | 368.14          |
| 2681.42      | 5.27         | 508.81          |
| 3117.77      | 6.25         | 498.84          |

Table 34 Experimental data for Freundlich isotherm of reactive red at room temperature on bead 300  $\mu\text{m}$

| $C_e$ (mg/l) | $q_e$ (mg/g) | $\log C_e$ | $\log q_e$ |
|--------------|--------------|------------|------------|
| 70.76        | 16.08        | 1.85       | 0.64       |
| 540.69       | 103.78       | 2.73       | 0.72       |
| 922.02       | 153.16       | 2.96       | 0.78       |
| 1576.44      | 300.85       | 3.20       | 0.72       |
| 2079.98      | 368.14       | 3.32       | 0.75       |
| 2681.42      | 508.81       | 3.43       | 0.72       |
| 3117.77      | 498.84       | 3.49       | 0.80       |

จุฬาลงกรณ์มหาวิทยาลัย

### 3.3 Particle Size 500 $\mu\text{m}$

Table 35 Equilibrium concentration of reactive red in solution at room temperature on bead 500  $\mu\text{m}$

| Initial dye concentration (mg/g) | Equilibrium dye concentration in solution: $C_e$ (mg/l) |         |         |            | SD   |
|----------------------------------|---|---------|---------|------------|------|
|                                  | 1   | 2       | 3       | Mean value |      |
| 511.08                           | 161.90  | 161.52  | 161.16  | 161.53     | 0.37 |
| 1062.03                          | 653.68  | 653.78  | 653.73  | 653.73     | 0.05 |
| 1524.50                          | 1148.19   | 1148.06 | 1147.50 | 1147.92    | 0.37 |
| 2100.09                          | 1729.19   | 1728.63 | 1727.25 | 1728.36    | 0.99 |
| 2644.84                          | 2181.25   | 2181.50 | 2180.75 | 2181.17    | 0.38 |
| 3208.00                          | 2746.25   | 2746.25 | 2746.25 | 2746.25    | 0    |
| 3742.79                          | 3210.25   | 3210.25 | 3209.25 | 3209.04    | 0.58 |

Table 36 Experimental data for equilibrium adsorption isotherm of reactive red at room temperature on bead 500  $\mu\text{m}$

| $C_o$ (mg/l) | $C_e$ (mg/l) | Weight of bead : W (g) | Dye adsorbed by bead : $q_e$ (mg/g) |
|--------------|--------------|------------------------|-------------------------------------|
| 511.08       | 161.53       | 0.5003                 | 3.49                                |
| 1062.03      | 653.73       | 0.5003                 | 4.08                                |
| 1524.50      | 1147.92      | 0.5003                 | 3.76                                |
| 2100.09      | 1728.36      | 0.5007                 | 3.71                                |
| 2644.84      | 2181.17      | 0.5000                 | 4.64                                |
| 3208.00      | 2746.25      | 0.5005                 | 4.61                                |
| 3742.79      | 3209.04      | 0.5004                 | 5.33                                |

Table 37 Experimental data for Langmuir isotherm of reactive red at room temperature on bead 500  $\mu\text{m}$

| $C_e$ (mg/l) | $q_e$ (mg/g) | $C_e/q_e$ (g/l) |
|--------------|--------------|-----------------|
| 161.53       | 3.49         | 46.28           |
| 653.73       | 4.08         | 160.23          |
| 1147.92      | 3.76         | 305.30          |
| 1728.36      | 3.71         | 465.87          |
| 2181.17      | 4.64         | 470.08          |
| 2746.25      | 4.61         | 595.72          |
| 3209.04      | 5.33         | 602.07          |

Table 38 Experimental data for Freundlich isotherm of reactive red at room temperature on bead 500  $\mu\text{m}$

| $C_e$ (mg/l) | $q_e$ (mg/g) | $\log C_e$ | $\log q_e$ |
|--------------|--------------|------------|------------|
| 161.53       | 3.49         | 2.21       | 0.54       |
| 653.73       | 4.08         | 2.82       | 0.61       |
| 1147.92      | 3.76         | 3.06       | 0.58       |
| 1728.36      | 3.71         | 3.24       | 0.57       |
| 2181.17      | 4.64         | 3.34       | 0.67       |
| 2746.25      | 4.61         | 3.44       | 0.66       |
| 3209.04      | 5.33         | 3.51       | 0.73       |

จุฬาลงกรณ์มหาวิทยาลัย

#### 4. Reactive Red at Temperature of 80°C

##### 4.1 Particle Size 150 µm

Table 39 Equilibrium concentration of reactive red in solution at 80°C on bead 150 µm

| Initial dye concentration (mg/g) | Equilibrium dye concentration in solution: $C_e$ (mg/l) |         |         |            | SD   |
|----------------------------------|---|---------|---------|------------|------|
|                                  | 1   | 2       | 3       | Mean value |      |
| 511.08                           | 34.32   | 34.33   | 34.37   | 34.34      | 0.03 |
| 1062.03                          | 53.72   | 53.83   | 54.09   | 53.88      | 0.19 |
| 1524.50                          | 738.38  | 736.55  | 736.95  | 737.29     | 0.96 |
| 2100.09                          | 1187.44   | 1186.44 | 1187.06 | 1187.31    | 0.22 |
| 2644.84                          | 1779.75   | 1777.50 | 1778.75 | 1778.66    | 1.13 |
| 3208.00                          | 2012.88   | 2013.38 | 2012.88 | 2013.05    | 0.29 |
| 3742.79                          | 2611.38   | 2611.35 | 2611.31 | 2611.35    | 0.04 |

Table 40 Experimental data for equilibrium adsorption isotherm of reactive red at 80°C on bead 150 µm

| $C_o$ (mg/l) | $C_e$ (mg/l) | Weight of bead : W (g) | Dye adsorbed by bead : $q_e$ (mg/g) |
|--------------|--------------|------------------------|-------------------------------------|
| 511.08       | 34.34        | 0.5002                 | 4.77                                |
| 1062.03      | 53.88        | 0.5002                 | 10.08                               |
| 1524.50      | 737.29       | 0.5007                 | 7.86                                |
| 2100.09      | 1187.31      | 0.5004                 | 9.12                                |
| 2644.84      | 1778.66      | 0.5002                 | 8.66                                |
| 3208.00      | 2013.05      | 0.5006                 | 11.94                               |
| 3742.79      | 2611.35      | 0.5002                 | 11.31                               |

Table 41 Experimental data for Langmuir isotherm of reactive red at 80°C on bead  
150  $\mu\text{m}$

| $C_e$ (mg/l) | $q_e$ (mg/g) | $C_e/q_e$ (g/l) |
|--------------|--------------|-----------------|
| 34.34        | 4.77         | 7.20            |
| 53.88        | 10.08        | 5.35            |
| 737.29       | 7.86         | 93.80           |
| 1187.31      | 9.12         | 130.19          |
| 1778.66      | 8.66         | 205.39          |
| 2013.05      | 11.94        | 168.60          |
| 2611.35      | 11.31        | 230.89          |

Table 42 Experimental data for Freundlich isotherm of reactive red at 80°C on bead  
150  $\mu\text{m}$

| $C_e$ (mg/l) | $q_e$ (mg/g) | $\log C_e$ | $\log q_e$ |
|--------------|--------------|------------|------------|
| 34.34        | 4.77         | 1.54       | 0.68       |
| 53.88        | 10.08        | 1.73       | 1.00       |
| 737.29       | 7.86         | 2.87       | 0.90       |
| 1187.31      | 9.12         | 3.07       | 0.96       |
| 1778.66      | 8.66         | 3.25       | 0.94       |
| 2013.05      | 11.94        | 3.30       | 1.08       |
| 2611.35      | 11.31        | 3.42       | 1.05       |

จุฬาลงกรณ์มหาวิทยาลัย

#### 4.2 Particle Size 300 $\mu\text{m}$

Table 43 Equilibrium concentration of reactive red in solution at 80°C on bead 300  $\mu\text{m}$

| Initial dye concentration (mg/g) | Equilibrium dye concentration in solution: $C_e$ (mg/l) |         |         |            | SD   |
|----------------------------------|---|---------|---------|------------|------|
|                                  | 1   | 2       | 3       | Mean value |      |
| 511.08                           | 48.12   | 48.21   | 48.16   | 48.16      | 0.05 |
| 1062.03                          | 546.93  | 546.28  | 546.05  | 546.42     | 0.46 |
| 1524.50                          | 1049.19   | 1048.56 | 1048.25 | 1048.67    | 0.48 |
| 2100.09                          | 1537.81   | 1537.25 | 1537.00 | 1537.35    | 0.41 |
| 2644.84                          | 2115.56   | 2115.19 | 2114.69 | 2115.15    | 0.44 |
| 3208.00                          | 2655.25   | 2655.75 | 2655.50 | 2655.50    | 0.25 |
| 3742.79                          | 3197.75   | 3197.80 | 3197.78 | 3197.78    | 0.03 |

สถาบันวิทยบริการ  
จุฬาลงกรณ์มหาวิทยาลัย

Table 44 Experimental data for equilibrium adsorption isotherm of reactive red at 80°C on bead 300  $\mu\text{m}$

| $C_o$ (mg/l) | $C_e$ (mg/l) | Weight of bead : W (g) | Dye adsorbed by bead : $q_e$ (mg/g) |
|--------------|--------------|------------------------|-------------------------------------|
| 511.08       | 48.16        | 0.5002                 | 4.63                                |
| 1062.03      | 546.42       | 0.5006                 | 5.15                                |
| 1524.50      | 1048.67      | 0.5004                 | 4.75                                |
| 2100.09      | 1537.35      | 0.5005                 | 5.62                                |
| 2644.84      | 2115.15      | 0.5001                 | 5.30                                |
| 3208.00      | 2655.50      | 0.5005                 | 5.52                                |
| 3742.79      | 3197.78      | 0.5003                 | 5.45                                |



สถาบันวิทยบริการ  
จุฬาลงกรณ์มหาวิทยาลัย

Table 45 Experimental data for Langmuir isotherm of reactive red at 80°C on bead  
300  $\mu\text{m}$

| $C_e$ (mg/l) | $q_e$ (mg/g) | $C_e / q_e$ (g/l) |
|--------------|--------------|-------------------|
| 48.16        | 4.63         | 10.40             |
| 546.42       | 5.15         | 106.10            |
| 1048.67      | 4.75         | 220.77            |
| 1537.35      | 5.62         | 273.55            |
| 2115.15      | 5.30         | 399.08            |
| 2655.50      | 5.52         | 481.07            |
| 3197.78      | 5.45         | 586.75            |

สถาบันวิทยบริการ  
จุฬาลงกรณ์มหาวิทยาลัย



Table 46 Experimental data for Freundlich isotherm of reactive red at 80°C on bead  
300  $\mu\text{m}$

| $C_e$ (mg/l) | $q_e$ (mg/g) | $\log C_e$ | $\log q_e$ |
|--------------|--------------|------------|------------|
| 48.16        | 4.63         | 1.68       | 0.67       |
| 546.42       | 5.15         | 2.74       | 0.71       |
| 1048.67      | 4.75         | 3.02       | 0.68       |
| 1537.35      | 5.62         | 3.19       | 0.75       |
| 2115.15      | 5.30         | 3.33       | 0.72       |
| 2655.50      | 5.52         | 3.42       | 0.74       |
| 3197.78      | 5.45         | 3.50       | 0.74       |



สถาบันวิทยบริการ  
จุฬาลงกรณ์มหาวิทยาลัย

### 4.3 Particle Size 500 $\mu\text{m}$

Table 47 Equilibrium concentration of reactive red in solution at 80°C on bead 500  $\mu\text{m}$

| Initial dye concentration (mg/g) | Equilibrium dye concentration in solution: $C_e$ (mg/l) |         |         |            | SD   |
|----------------------------------|---|---------|---------|------------|------|
|                                  | 1   | 2       | 3       | Mean value |      |
| 511.08                           | 118.83  | 118.80  | 118.78  | 118.80     | 0.03 |
| 1062.03                          | 668.00  | 667.70  | 667.50  | 667.73     | 0.25 |
| 1524.50                          | 1094.25   | 1093.63 | 1090.69 | 1092.86    | 1.90 |
| 2100.09                          | 1715.44   | 1714.88 | 1725.25 | 1715.19    | 0.28 |
| 2644.84                          | 2187.75   | 2185.00 | 2186.75 | 2186.50    | 1.39 |
| 3208.00                          | 2699.13   | 2698.25 | 2700.25 | 2699.21    | 1.00 |
| 3742.79                          | 3223.38   | 3221.50 | 3221.75 | 3222.21    | 1.02 |

Table 48 Experimental data for equilibrium adsorption isotherm of reactive red at 80°C on bead 500  $\mu\text{m}$

| $C_o$ (mg/l) | $C_e$ (mg/l) | Weight of bead : W (g) | Dye adsorbed by bead : $q_e$ (mg/g) |
|--------------|--------------|------------------------|-------------------------------------|
| 511.08       | 118.80       | 0.5000                 | 3.92                                |
| 1062.03      | 667.73       | 0.5000                 | 3.94                                |
| 1524.50      | 1092.86      | 0.5000                 | 4.32                                |
| 2100.09      | 1715.19      | 0.5007                 | 3.84                                |
| 2644.84      | 2186.50      | 0.5000                 | 4.58                                |
| 3208.00      | 2699.21      | 0.5004                 | 5.08                                |
| 3742.79      | 3222.21      | 0.5004                 | 5.20                                |

Table 49 Experimental data for Langmuir isotherm of reactive red at 80°C on bead 500  $\mu\text{m}$

| $C_e$ (mg/l) | $q_e$ (mg/g) | $C_e/q_e$ (g/l) |
|--------------|--------------|-----------------|
| 118.80       | 3.92         | 30.31           |
| 667.73       | 3.94         | 169.47          |
| 1092.86      | 4.32         | 252.98          |
| 1715.19      | 3.84         | 446.66          |
| 2186.50      | 4.58         | 477.40          |
| 2699.21      | 5.08         | 531.34          |
| 3222.21      | 5.20         | 619.66          |

Table 50 Experimental data for Freundlich isotherm of reactive red at 80°C on bead 500  $\mu\text{m}$

| $C_e$ (mg/l) | $q_e$ (mg/g) | $\log C_e$ | $\log q_e$ |
|--------------|--------------|------------|------------|
| 118.80       | 3.92         | 2.07       | 0.59       |
| 667.73       | 3.94         | 2.82       | 0.60       |
| 1092.86      | 4.32         | 3.04       | 0.64       |
| 1715.19      | 3.84         | 3.23       | 0.58       |
| 2186.50      | 4.58         | 3.34       | 0.66       |
| 2699.21      | 5.08         | 3.43       | 0.71       |
| 3222.21      | 5.20         | 3.51       | 0.72       |

จุฬาลงกรณ์มหาวิทยาลัย

## 5. Reactive Yellow at Room Temperature

### 5.1 Particle Size 150 $\mu\text{m}$

Table 51 Initial dye concentration of reactive yellow

| Concentration number | Initial dye concentration : $C_0$ (mg/l) |         |         |            | SD   |
|----------------------|--|---------|---------|------------|------|
|                      | 1  | 2       | 3       | Mean value |      |
| 1                    | 542.96                                   | 542.59  | 542.55  | 542.70     | 0.23 |
| 2                    | 1108.10                                  | 1107.89 | 1107.43 | 1107.81    | 0.34 |
| 3                    | 1638.82                                  | 1639.16 | 1638.85 | 1638.94    | 0.19 |
| 4                    | 2186.38                                  | 2185.96 | 2186.38 | 2186.24    | 0.24 |
| 5                    | 2650.38                                  | 2649.51 | 2649.15 | 2649.68    | 0.63 |
| 6                    | 3287.73                                  | 3287.73 | 3288.56 | 3288.01    | 0.48 |
| 7                    | 3762.89                                  | 3762.23 | 3761.70 | 3762.27    | 0.60 |

Table 52 Equilibrium concentration of reactive yellow in solution at room temperature on bead 150  $\mu\text{m}$

| Initial dye concentration (mg/g) | Equilibrium dye concentration in solution: $C_e$ (mg/l) |         |         |            | SD   |
|----------------------------------|---|---------|---------|------------|------|
|                                  | 1   | 2       | 3       | Mean value |      |
| 542.70                           | 27.27   | 27.25   | 27.26   | 27.26      | 0.01 |
| 1107.81                          | 80.47   | 80.53   | 80.54   | 80.51      | 0.04 |
| 1638.94                          | 440.65  | 440.24  | 440.08  | 440.32     | 0.29 |
| 2186.24                          | 855.67  | 855.67  | 857.10  | 856.15     | 0.83 |
| 2649.68                          | 1154.14   | 1153.11 | 1153.00 | 1153.42    | 0.63 |
| 3288.01                          | 1699.09   | 1698.28 | 1699.88 | 1699.08    | 0.80 |
| 3762.27                          | 2193.08   | 2199.99 | 2191.99 | 2192.35    | 0.63 |

Table 53 Experimental data for equilibrium adsorption isotherm of reactive yellow at room temperature on bead 300  $\mu\text{m}$

| $C_o$ (mg/l) | $C_e$ (mg/l) | Weight of bead : W (g) | Dye adsorbed by bead : $q_e$ (mg/g) |
|--------------|--------------|------------------------|-------------------------------------|
| 542.70       | 27.26        | 0.5009                 | 5.15                                |
| 1107.81      | 80.51        | 0.5000                 | 10.27                               |
| 1638.94      | 440.32       | 0.5002                 | 11.98                               |
| 2186.24      | 856.15       | 0.5001                 | 13.30                               |
| 2649.68      | 1153.42      | 0.5005                 | 14.95                               |
| 3288.01      | 1699.08      | 0.5005                 | 15.87                               |
| 3762.27      | 2192.35      | 0.5008                 | 15.67                               |

Table 54 Experimental data for Langmuir isotherm of reactive yellow at room temperature on bead 150  $\mu\text{m}$

| $C_e$ (mg/l) | $q_e$ (mg/g) | $C_e/q_e$ (g/l) |
|--------------|--------------|-----------------|
| 27.26        | 5.15         | 5.29            |
| 80.51        | 10.27        | 7.84            |
| 440.32       | 11.98        | 36.75           |
| 856.15       | 13.30        | 64.37           |
| 1153.42      | 14.95        | 77.15           |
| 1699.08      | 15.87        | 107.06          |
| 2192.35      | 15.67        | 139.91          |

สถาบันวิทยบริการ  
จุฬาลงกรณ์มหาวิทยาลัย

Table 55 Experimental data for Freundlich isotherm of reactive yellow at room temperature on bead 150  $\mu\text{m}$

| $C_e$ (mg/l) | $q_e$ (mg/g) | $\log C_e$ | $\log q_e$ |
|--------------|--------------|------------|------------|
| 27.26        | 5.15         | 1.44       | 0.71       |
| 80.51        | 10.27        | 1.91       | 1.01       |
| 440.32       | 11.98        | 2.64       | 1.08       |
| 856.15       | 13.30        | 2.93       | 1.12       |
| 1153.42      | 14.95        | 3.06       | 1.17       |
| 1699.08      | 15.87        | 3.23       | 1.20       |
| 2192.35      | 15.67        | 3.34       | 1.20       |

สถาบันวิทยบริการ  
จุฬาลงกรณ์มหาวิทยาลัย

## 5.2 Particle Size 300 $\mu\text{m}$

Table 56 Equilibrium concentration of reactive yellow in solution at room temperature on bead 300  $\mu\text{m}$

| Initial dye concentration (mg/g) | Equilibrium dye concentration in solution: $C_e$ (mg/l) |         |         |            | SD   |
|----------------------------------|---|---------|---------|------------|------|
|                                  | 1   | 2       | 3       | Mean value |      |
| 542.70                           | 105.65  | 105.75  | 105.65  | 105.68     | 0.06 |
| 1107.81                          | 336.03  | 334.93  | 334.73  | 335.23     | 0.70 |
| 1638.94                          | 833.13  | 832.50  | 833.31  | 832.98     | 0.43 |
| 2186.24                          | 1334.53   | 1334.73 | 1334.94 | 1334.73    | 0.21 |
| 2649.68                          | 1556.27   | 1556.42 | 1557.19 | 1556.62    | 0.49 |
| 3288.01                          | 2336.39   | 2336.56 | 2336.23 | 2336.39    | 0.17 |
| 3762.27                          | 2767.38   | 2767.31 | 2767.35 | 2767.35    | 0.04 |

Table 57 Experimental data for equilibrium adsorption isotherm of reactive yellow at room temperature on bead 300  $\mu\text{m}$

| $C_o$ (mg/l) | $C_e$ (mg/l) | Weight of bead : W (g) | Dye adsorbed by bead : $q_e$ (mg/g) |
|--------------|--------------|------------------------|-------------------------------------|
| 542.70       | 105.68       | 0.5006                 | 4.36                                |
| 1107.81      | 335.23       | 0.5003                 | 7.72                                |
| 1638.94      | 832.98       | 0.5001                 | 8.06                                |
| 2186.24      | 1334.73      | 0.5000                 | 8.52                                |
| 2649.68      | 1556.62      | 0.5010                 | 10.91                               |
| 3288.01      | 2336.39      | 0.5000                 | 9.52                                |
| 3762.27      | 2767.35      | 0.5003                 | 9.94                                |

Table 58 Experimental data for Langmuir isotherm of reactive yellow at room temperature on bead 300  $\mu\text{m}$

| $C_e$ (mg/l) | $q_e$ (mg/g) | $C_e/q_e$ (g/l) |
|--------------|--------------|-----------------|
| 105.68       | 4.36         | 24.24           |
| 335.23       | 7.72         | 43.42           |
| 832.98       | 8.06         | 103.35          |
| 1334.73      | 8.52         | 156.66          |
| 1556.62      | 10.91        | 142.68          |
| 2336.39      | 9.52         | 245.42          |
| 2767.35      | 9.94         | 278.41          |

Table 59 Experimental data for Freundlich isotherm of reactive yellow at room temperature on bead 300  $\mu\text{m}$

| $C_e$ (mg/l) | $q_e$ (mg/g) | $\log C_e$ | $\log q_e$ |
|--------------|--------------|------------|------------|
| 105.68       | 4.36         | 2.02       | 0.64       |
| 335.23       | 7.72         | 2.53       | 0.89       |
| 832.98       | 8.06         | 2.92       | 0.90       |
| 1334.73      | 8.52         | 3.13       | 0.93       |
| 1556.62      | 10.91        | 3.19       | 1.04       |
| 2336.39      | 9.52         | 3.37       | 0.98       |
| 2767.35      | 9.94         | 3.44       | 1.00       |

จุฬาลงกรณ์มหาวิทยาลัย



### 5.3 Particle Size 500 $\mu\text{m}$

Table 60 Equilibrium concentration of reactive yellow in solution at room temperature on bead 500  $\mu\text{m}$

| Initial dye concentration (mg/g) | Equilibrium dye concentration in solution: $C_e$ (mg/l) |         |         |            | SD   |
|----------------------------------|---|---------|---------|------------|------|
|                                  | 1   | 2       | 3       | Mean value |      |
| 542.70                           | 68.01   | 68.58   | 68.21   | 68.27      | 0.29 |
| 1107.81                          | 455.31  | 455.30  | 455.46  | 455.36     | 0.09 |
| 1638.94                          | 860.63  | 858.34  | 859.39  | 859.45     | 1.15 |
| 2186.24                          | 1380.03   | 1379.53 | 1379.37 | 1379.64    | 0.34 |
| 2649.68                          | 1922.14   | 1922.14 | 1921.58 | 1921.95    | 0.32 |
| 3288.01                          | 2351.26   | 2351.26 | 2350.09 | 2350.87    | 0.68 |
| 3762.27                          | 2899.10   | 2899.15 | 2899.20 | 2899.15    | 0.05 |

Table 61 Experimental data for equilibrium adsorption isotherm of reactive yellow at room temperature on bead 500  $\mu\text{m}$

| $C_o$ (mg/l) | $C_e$ (mg/l) | Weight of bead : W (g) | Dye adsorbed by bead : $q_e$ (mg/g) |
|--------------|--------------|------------------------|-------------------------------------|
| 542.70       | 68.27        | 0.5000                 | 4.74                                |
| 1107.81      | 455.36       | 0.5004                 | 6.52                                |
| 1638.94      | 859.45       | 0.5002                 | 7.79                                |
| 2186.24      | 1379.64      | 0.5004                 | 8.06                                |
| 2649.68      | 1921.95      | 0.5005                 | 7.27                                |
| 3288.01      | 2350.87      | 0.5000                 | 9.37                                |
| 3762.27      | 2899.15      | 0.5000                 | 8.63                                |

Table 62 Experimental data for Langmuir isotherm of reactive yellow at room temperature on bead 500  $\mu\text{m}$

| $C_e$ (mg/l) | $q_e$ (mg/g) | $C_e/q_e$ (g/l) |
|--------------|--------------|-----------------|
| 68.27        | 4.74         | 14.40           |
| 455.36       | 6.52         | 69.84           |
| 859.45       | 7.79         | 110.33          |
| 1379.64      | 8.06         | 171.17          |
| 1921.95      | 7.27         | 264.37          |
| 2350.87      | 9.37         | 250.89          |
| 2899.15      | 8.63         | 335.94          |

Table 63 Experimental data for Freundlich isotherm of reactive yellow at room temperature on bead 500  $\mu\text{m}$

| $C_e$ (mg/l) | $q_e$ (mg/g) | $\log C_e$ | $\log q_e$ |
|--------------|--------------|------------|------------|
| 68.27        | 4.74         | 1.83       | 0.68       |
| 455.36       | 6.52         | 2.66       | 0.81       |
| 859.45       | 7.79         | 2.93       | 0.89       |
| 1379.64      | 8.06         | 3.14       | 0.91       |
| 1921.95      | 7.27         | 3.28       | 0.86       |
| 2350.87      | 9.37         | 3.37       | 0.97       |
| 2899.15      | 8.63         | 3.46       | 0.94       |

จุฬาลงกรณ์มหาวิทยาลัย

## 6. Reactive Yellow at Temperature of 80°C

### 6.1 Particle Size 150 $\mu\text{m}$

Table 64 Equilibrium concentration of reactive yellow in solution at 80°C on bead  
150  $\mu\text{m}$

| Initial dye concentration (mg/g) | Equilibrium dye concentration in solution: $C_e$ (mg/l) |         |         |            | SD   |
|----------------------------------|---|---------|---------|------------|------|
|                                  | 1   | 2       | 3       | Mean value |      |
| 542.70                           | 37.47   | 37.52   | 37.52   | 37.50      | 0.03 |
| 1107.81                          | 66.05   | 66.13   | 66.12   | 66.10      | 0.04 |
| 1638.94                          | 324.27  | 324.31  | 324.43  | 324.34     | 0.08 |
| 2186.24                          | 703.50  | 703.27  | 703.59  | 703.45     | 0.17 |
| 2649.69                          | 1152.64   | 1152.56 | 1152.83 | 1152.68    | 0.14 |
| 3288.01                          | 1573.53   | 1573.27 | 1573.43 | 1573.41    | 0.13 |
| 3762.27                          | 2150.64   | 2150.74 | 2150.77 | 2150.72    | 0.07 |

Table 65 Experimental data for equilibrium adsorption isotherm of reactive yellow at 80°C on bead 150  $\mu\text{m}$

| $C_o$ (mg/l) | $C_e$ (mg/l) | Weight of bead : W (g) | Dye adsorbed by bead : $q_e$ (mg/g) |
|--------------|--------------|------------------------|-------------------------------------|
| 542.70       | 37.50        | 0.5009                 | 5.04                                |
| 1107.81      | 66.10        | 0.5001                 | 10.42                               |
| 1638.94      | 324.34       | 0.5003                 | 13.14                               |
| 2186.24      | 703.45       | 0.5000                 | 14.83                               |
| 2649.69      | 1152.68      | 0.5001                 | 14.97                               |
| 3288.01      | 1573.41      | 0.5000                 | 17.15                               |
| 3762.27      | 2150.72      | 0.5008                 | 16.09                               |

Table 66 Experimental data for Langmuir isotherm of reactive yellow at 80°C on bead 150  $\mu\text{m}$

| $C_e$ (mg/l) | $q_e$ (mg/g) | $C_e/q_e$ (g/l) |
|--------------|--------------|-----------------|
| 37.50        | 5.04         | 7.44            |
| 66.10        | 10.42        | 6.34            |
| 324.34       | 13.14        | 24.68           |
| 703.45       | 14.83        | 47.43           |
| 1152.68      | 14.97        | 77.00           |
| 1573.41      | 17.15        | 91.74           |
| 2150.72      | 16.09        | 133.67          |

Table 67 Experimental data for Freundlich isotherm of reactive yellow at 80°C on bead 150  $\mu\text{m}$

| $C_e$ (mg/l) | $q_e$ (mg/g) | $\log C_e$ | $\log q_e$ |
|--------------|--------------|------------|------------|
| 37.50        | 5.04         | 1.57       | 0.70       |
| 66.10        | 10.42        | 1.82       | 1.02       |
| 324.34       | 13.14        | 2.51       | 1.12       |
| 703.45       | 14.83        | 2.85       | 1.17       |
| 1152.68      | 14.97        | 3.06       | 1.18       |
| 1573.41      | 17.15        | 3.20       | 1.23       |
| 2150.72      | 16.09        | 3.33       | 1.21       |

จุฬาลงกรณ์มหาวิทยาลัย

## 6.2 Particle Size 300 $\mu\text{m}$

Table 68 Equilibrium concentration of reactive yellow in solution at 80°C on bead

300  $\mu\text{m}$

| Initial dye concentration (mg/g) | Equilibrium dye concentration in solution: $C_e$ (mg/l) |         |         |            | SD   |
|----------------------------------|---|---------|---------|------------|------|
|                                  | 1   | 2       | 3       | Mean value |      |
| 542.70                           | 60.46   | 60.44   | 60.66   | 60.52      | 0.12 |
| 1107.81                          | 327.66  | 326.57  | 326.81  | 327.01     | 0.57 |
| 1638.94                          | 728.86  | 727.89  | 728.90  | 728.55     | 0.57 |
| 2186.24                          | 1214.37   | 1215.20 | 1214.03 | 1214.53    | 0.60 |
| 2649.69                          | 1636.97   | 1635.89 | 1635.46 | 1636.11    | 0.78 |
| 3288.01                          | 2188.85   | 2188.85 | 2188.43 | 2188.71    | 0.24 |
| 3762.27                          | 2634.45   | 2632.13 | 2633.36 | 2633.31    | 1.16 |

Table 69 Experimental data for equilibrium adsorption isotherm of reactive yellow at 80°C on bead 300  $\mu\text{m}$

| $C_o$ (mg/l) | $C_e$ (mg/l) | Weight of bead : W (g) | Dye adsorbed by bead : $q_e$ (mg/g) |
|--------------|--------------|------------------------|-------------------------------------|
| 542.70       | 60.52        | 0.5000                 | 4.82                                |
| 1107.81      | 327.01       | 0.5005                 | 7.80                                |
| 1638.94      | 728.55       | 0.5002                 | 9.10                                |
| 2186.24      | 1214.53      | 0.5004                 | 9.71                                |
| 2649.69      | 1636.11      | 0.5002                 | 10.13                               |
| 3288.01      | 2188.71      | 0.5002                 | 10.99                               |
| 3762.27      | 2633.31      | 0.5009                 | 11.27                               |

Table 70 Experimental data for Langmuir isotherm of reactive yellow at 80°C on bead 300  $\mu\text{m}$

| $C_e$ (mg/l) | $q_e$ (mg/g) | $C_e/q_e$ (g/l) |
|--------------|--------------|-----------------|
| 60.52        | 4.82         | 12.56           |
| 327.01       | 7.80         | 41.92           |
| 728.55       | 9.10         | 80.06           |
| 1214.53      | 9.71         | 125.08          |
| 1636.11      | 10.13        | 161.51          |
| 2188.71      | 10.99        | 199.15          |
| 2633.31      | 11.27        | 233.66          |

Table 71 Experimental data for Freundlich isotherm of reactive yellow at 80°C on bead 300  $\mu\text{m}$

| $C_e$ (mg/l) | $q_e$ (mg/g) | $\log C_e$ | $\log q_e$ |
|--------------|--------------|------------|------------|
| 60.52        | 4.82         | 1.78       | 0.68       |
| 327.01       | 7.80         | 2.51       | 0.89       |
| 728.55       | 9.10         | 2.86       | 0.96       |
| 1214.53      | 9.71         | 3.08       | 0.99       |
| 1636.11      | 10.13        | 3.21       | 1.01       |
| 2188.71      | 10.99        | 3.34       | 1.04       |
| 2633.31      | 11.27        | 3.42       | 1.05       |

จุฬาลงกรณ์มหาวิทยาลัย

### 6.3 Particle Size 500 $\mu\text{m}$

Table 72 Equilibrium concentration of reactive yellow in solution at 80°C on bead

500  $\mu\text{m}$

| Initial dye concentration (mg/g) | Equilibrium dye concentration in solution: $C_e$ (mg/l) |         |         |            | SD   |
|----------------------------------|---|---------|---------|------------|------|
|                                  | 1   | 2       | 3       | Mean value |      |
| 542.70                           | 35.47   | 35.43   | 35.42   | 35.44      | 0.03 |
| 1107.81                          | 367.36  | 367.68  | 367.67  | 367.57     | 0.18 |
| 1638.94                          | 840.47  | 840.72  | 839.84  | 840.34     | 0.45 |
| 2186.24                          | 1306.41   | 1306.26 | 1305.18 | 1305.95    | 0.67 |
| 2649.69                          | 1787.45   | 1787.45 | 1786.90 | 1787.27    | 0.32 |
| 3288.01                          | 2373.98   | 2372.06 | 2371.29 | 2372.44    | 1.39 |
| 3762.27                          | 2742.70   | 2742.70 | 2742.65 | 2742.68    | 0.03 |

Table 73 Experimental data for equilibrium adsorption isotherm of reactive yellow at 80°C on bead 500  $\mu\text{m}$

| $C_o$ (mg/l) | $C_e$ (mg/l) | Weight of bead : W (g) | Dye adsorbed by bead : $q_e$ (mg/g) |
|--------------|--------------|------------------------|-------------------------------------|
| 542.70       | 35.44        | 0.5000                 | 5.07                                |
| 1107.81      | 367.57       | 0.5000                 | 7.40                                |
| 1638.94      | 840.34       | 0.5000                 | 7.99                                |
| 2186.24      | 1305.95      | 0.5004                 | 8.80                                |
| 2649.69      | 1787.27      | 0.5005                 | 8.62                                |
| 3288.01      | 2372.44      | 0.5000                 | 9.16                                |
| 3762.27      | 2742.68      | 0.5009                 | 10.18                               |

Table 74 Experimental data for Langmuir isotherm of reactive yellow at 80°C on bead 500  $\mu\text{m}$

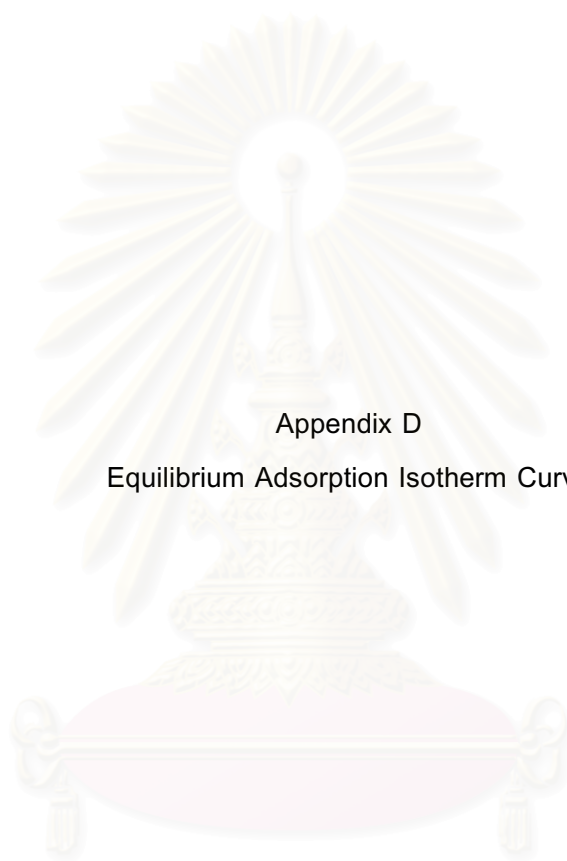
| $C_e$ (mg/l) | $q_e$ (mg/g) | $C_e/q_e$ (g/l) |
|--------------|--------------|-----------------|
| 35.44        | 5.07         | 6.99            |
| 367.57       | 7.40         | 49.67           |
| 840.34       | 7.99         | 105.17          |
| 1305.95      | 8.80         | 148.40          |
| 1787.27      | 8.62         | 207.34          |
| 2372.44      | 9.16         | 259.00          |
| 2742.68      | 10.18        | 269.42          |

Table 75 Experimental data for Freundlich isotherm of reactive yellow at 80°C on bead 500  $\mu\text{m}$

| $C_e$ (mg/l) | $q_e$ (mg/g) | $\log C_e$ | $\log q_e$ |
|--------------|--------------|------------|------------|
| 35.44        | 5.07         | 1.55       | 0.71       |
| 367.57       | 7.40         | 2.57       | 0.87       |
| 840.34       | 7.99         | 2.92       | 0.90       |
| 1305.95      | 8.80         | 3.12       | 0.94       |
| 1787.27      | 8.62         | 3.25       | 0.94       |
| 2372.44      | 9.16         | 3.38       | 0.96       |
| 2742.68      | 10.18        | 3.44       | 1.01       |

จุฬาลงกรณ์มหาวิทยาลัย

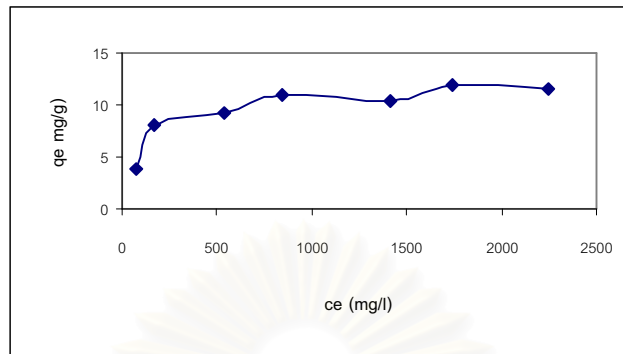




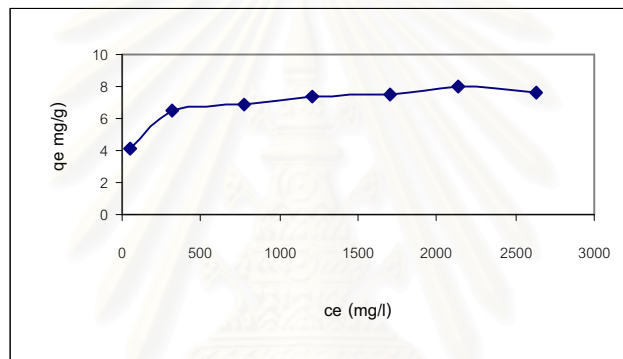
Appendix D

Equilibrium Adsorption Isotherm Curve

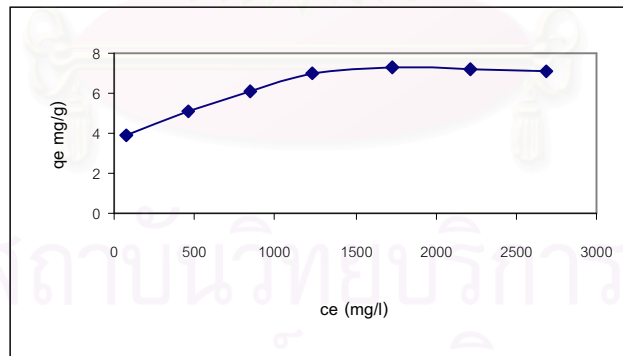
สถาบันวิทยบริการ  
จุฬาลงกรณ์มหาวิทยาลัย



(a)



(b)



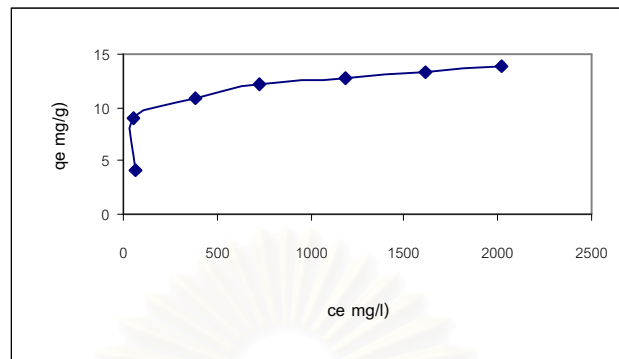
(c)

Figure 1 Equilibrium adsorption isotherms of reactive blue at room temperature on polymer bead.

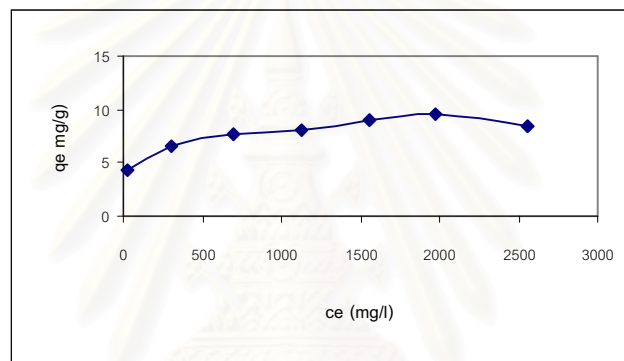
(a) particle size 150  $\mu\text{m}$

(b) particle size 300  $\mu\text{m}$

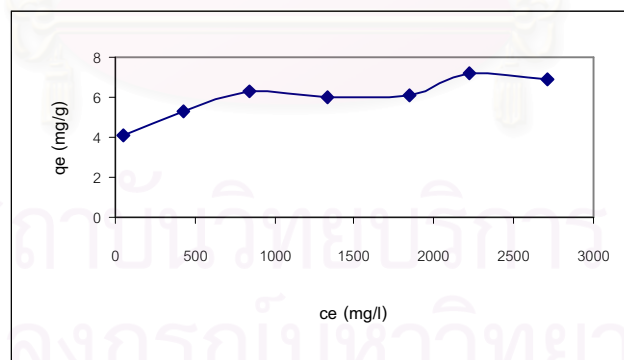
(c) particle size 500  $\mu\text{m}$



(a)



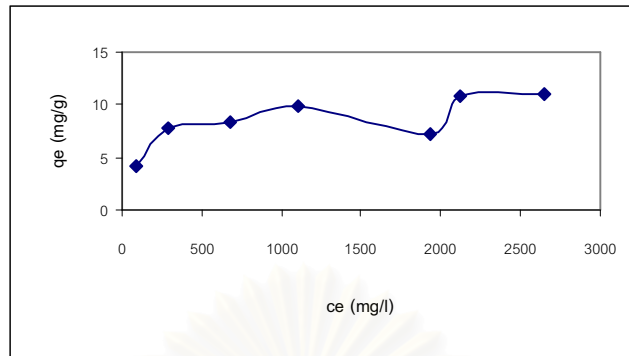
(b)



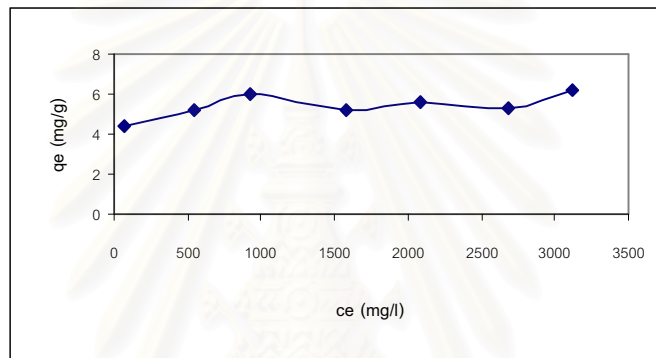
(c)

Figure 2 Equilibrium adsorption isotherms of reactive blue at temperature of 80°C on polymer bead.

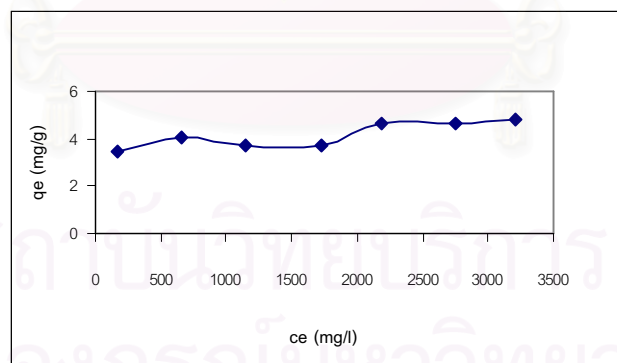
(a) particle size 150 μm    (b) particle size 300 μm    (c) particle size 500 μm



(a)



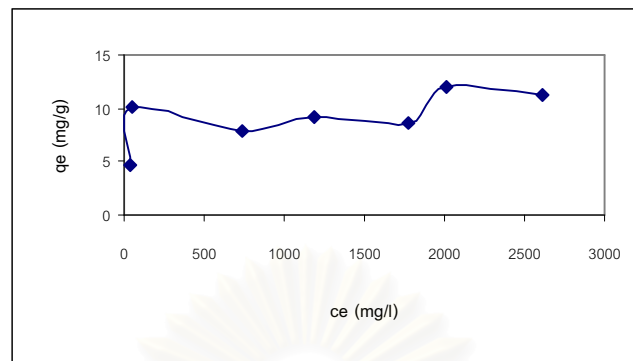
(b)



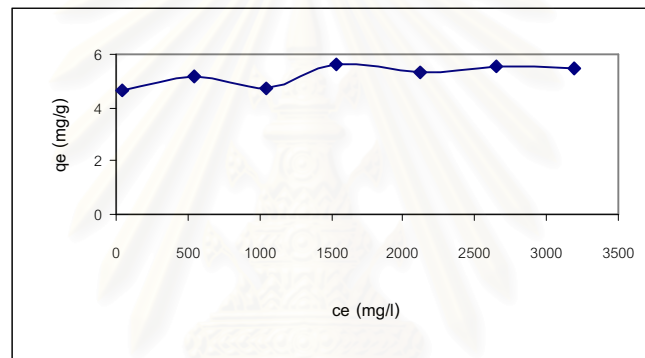
(c)

Figure 3 Equilibrium adsorption isotherms of reactive red at room temperature on polymer bead.

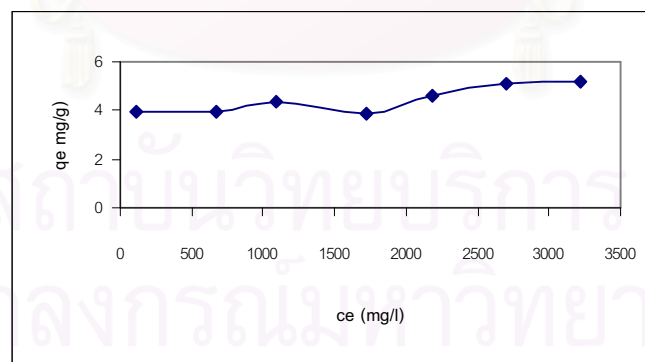
(a) particle size 150  $\mu\text{m}$  (b) particle size 300  $\mu\text{m}$  (c) particle size 500  $\mu\text{m}$



(a)



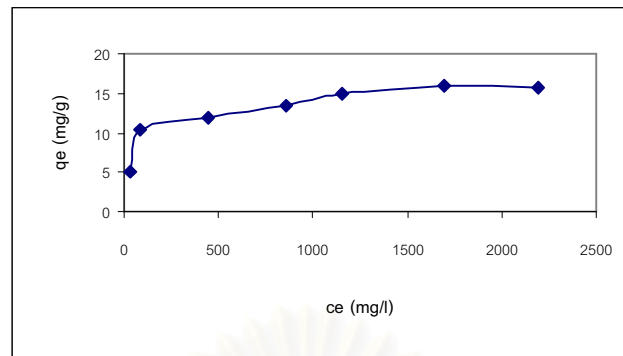
(b)



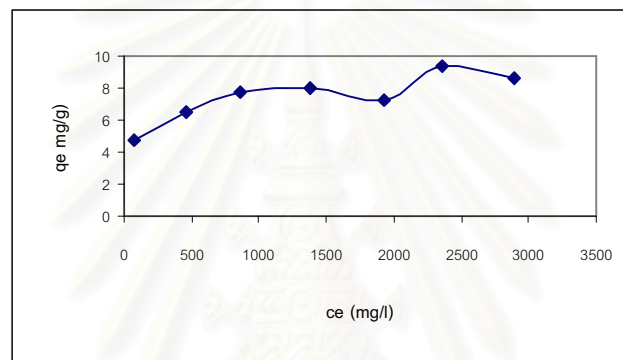
(c)

Figure 4 Equilibrium adsorption isotherms of reactive red at temperature of of 80°C on polymer bead.

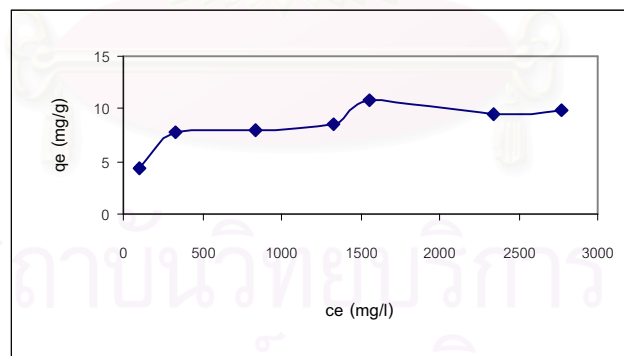
(a) particle size 150  $\mu\text{m}$     (b) particle size 300  $\mu\text{m}$     (c) particle size 500  $\mu\text{m}$



(a)



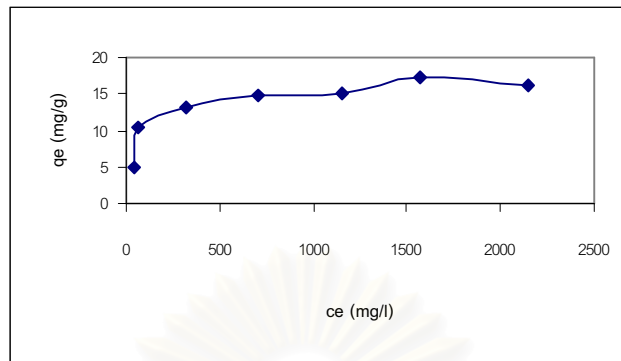
(b)



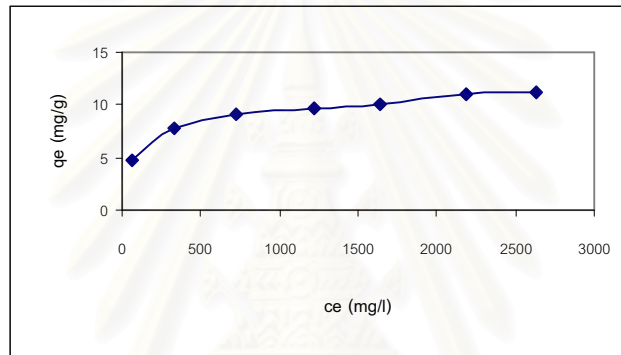
(c)

Figure 5 Equilibrium adsorption isotherms of reactive yellow at room temperature on polymer bead.

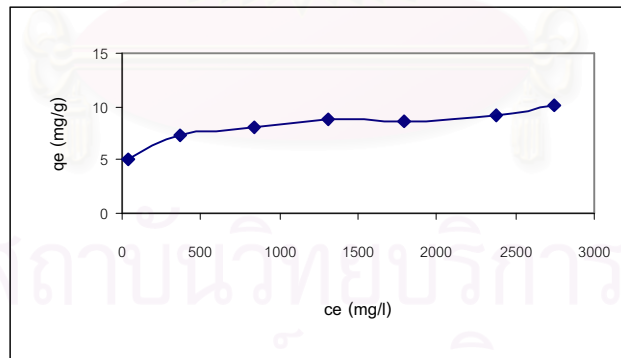
(a) particle size 150 μm      (b) particle size 300 μm      (c) particle size 500 μm



(a)



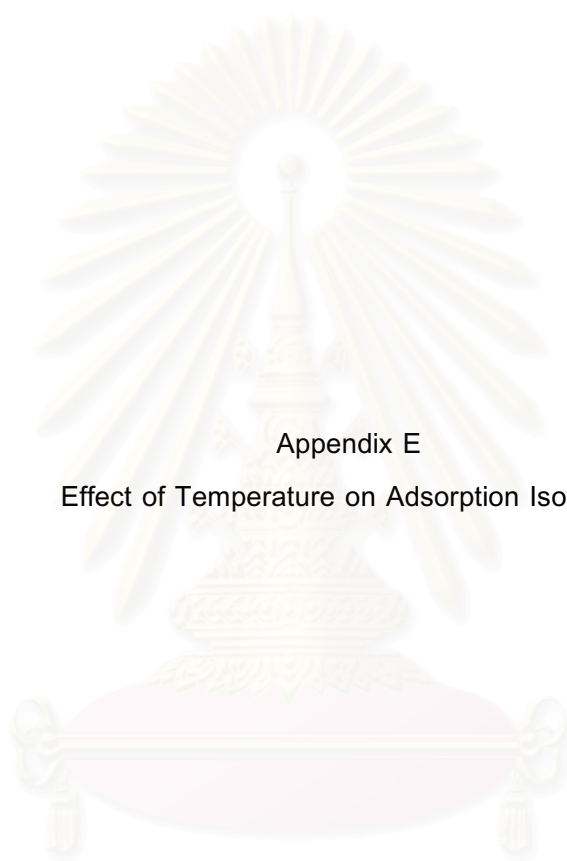
(b)



(c)

Figure 6 Equilibrium adsorption isotherms of reactive yellow at temperature of 80°C on polymer bead.

(a) particle size 150 μm      (b) particle size 300 μm      (c) particle size 500 μm

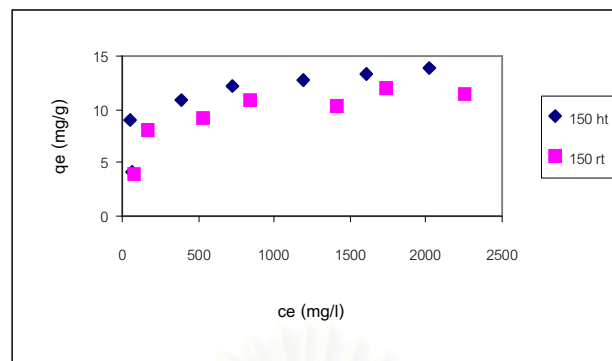


Appendix E

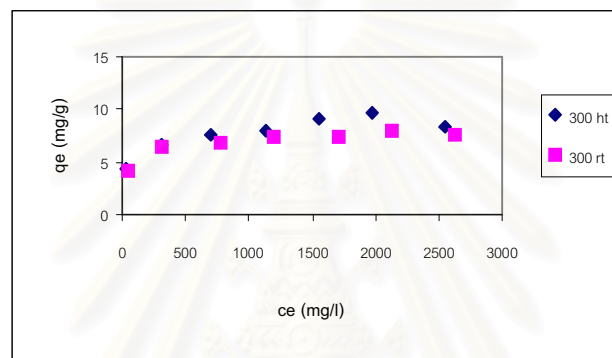
Effect of Temperature on Adsorption Isotherm

สถาบันวิทยบริการ  
จุฬาลงกรณ์มหาวิทยาลัย

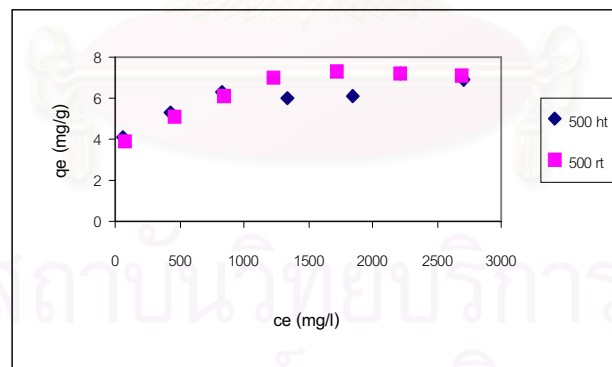




(a)



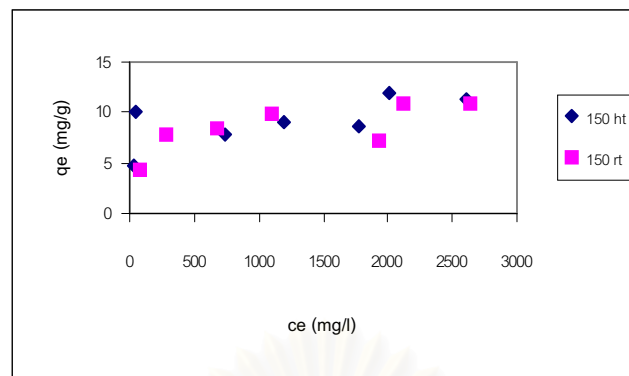
(b)



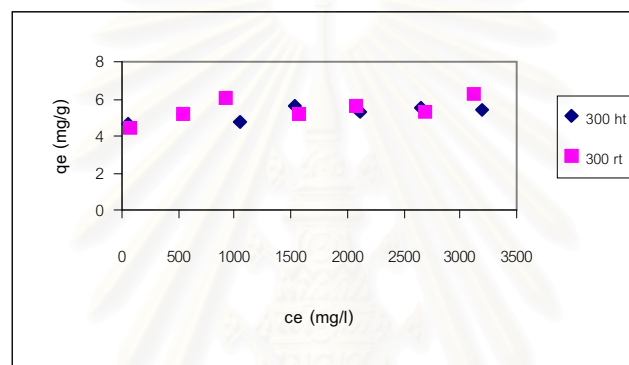
(c)

Figure 1 Effect of temperature on the equilibrium adsorption isotherm of reactive blue on polymer bead.

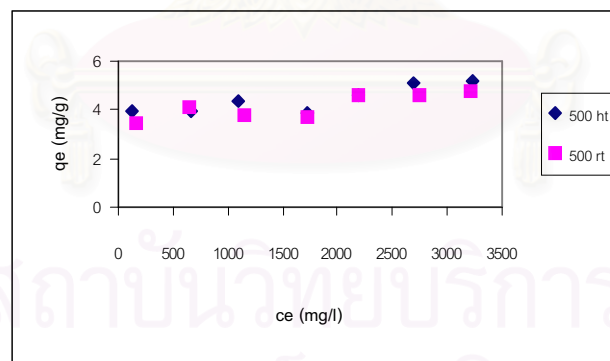
(a) particle size 150  $\mu\text{m}$       (b) particle size 300  $\mu\text{m}$       (c) particle size 500  $\mu\text{m}$



(a)



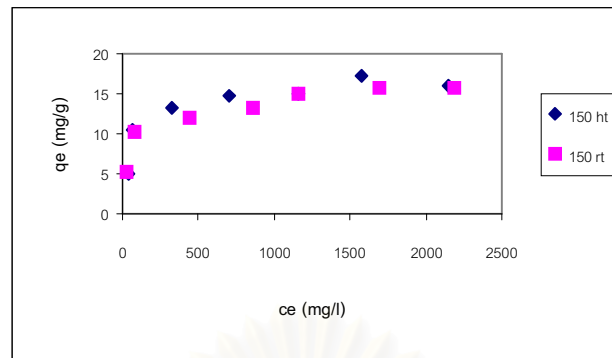
(b)



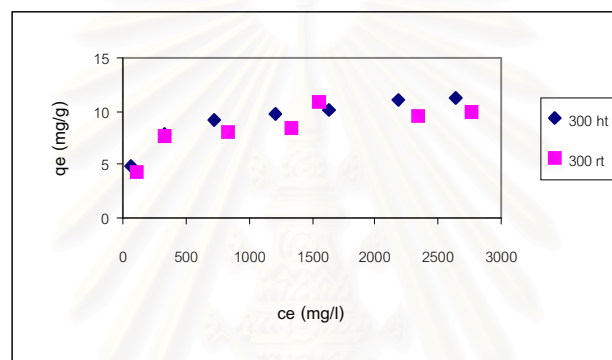
(c)

Figure 2 Effect of temperature on the equilibrium adsorption isotherm of reactive red on polymer bead.

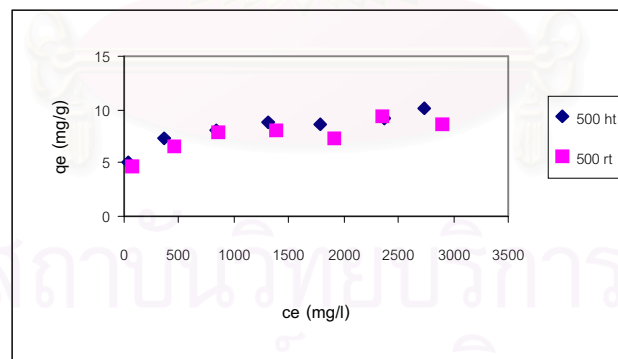
(a) particle size 150  $\mu\text{m}$       (b) particle size 300  $\mu\text{m}$       (c) particle size 500  $\mu\text{m}$



(a)



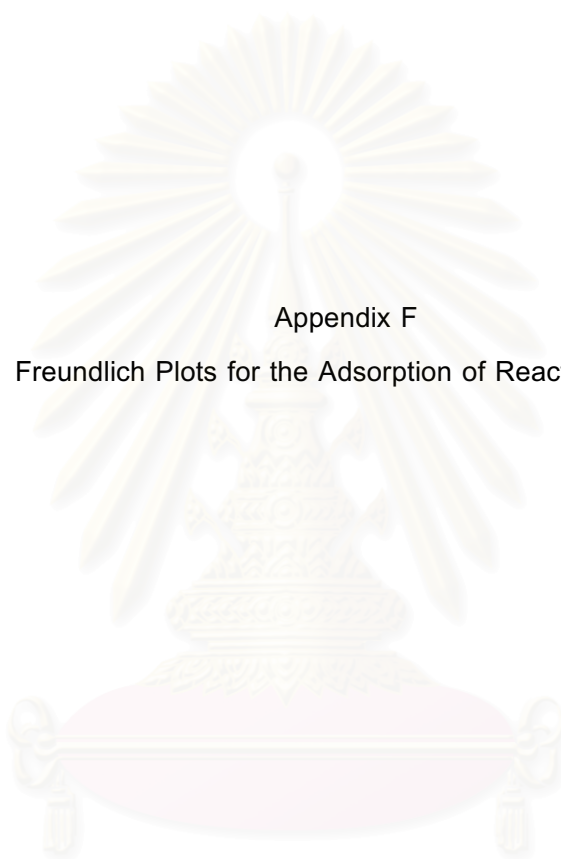
(b)



(c)

Figure 3 Effect of temperature on the equilibrium adsorption isotherm of reactive yellow on polymer bead.

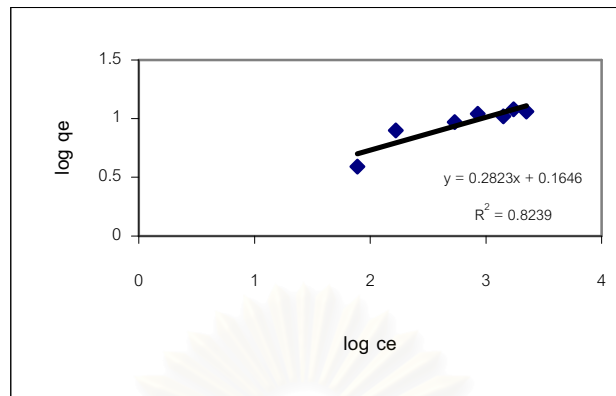
(a) particle size 150  $\mu\text{m}$       (b) particle size 300  $\mu\text{m}$       (c) particle size 500  $\mu\text{m}$



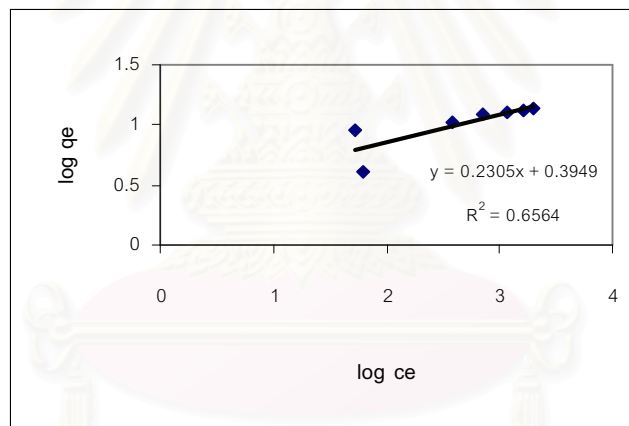
Appendix F

Freundlich Plots for the Adsorption of Reactive Dyes

สถาบันวิทยบริการ  
จุฬาลงกรณ์มหาวิทยาลัย



(a)

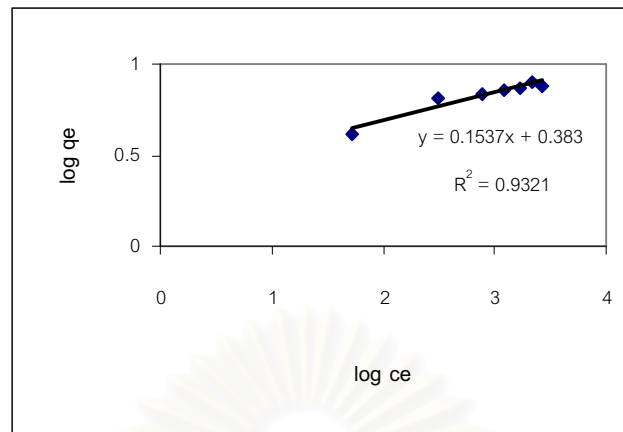


(b)

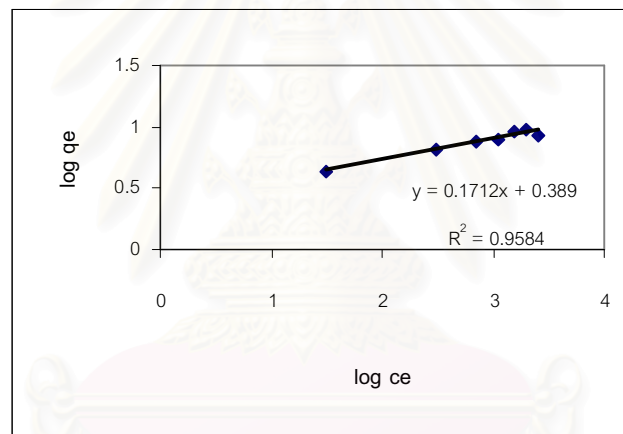
Figure 1 Freundlich plots for the adsorption of reactive blue on bead 150  $\mu\text{m}$ .

(a) at room temperature

(b) at 80°C



(a)

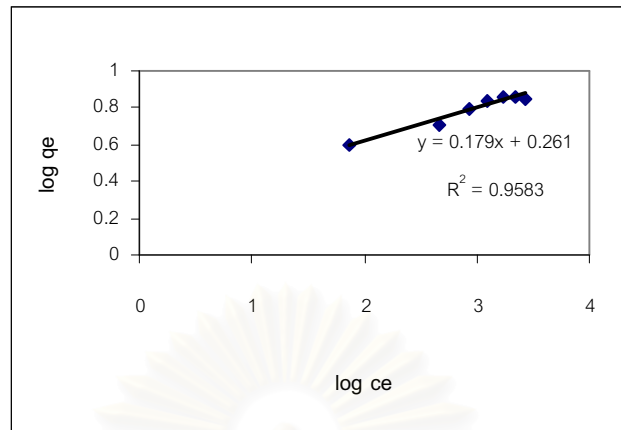


(b)

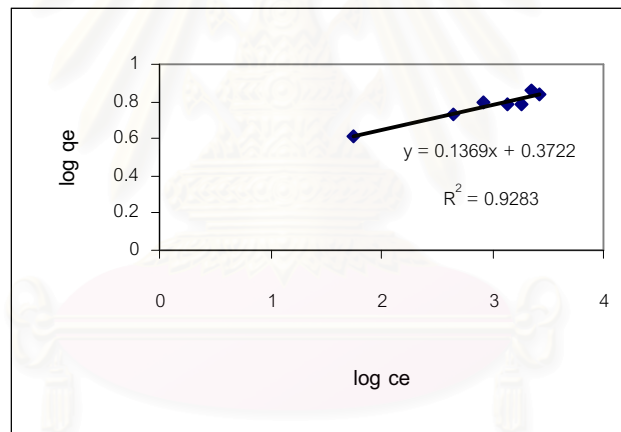
Figure 2 Freundlich plots for the adsorption of reactive blue on bead 300  $\mu\text{m}$ .

(a) at room temperature

(b) at 80°C



(a)

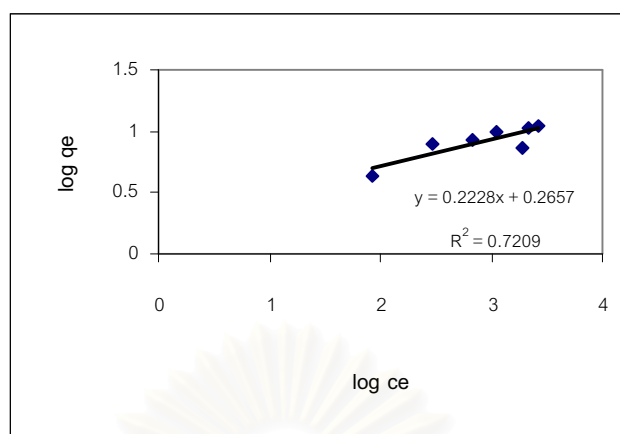


(b)

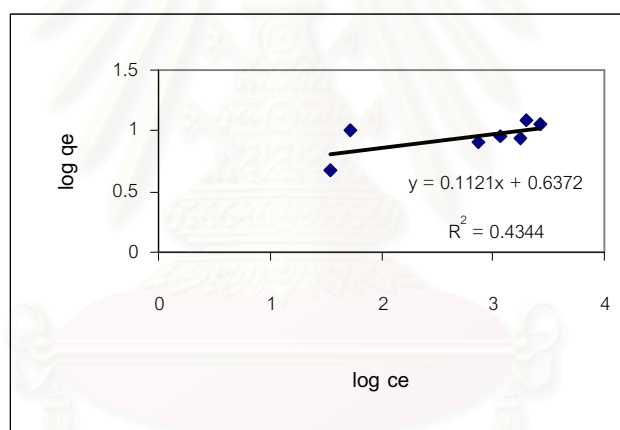
Figure 3 Freundlich plots for the adsorption of reactive blue on bead 500  $\mu\text{m}$ .

(a) at room temperature

(b) at 80°C



(a)



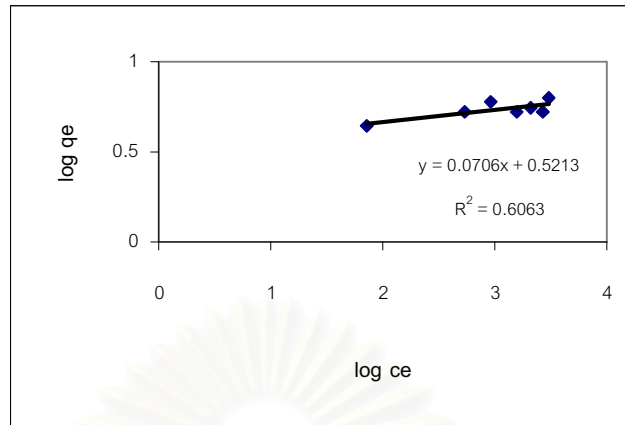
(b)

Figure 4 Freundlich plots for the adsorption of reactive red on bead 150  $\mu\text{m}$ .

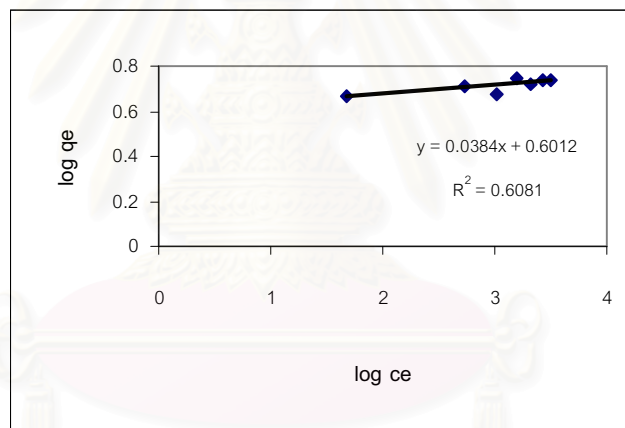
(a) at room temperature

(b) at 80°C





(a)

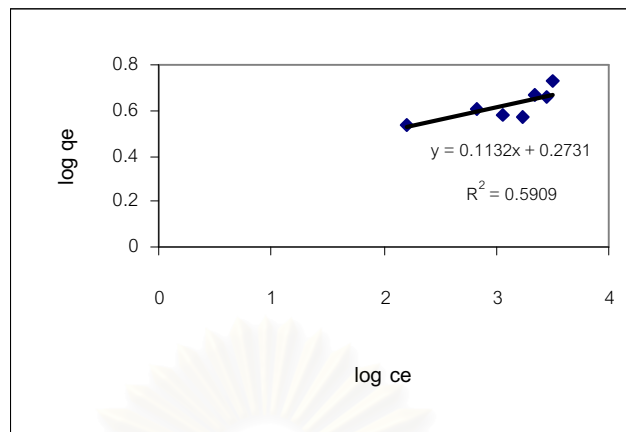


(b)

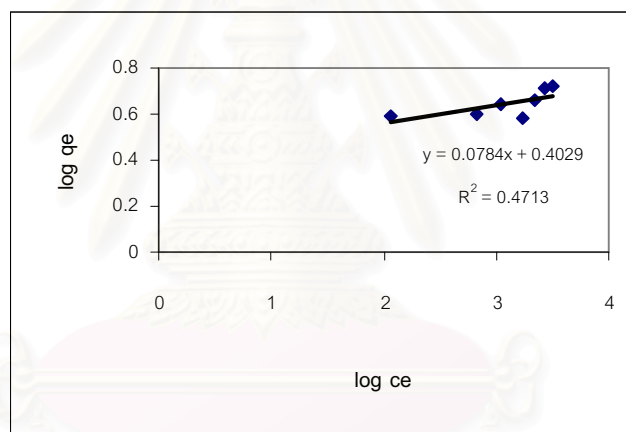
Figure 5 Freundlich plots for the adsorption of reactive red on bead  $300 \mu\text{m}$ .

(a) at room temperature

(b) at  $80^\circ\text{C}$



(a)

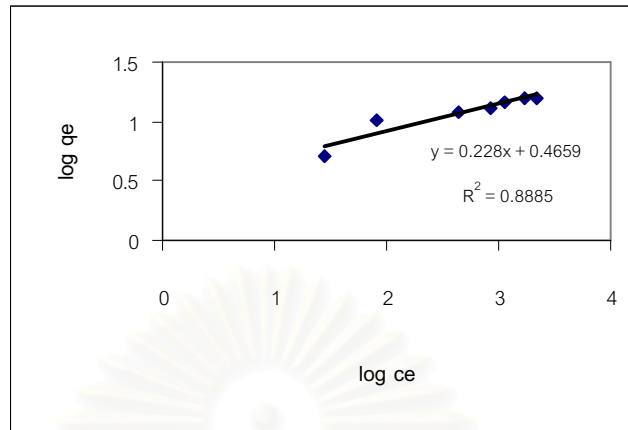


(b)

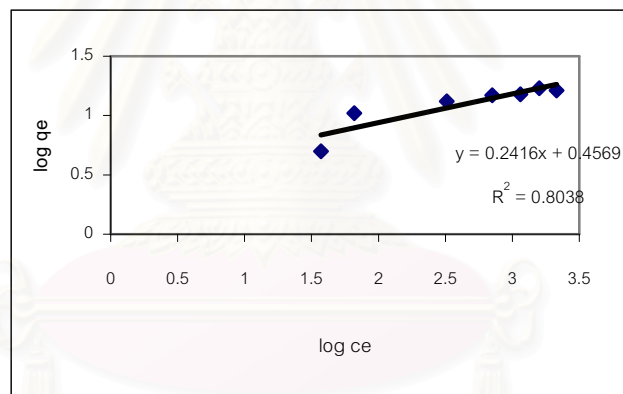
Figure 6 Freundlich plots for the adsorption of reactive red on bead 500  $\mu\text{m}$ .

(a) at room temperature

(b) at 80°C



(a)

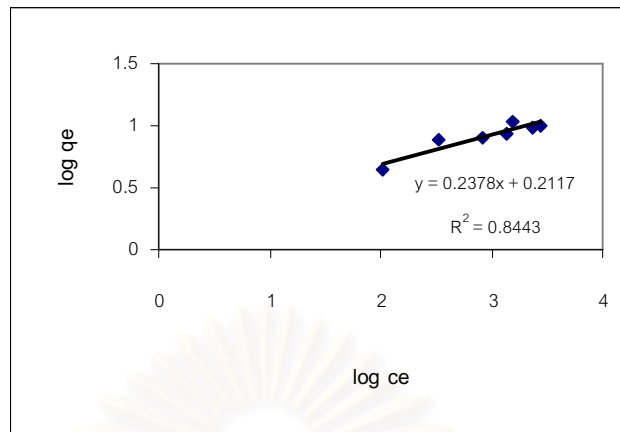


(b)

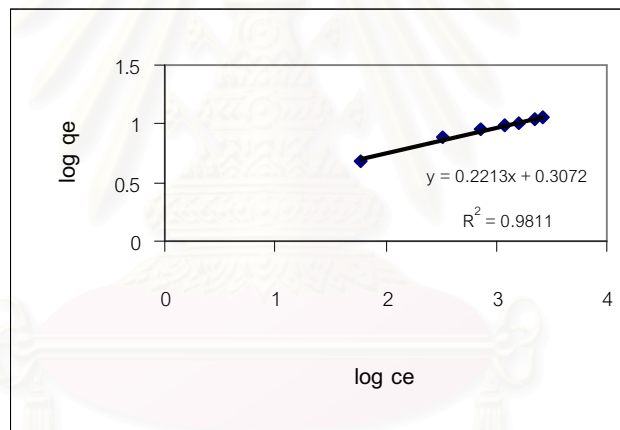
Figure 7 Freundlich plots for the adsorption of reactive yellow on bead 150  $\mu\text{m}$ .

(a) at room temperature

(b) at 80°C



(a)

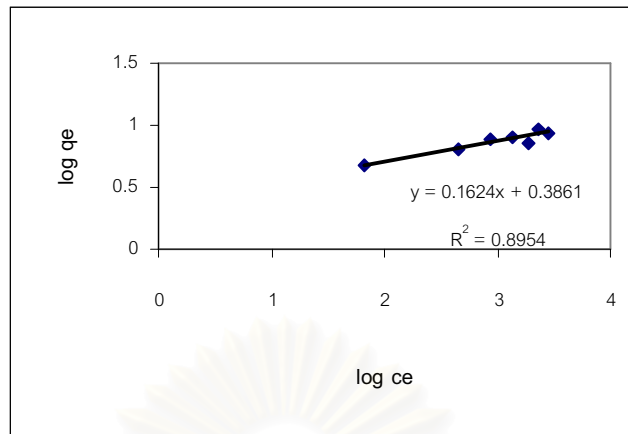


(b)

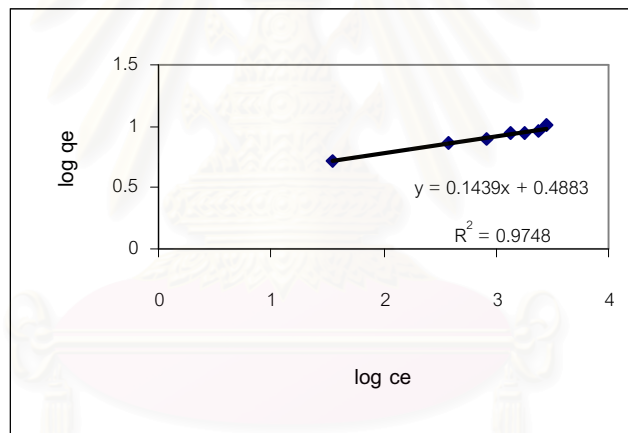
Figure 8 Freundlich plots for the adsorption of reactive yellow on bead 300  $\mu\text{m}$ .

(a) at room temperature

(b) at 80°C



(a)



(b)

Figure 9 Freundlich plots for the adsorption of reactive yellow on bead 500  $\mu\text{m}$ .

(a) at room temperature

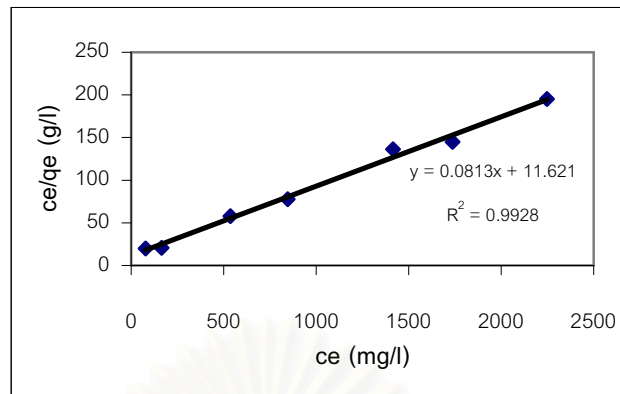
(b) at 80°C

## Appendix G

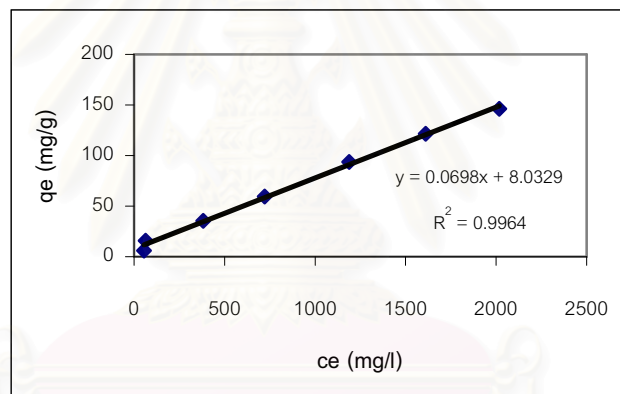
Langmuir Plots for the Adsorption of Reactive Dyes



สถาบันวิทยบริการ  
จุฬาลงกรณ์มหาวิทยาลัย



(a)

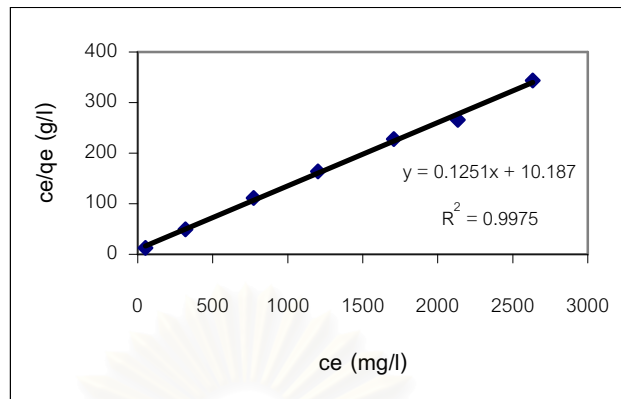


(b)

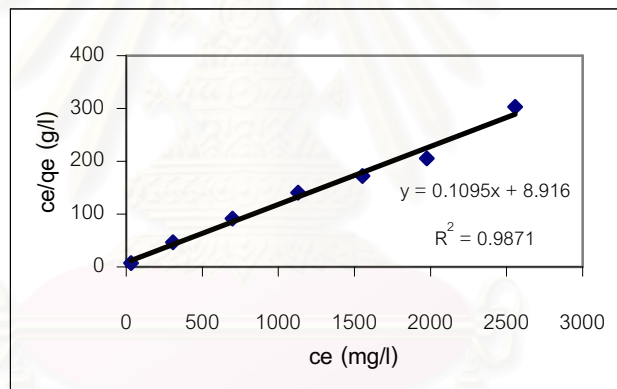
Figure 1 Langmuir plots for the adsorption of reactive blue on bead 150  $\mu\text{m}$ .

(a) at room temperature

(b) at 80°C



(a)



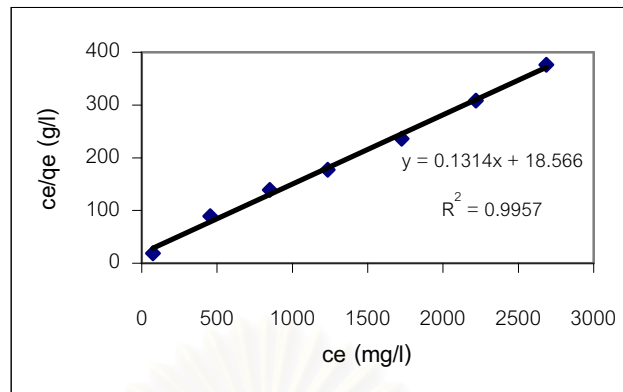
(b)

Figure 2 Langmuir plots for the adsorption of reactive blue on bead 300  $\mu\text{m}$ .

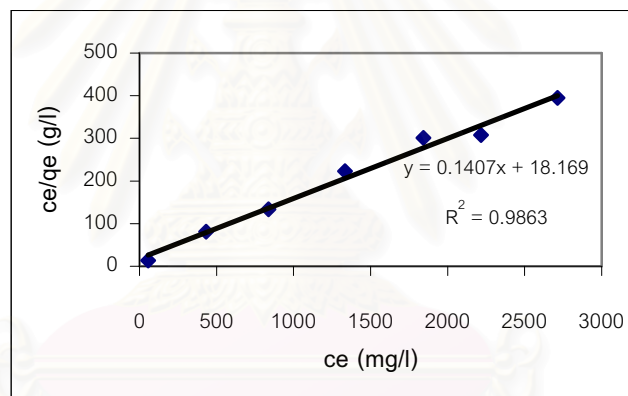
(a) at room temperature

(b) at 80°C





(a)

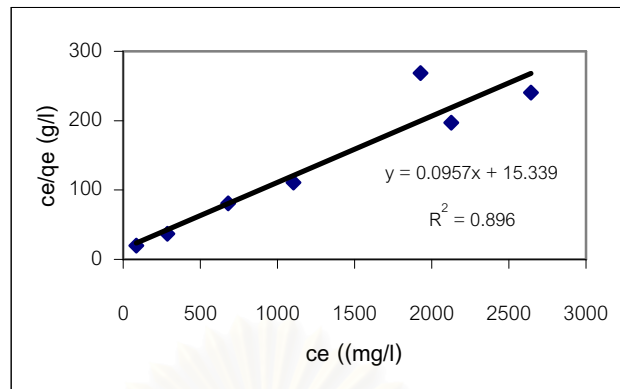


(b)

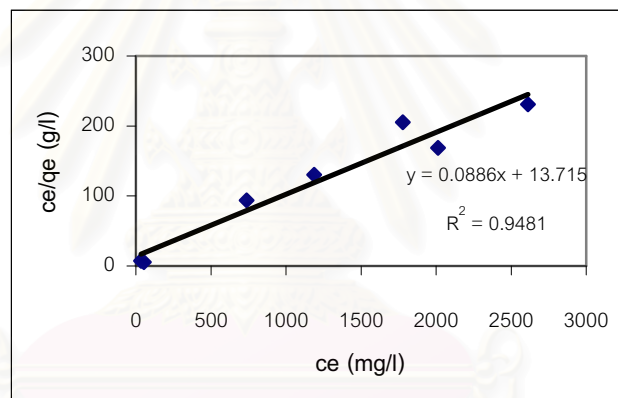
Figure 3 Langmuir plots for the adsorption of reactive blue on bead 500  $\mu\text{m}$ .

(a) at room temperature

(b) at 80°C



(a)

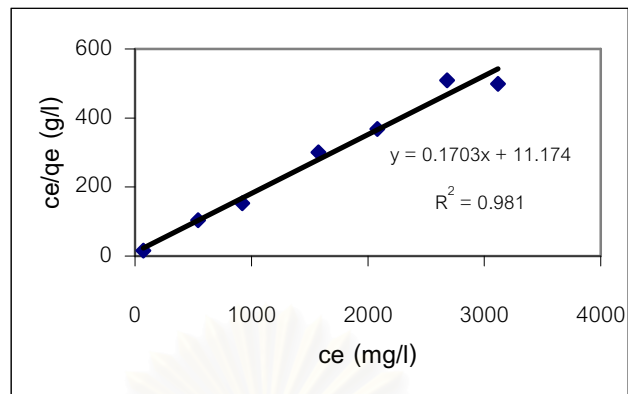


(b)

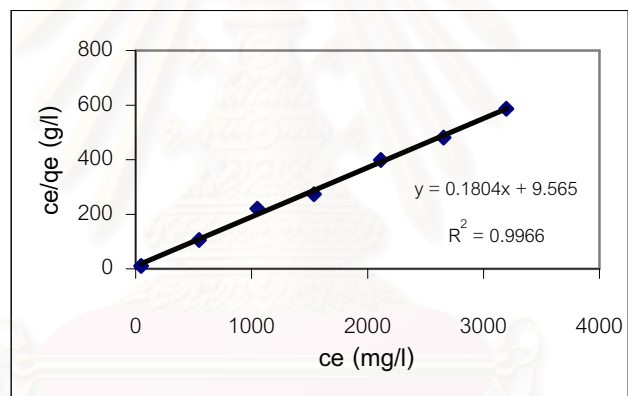
Figure 4 Langmuir plots for the adsorption of reactive red on bead 150  $\mu\text{m}$ .

(a) at room temperature

(b) at 80°C



(a)

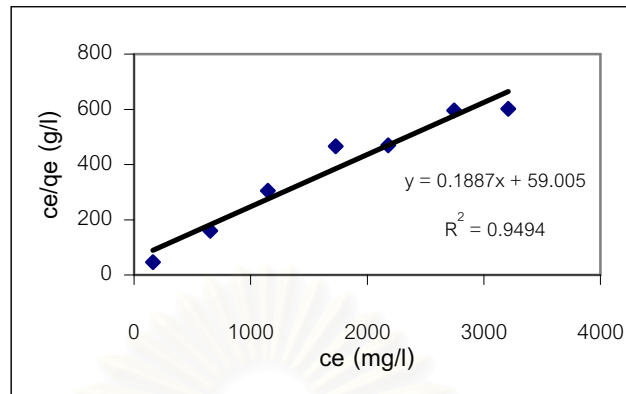


(b)

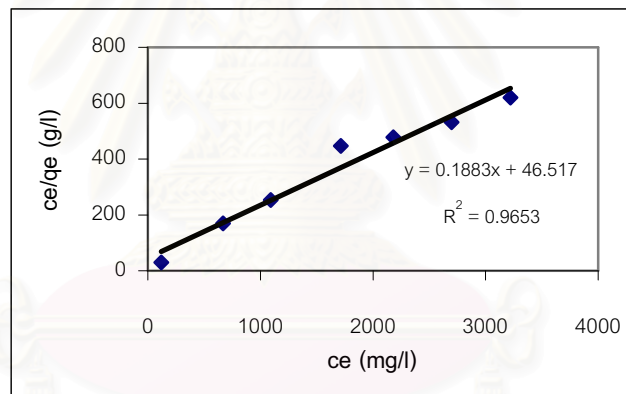
Figure 5 Langmuir plots for the adsorption of reactive red on bead 300  $\mu\text{m}$ .

(a) at room temperature

(b) at 80°C



(a)

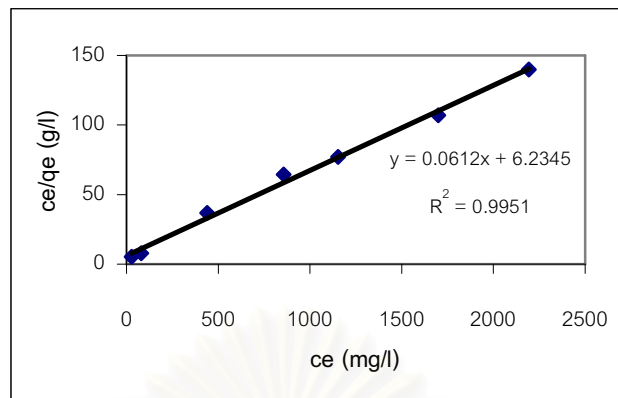


(b)

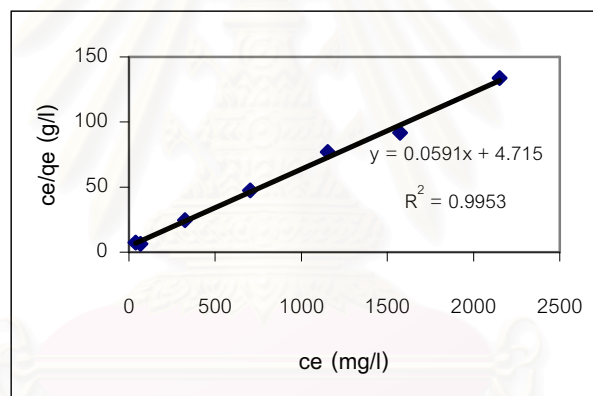
Figure 6 Langmuir plots for the adsorption of reactive red on bead  $500 \mu\text{m}$ .

(a) at room temperature

(b) at  $80^\circ\text{C}$



(a)

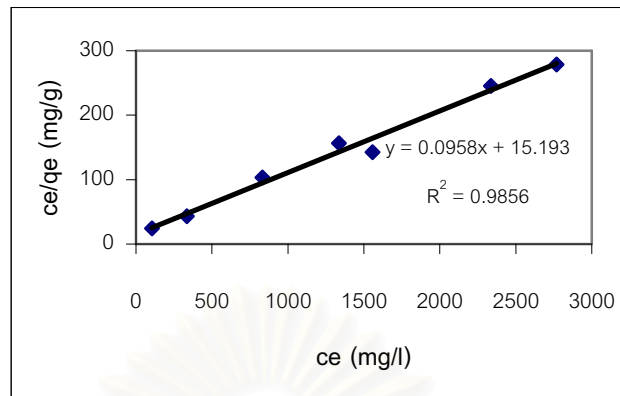


(b)

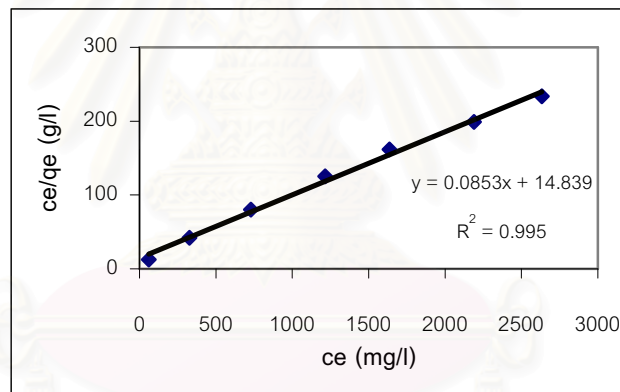
Figure 7 Langmuir plots for the adsorption of reactive yellow on bead 150  $\mu\text{m}$ .

(a) at room temperature

(b) at 80°C



(a)

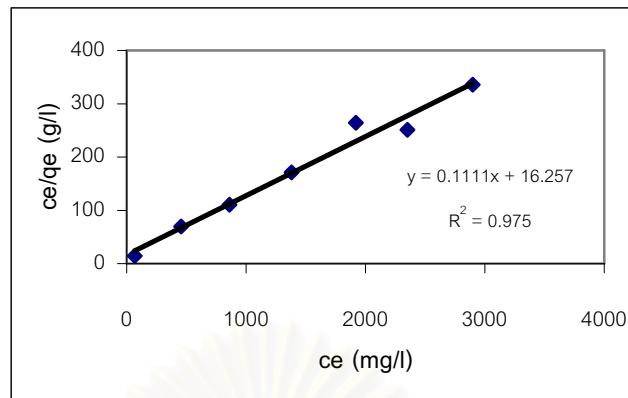


(b)

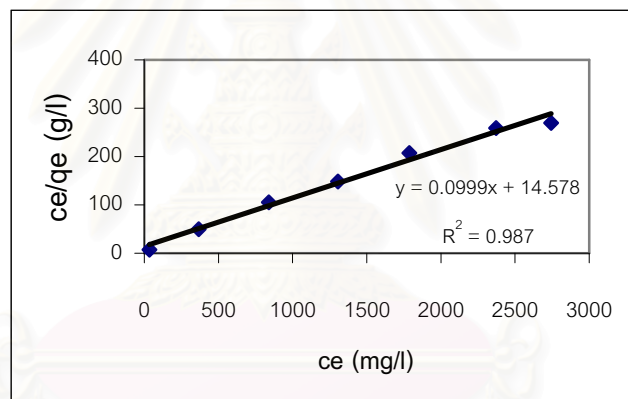
Figure 8 Langmuir plots for the adsorption of reactive yellow on bead 300  $\mu\text{m}$ .

(a) at room temperature

(b) at 80°C



(a)



(b)

Figure 9 Langmuir plots for the adsorption of reactive yellow on bead 500  $\mu\text{m}$ .

(a) at room temperature

(b) at 80°C

## BIOGRAPHY

Miss Boonsri Kusuktham was born in Bangkok, Thailand, on July 20, 1964. She received a Bachelor of Education degree with a major in Science-Chemistry from Srinakharinwirot University in 1986. She graduated a master of Education degree with a major in Chemistry from Srinakharinwirot University in 1989 and a Master of Science with a major in Polymer Science from Mahidol University in 1996. She started as a graduate student in the Department of Materials Science with a major in Materials Science, Chulalongkorn University in June 2001, and Completed the program in 2004.



สถาบันวิทยบริการ  
จุฬาลงกรณ์มหาวิทยาลัย